DESIGN OF ISOLATED DC-DC AND DC-DC-AC CONVERTERS WITH REDUCED NUMBER OF POWER SWITCHES

A Thesis

Submitted to the Faculty

of

Purdue University

by

Dhara I. Mallik

In Partial Fulfillment of the

Requirements for the Degree

of

Master of Science in Electrical and Computer Engineering

August 2017

Purdue University

Indianapolis, Indiana

THE PURDUE UNIVERSITY GRADUATE SCHOOL
STATEMENT OF COMMITTEE APPROVAL

Dr. Euzeli Cipriano dos Santos, Chair

Department of Electrical and Computer Engineering

Dr. Mohamed El-Sharkawy

Department of Electrical and Computer Engineering

Dr. Maher Rizkalla

Department of Electrical and Computer Engineering

Approved by:

Dr. Brian King

Head of the Graduate Program

Dedicated to my beloved parents

Munmun Manabee and Dr. M S I Mullick

Ma ♥ Bapi

ACKNOWLEDGMENTS

I would like to thank my thesis supervisor and mentor Dr. Euzeli C. dos Santos, for his guidance and inspiration through the research process and course-works. I am grateful to all my committee members.

I am immensely indebted to Dr. Brian King, the Head of the Department, not only for his guidance since the very first year of my graduate studies but also for being a continuous support.

I am grateful to the other faculty members and staff. I would especially like to mention Sherrie for keep enduring my constant nudging always with a welcoming smile. I want to thank my lab-mates for their support whenever I asked and even when I did not ask.

I owe everything to my loving parents who kept sacrificing for me since the day I was born. Even being a thousand of miles away, they never stopped encouraging, motivating and telling me to dream bigger. I am also grateful to my other family members for keeping me going. Finally, I would like to thank Ragib, for having the courage to hold my hands even during the most struggling and uncertain times.

TABLE OF CONTENTS

Page

LIST OF TABLES viii

LIST OF FIGURES ix

SYMBOLS xii

ABBREVIATIONS xiii

ABSTRACT xiv

1 INTRODUCTION 1

1.1 Power Processing 1

1.2 Dc-dc Converter 3

1.2.1 Isolated dc-dc Converter 4

1.3 Dc-ac Converter 4

1.4 Multiple Output Converters 5

2 CONVENTIONAL CONFIGURATIONS 6

2.1 Introduction 6

2.2 Single Input Single Output Dc-dc Converter 6

2.2.1 Converter Configuration 6

2.2.2 Transfer Function 7

2.2.3 Switching Signals 7

2.2.4 Generation Gating Signals 8

2.3 Single Input Dual Output Dc-dc Converter 12

2.3.1 Converter Configuration 13

2.3.2 Gating Signal Circuitry 13

2.3.3 Transfer Function 14

2.4 Dc-Ac Converter 15

3 PROPOSED DC-DC CONVERTER 19

Page

3.1 Introduction 19
3.2 Motivation 19
3.3 Design Requirements 21
3.4 Converter Design and Layout 22
3.5 Switching States 22
3.6 Gating Signals 25
3.6.1 Serially Connected Loads Operate Together 26
3.6.2 Serially Connected Loads Operate Separately 26
3.6.3 Parallel Connection of the Load 30
3.7 Selection of Gating Signal for the Proposed Converter 30
3.8 Switching State Diagrams 34
3.9 Switching Signal Circuitry 37
3.10 Steady State Analysis 41
3.11 Feedback Control System 43
4 RESULTS OBTAINED FROM THE PROPOSED DC-DC CONVERTER 46
4.1 Introduction 46
4.2 Circuit Diagrams to Simulate Proposed Dc-dc Converter 46
4.3 Results From Simulation 49
4.4 Calculations 50
4.5 Special Condition 52
4.6 Comparison with The Conventional Converter 54
4.6.1 Generation of Output Voltage 54
4.6.2 Power Loss 55
4.6.3 Number of Components Required 66
5 PROPOSED DC-DC-AC CONVERTER 67
5.1 Introduction 67
5.2 Motivation 68
5.3 Design Layout 68

Page

5.3.1 Dc-dc Converter 69
5.3.2 Dc-ac Converter 70
5.4 Three Phase Voltage Source Inverters 70
5.5 Converter Layout 71
5.5.1 Dual Output Converter with Eight Switches 71
5.5.2 Dual Output Converter with Six Switches 72
5.5.3 Dual Output Converter with Fault Correction 72
5.6 Gating Signal 73
6 RESULTS FROM DESIGNED DC-DC-AC CONVERTER 76
6.1 Introduction 76
6.2 Gating Signals 76
6.3 Single Input Dual Output Dc-ac Converter 79
7 CONCLUSION 82
7.1 Discussions on the Designed Converters 82
7.1.1 Single Input Dual Output Dc to Dc Converter 82
7.1.2 Single Input Dual Output Dc to Ac Converter 82
7.2 Suggested Improvements 82
REFERENCES 84

LIST OF TABLES

Table		Page
2.1	All Possible States of the Four Switches	8
2.2	States Considered to Generate the Gating Signals	9
2.3	Generating the Four Required Signals	9
3.1	All topological states	23
3.2	States Considered to Generate the Gating Signals	27
3.3	Logic Table to Generate the Gating Signals	27
3.4	Desired Switching States	32
3.5	Generation of the Switching Signals for the Switches Q1 and Q2	32
3.6	Generation of the Switching Signals for the Switch Q3 (Initial)	33
3.7	Generation of the Switching Signals for the Switch Q3 (Final)	34
3.8	Generation of the Switching Signals for the Switch Q4	35
4.1	Parameters of Simulation Control	49
4.2	Output Voltage of Conventional and Proposed Converter with Changing Input Voltage	54
6.1	Parameters Included for the Triangular Wave	76
6.2	Parameters Included for the Sine Waves	77

LIST OF FIGURES

Figure		Page
1.1	Electric Power Conversion System	1
1.2	Converter Power Loss vs. Efficiency	3
2.1	Full-bridge Single Input Single Output Dc-dc Converter	6
2.2	Logic Circuit to Generate Switching Signals	10
2.3	Generation of Sig1 from a Triangular Wave and a Dc Voltage	11
2.4	Generation of Sig2 from a Triangular Wave and a Dc Voltage	11
2.5	Generation of Q1 from Sig1 and Sig2	12
2.6	Generation of Q2 from Sig1' and Sig2'	13
2.7	Full-bridge Single Input Dual Output Dc-dc Converter	14
2.8	Logic Circuit to Generate Switching Signals	15
2.9	Conventional Single-Input Single-output Inverter	16
2.10	Single-input Dual-output Dc-dc-ac Converter with Eight Switches	16
2.11	Switching Signal Generation of Dc-ac Converter	17
3.1	Proposed Single Input Dual Output Dc-dc Converter	22
3.2	Primary Side Voltages of the Loads for Series Connection	28
3.3	Primary Side Voltages with Increased Duty Cycle for Load-1	29
3.4	Primary Side Voltages of the Loads for Parallel Connection	31
3.5	Equivalent Circuit for the First State	36
3.6	Equivalent Circuit for the Second State	37
3.7	Equivalent Circuit for the Third State	38
3.8	Equivalent Circuit for the Fourth State	39
3.9	All Six Switching Signals	40
3.10	Circuitry to Generate Gating Signals	41
3.11	Inductor Voltages and Currents for Output1 and Output2	42

Figure Page

3.12 Basic Feedback Control System for the Converter 44
3.13 Feedback Control System for the Converter 44
4.1 Diagram in PSIM to Simulate the Designed Converter 47
4.2 Gating Circuitry to Generate the Switching Signals 48
4.3 Four Switching Signals Generated to Control the Voltage at Primary Side . . . 50
4.4 Primary Side Voltages [Upper one with 0.8 duty cycle and lower one with 0.5 duty cycle] 51
4.5 Output Voltages of Load-1 and Load-2 51
4.6 Primary Side Voltages [Upper one with 0.5 duty cycle and lower one with 0.8 duty cycle] 53
4.7 Output Voltages of Load-1 and Load-2 [Upper one with 0.5 duty cycle and lower one with 0.8 duty cycle] 53
4.8 MOSFET Properties in the PcdEditor Window in PSIM 56
4.9 Diode Voltage Drop vs Diode Forward Current of the Switch 57
4.10 Diagram to Calculate the Losses in Conventional Configuration 58
4.11 Diagram to Calculate the Losses in Conventional Configuration 58
4.12 Conduction Losses of the Switches in the Conventional Configuration 59
4.13 Conduction Losses of the Switches in the Proposed Design 60
4.14 Comparison Between the Conduction Losses of the Conventional and Proposed Configuration 61
4.15 Switching Losses of the Switches in the Conventional Configuration 62
4.16 Switching Losses of the Switches in the Proposed Design 63
4.17 Comparison Between the Switching Losses of the Conventional and Proposed Configuration 64
4.18 Total Loss in the Conventional Configuration 65
4.19 Total Loss in the Proposed Design 65
4.20 Comparison Between the Total Losses of the Conventional and Proposed Configuration 66
5.1 The Planned Layout of the Converter 69
5.2 Triangular Wave and Three Sine Waves to Generate Switching Signals 71

Figure Page

5.3 Single-input Dual-output Inverter with Eight Switches 72
5.4 Single-input Dual-output Inverter with Six Switches 73
5.5 Open-end Winding System 74
5.6 Switching Signal Generation of Dc-ac Converter 75
6.1 Gating Signal Generation Circuitry 78
6.2 Waves to Generate Switching Signals 78
6.3 Generated Switching Signals for Six Switches 79
6.4 Circuit Diagram for the Proposed Design 80
6.5 Output Currents 80
6.6 Line to Line Voltages 81

SYMBOLS

m	mass
V	voltage
I	current
P	power
η	turns ratio
D	duty cycle
$^{\circ}C$	degree Celsius
&	AND gate
|	OR gate
$\overline{x}$	NOT gate(NOT x)
$\bigoplus$	XOR gate

ABBREVIATIONS

SISO	single input single output
SIDO	single input dual output
PWM	pulse width modulation
dc	direct current
ac	alternating current
Op-Amp	operational amplifier
RoHS	restriction of hazardous substances

ABSTRACT

Mallik, Dhara I. M.S.E.C.E., Purdue University, August 2017. Design of Isolated Dc-dc and Dc-dc-ac Converters with Reduced Number of Power Switches. Major Professor: Euzeli C. dos Santos.

There are various types of power electronic converters available in recent days. In some applications (e.g. PC power supply), it is required to supply more than one load from a single power supply. One of the main challenges while designing a power converter is to increase its efficiency especially when the number of power switches employed is relatively large. While several loads are supplied from a single source, if the power loss in the switches cannot be reduced, then the expected utilization of using a single source is not very feasible. To reduce the loss and increase efficiency, the thesis presents a novel design with reduced number of switches.

The scope of this thesis is not limited to the dc-dc converter only, the converter to supply three phase ac loads from a single dc source is also presented. This discussion includes an improved fault tolerant configuration of the inverter part. The generated waveforms from the simulations are included as a demonstration of satisfactory results.

1. INTRODUCTION

Since the time of ancient Greek through the discovery of electricity by Benjamin Franklin, electricity has been an inseparable part of human life. Communication, entertainment, mechanical work, light, computing and all tangible benefits of energy and electricity cannot be denied. The enormous involvement of electricity requires control and conversion to meet modern day requirements. From the need to control the flow of electricity to manage the conversion of energy the area of Power Electronics was introduced [1].

1.1 Power Processing

Since the invention of mercury arc rectifier in 1902 to convert alternating current to direct current [2] [3], the revolutionary era of power electronic devices had been started. Application of mercury arc valves in power grids, the high-vacuum and gas-filled diode thermionic rectifiers, triggered devices such as the thyratron and ignitron were being widely used. In the beginning, power electronics [4], [5], [6], [7] mainly focused on advancing devices that provide the capability to handle high power levels. Then the focus transitioned to the application of the semiconductor devices [8] with suitable power rating to meet broader requirements of novel products. Recently it was expanded to multidisciplinary technology such as artificial intelligence and neural network [9].

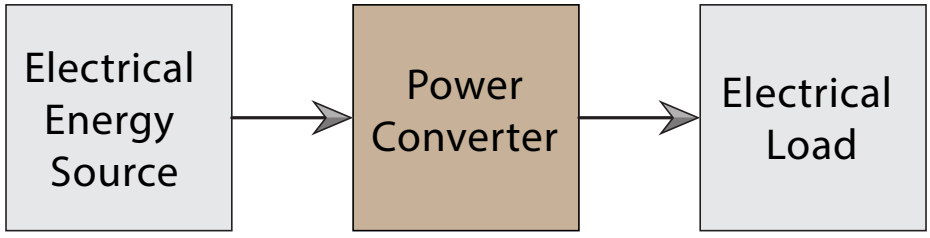

Fig. 1.1. Electric Power Conversion System

To meet the user requirements, a systematic method was developed in [10] to link technical power packaging issues. The framework explores the general power conversion system as depicted in figure 1.1. The input power is processed by the converter as specified and yield to the conditioned output power to supply to the load.

In power processing applications, efficiency is a crucial factor. Construction of low efficiency converters producing substantial output power does not simply meet the practical necessity [11]. If *Pout* is the output power and *Pin* is the input power then efficiency η is,

$$\eta = \frac{Pout}{Pin} \tag{1.1}$$

During the conversion process the lost power is the difference between the input and output power. The lost power $Ploss$ is,

$$Ploss = Pin - Pout \tag{1.2}$$

$$= \frac{Pout}{\eta} - Pout \tag{1.3}$$

$$= Pout(\frac{1}{\eta} - 1) \tag{1.4}$$

From equation (1.3), if the efficiency is needed to be plotted, then,

$$\frac{Ploss}{Pout} = \frac{1}{\eta} - 1 \tag{1.5}$$

The equation (1.5) is plotted in Matlab to generate the graph to depict the ratio of power loss to output power vs. the efficiency of the converter.

Figure 1.2 shows the plotted data. According to [11], if the converter has an efficiency of 50 percent, then the loss during the conversion is equal to the output power. This energy is converted to heat which needs to be removed from the converter. Therefore a large and expensive cooling process is required for the system. So only increasing the efficiency can lead to reducing the expense and producing higher output. So much effort is given in the converter design process to improve the efficiency.

The power electronic conversion process can be one of four types:

1. Alternating current (AC) to direct current(DC)

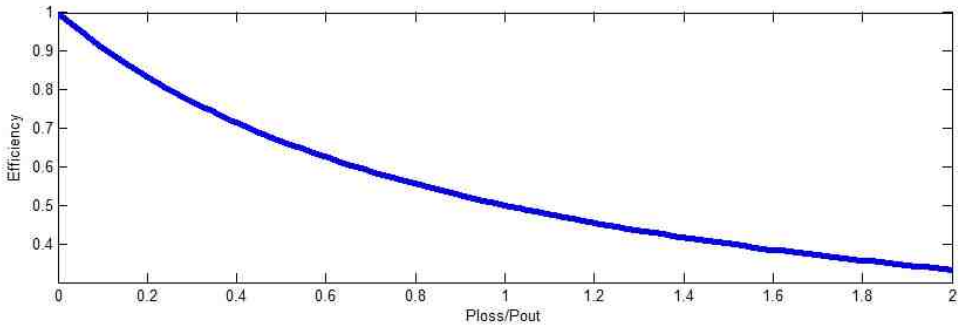

Fig. 1.2. Converter Power Loss vs. Efficiency

2. Direct current (DC) to alternating current(DC)

3. Direct current (DC) to direct current(DC)

4. Alternating current (AC) to alternating current(DC)

In this thesis, the dc to dc conversion and then dc to ac conversion were taken into consideration.

1.2 Dc-dc Converter

Since the 1940's, the growth of dc-dc converters has increased due to the high demand of dc-dc converter in industrial applications, computer hardware circuitry and trend in high power and high voltage density related applications [12]. Switching mode dc-dc converters are more efficient than linear converters as the transistors operate as switches and dissipate less power. PWM dc-dc converters are capable of conducting in step-up, step-down mode and can have multiple output voltages whereas linear regulators can operate only as step-down converters [13]. High step-up converters are especially required in the wide range of applications of energy sources like photo-voltaic panels and fuel cells which have variable input voltage range and low output voltage [14], [15]. In the systems where the generated power is needed to transmit to a long distance like offshore wind power [16], high-voltage

direct current (HVDC) transmission systems have lower cable loss than high-voltage alternating current (HVAC) transmission systems [17]. HVDC technology is considered as the main element of multi-terminal grid [18].

1.2.1 Isolated dc-dc Converter

As discussed above,in HVDC transmission systems, the regulation of voltage is very important and for that reason a stable control system is needed for the dc-dc converter. In [19], PWM based adaptive sliding mode control was presented for boost converter. An interleaved converter with voltage multiplier was proposed in [20] that has reduced switching loss but this kind of converter lacks proper control system in applications other than electric vehicles. Cascode technique along with inductor coupling was implemented for high step-up operation in [21]. But over these traditional converters, isolated dc-dc converters have many advantages in electrical isolation, high reliability, ease of realizing soft-switching control and bidirectional energy flow [22]. Another investigation [23] showed that three-level full bridge dc-dc converters are capable of improving light load efficiency compared to two-level dc-dc converters as the switches are exposed to lesser dc voltage.

Therefore, in this work, while designing converter, full bridge isolated type was considered.

1.3 Dc-ac Converter

Dc to ac converter is called the power inverter which converts direct current to alternating current. From the 1970's different prototypes of dc to ac conversion process started to formed for various uses such as supply a low-pressure mercury vapor discharge pump [24], then later transformer [25], [26] were utilized.

1.4 Multiple Output Converters

Dc-dc converter with single output is insufficient in many applications. For doubly fed machines like electric tractor locomotives or elevators are required to operate from one input source [27]. Multiple outputs with wide range applications in hybrid electric vehicles [28], LED lighting [29], dc based nano-grids [30], stand-by power supplies etc. [31], [32]. In addition, the setup where two loads can be operated from the same source reduce the bulkiness of the conventional converters and provide more compactness, cost effectiveness [33] and have higher efficiency [34]. Single input dual output buck converters were also explored for both unidirectional and bidirectional operations and utilization of power switches [35], [36]. Similar characteristics in reducing power loss and improving efficiency in full-bridge isolated dc-dc converter was explored in this thesis.

Many applications require ac output voltage that matches the frequency of the grid. Novel inverters are discovered day by day as they have broad applications like induction heating cooking appliances [37], inverter based microgrid system [38], hybrid multilevel conversion [39] and so on. Hybrid inverter is used in high voltage heating, ventilation and air conditioning system [40]. In such applications especially where the load is supplied from two separate dc-ac converters, the use of single input to dual ac output can be very cost effective. In this thesis, a dual ac output from a single dc input was investigated and proposed.

2. CONVENTIONAL CONFIGURATIONS

2.1 Introduction

A bidirectional isolated dc-dc converter was proposed in [41] for operation in medium voltage range. This type of galvanic isolation of the converters are suitable for energy storage system [42]. According to [43], when full-bridge switching circuit is used, the input and output voltage are significantly proportionate. For distributed power generation in residential systems, isolated dc-dc step up converters can be utilized [44].

2.2 Single Input Single Output Dc-dc Converter

2.2.1 Converter Configuration

A full-bridge dc-dc converter is shown in Fig. 2.1. The converter has a single dc source.

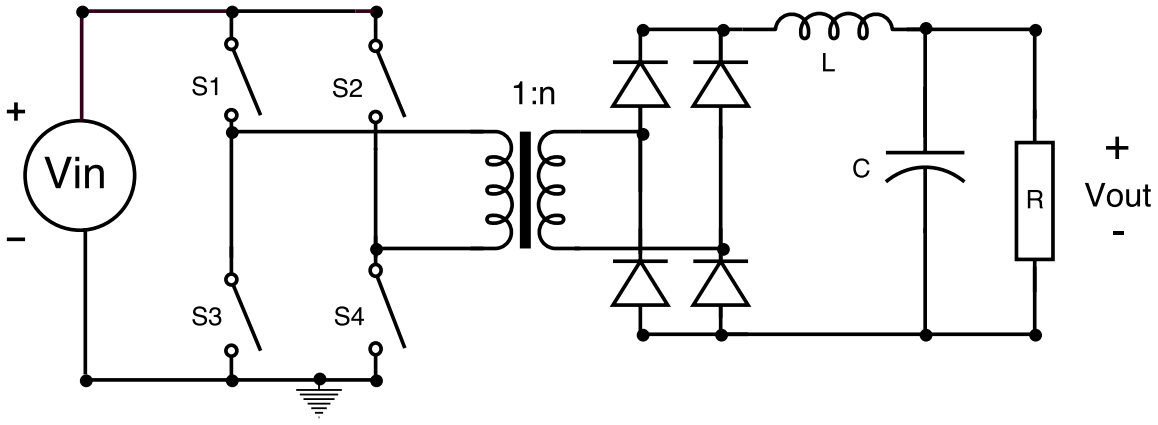

Fig. 2.1. Full-bridge Single Input Single Output Dc-dc Converter

The primary side of the transformer consists of four switches to build full-bridge switching circuitry. Transformer turns ratio is $1 : n$ from primary to secondary side. A rectifier and LC filter is used in the secondary side to generate the desired output voltage without distortion and enhance smoothness.

2.2.2 Transfer Function

Control of the converter voltage is dependent on the transfer function of the converter.

$$\frac{Vout}{Vpri} = n * D \tag{2.1}$$

Duty cycle is the fraction or period of time during which the system stays active [45], [46], [47].

2.2.3 Switching Signals

The switching signals of the converter need to be such that it generates an ac voltage in the transformer primary winding as the transformer cannot convert a dc voltage. The generated voltage at the primary winding should be such that it can be controlled by changing duty cycle of the signal. The converter has four switches. So the possible switching states are $2^4 = 16$. All 16 possible states and the generated voltage at the primary side are showed in table 2.1.

If the primary side is open circuited or shorted, it gives a zero voltage. State number 10 generates a positive voltage equal to the source voltage. Similarly, the seventh state generates a negative source voltage. So while taking the switching states for consideration, state 7 and state 10 are must be included in the desired states.

Also while choosing the zero voltage states it should be such that it makes the boolean expression less complicated and compact to implement. The number of logic gates used should also made optimum.

Table 2.1.
All Possible States of the Four Switches

State	**Q1**	**Q2**	**Q3**	**Q4**	V_{Pri}
1	0	0	0	0	0
2	0	0	0	1	0
3	0	0	1	0	0
4	0	0	1	1	0
5	0	1	0	0	0
6	0	1	0	1	0
7	0	1	1	0	-Vin
8	0	1	1	1	0
9	1	0	0	0	0
10	1	0	0	1	Vin
11	1	0	1	0	0
12	1	0	1	1	0
13	1	1	0	0	0
14	1	1	0	1	0
15	1	1	1	0	-
16	1	1	1	1	0

2.2.4 Generation Gating Signals

The states that are considered for the generation of gating signals are shown in table 2.2. The voltage goes from positive to negative and stay as zero in between so that the duty cycle is well defined. From equation 2.2, it can be seen that the ratio of output voltage to input voltage is directly proportional to the duty cycle. So if the duty cycle is changed then the output voltage will change accordingly. So the time the voltage keeps a value (positive and negative) should be increased with increased duty cycle and the time of zero voltage

Table 2.2.
States Considered to Generate the Gating Signals

Q1	**Q2**	**Q3**	**Q4**	V_{Pri}
1	0	0	1	Vin
1	1	1	1	0
0	1	1	0	-Vin
1	1	1	1	0

needs to be decreased at the same time. Similarly for decreased duty cycle, time of the signal keeping a value (positive and negative) should be decreased and the time of zero voltage needs to be increased during that state.

Table 2.3.
Generating the Four Required Signals

Sig1	**Sig2**	**!Sig2**	**Sig1|$\overline{\text{Sig2}}$=Q1=Q4**
1	1	0	1
1	0	1	1
0	1	0	0
0	0	1	1

$\overline{\text{Sig1}}$	**$\overline{\text{Sig2}}$**	**$\overline{\text{Sig1}}$|$\overline{\text{Sig2}}$=Q2=Q3**
0	0	1
0	1	1
1	0	0
1	1	1

The required switching signals can be generated from two signals Sig1 and Sig2. Signals Q1 and Q4 are same. Similarly signals Q2 and Q3 are same. Signal-1 can be generated

by comparing a triangular wave with a dc voltage using an op-amp. The pulse width modulation (PWM) is a traditional technology that is used in the switching mode power converter to control and regulate the output power [48]. The analog implementation of PWM, also known as naturally sampled PWM, is simpler compared to other methods and it only the generation of a suitable carrier and a comparator [49]. Figure 2.2 shows the gating cir-

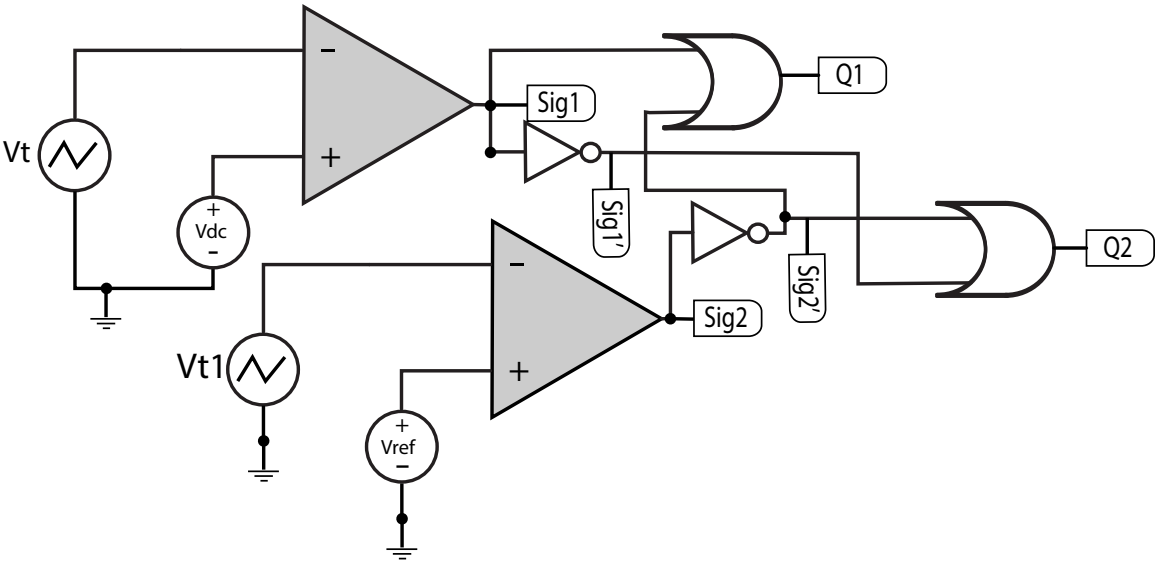

Fig. 2.2. Logic Circuit to Generate Switching Signals

cuitry to generate the switching signals. As can be seen from figure 2.2, the triangular wave is connected to the inverting input of the operational amplifier and the dc voltage which is a constant voltage with half the amplitude of the triangular wave is connected to the non-inverting input of the operational amplifier.

When Vdc is greater than the triangular voltage Vt, the op-amp produces a positive voltage. When Vt is greater than Vdc, it gives zero voltage as the non-inverting input node is connected to Vt. So it generates an output pulse every time Vdc is greater than Vt. Sig2 is generated similarly. The reference voltage Vref, controls the duty cycle. If the magnitude of Vref is increased, then the duration it is greater than Vt will increase. Hence

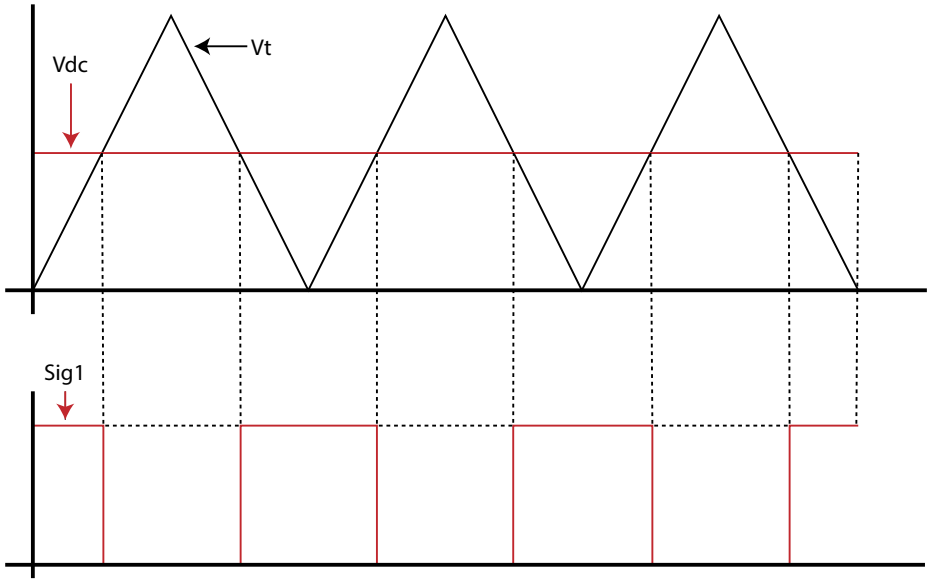

Fig. 2.3. Generation of Sig1 from a Triangular Wave and a Dc Voltage

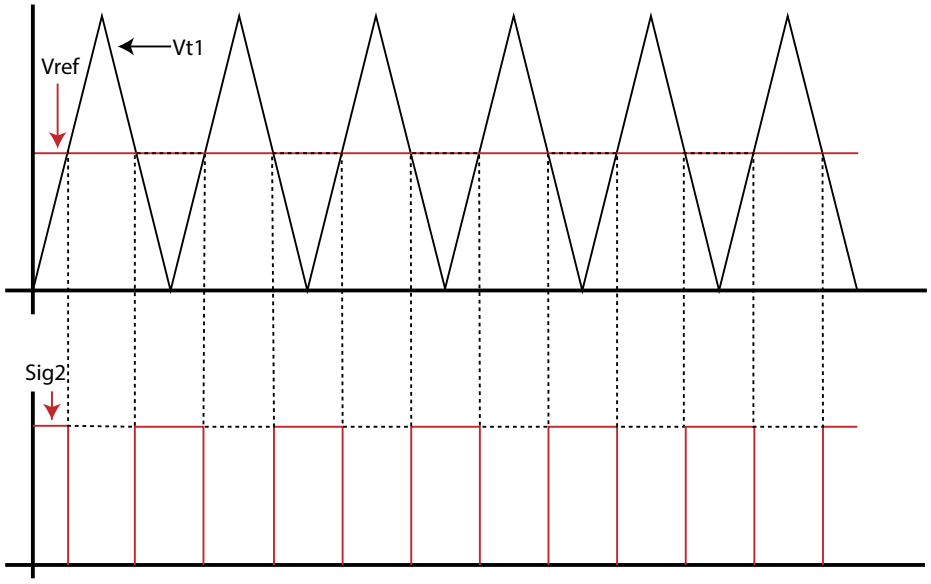

Fig. 2.4. Generation of Sig2 from a Triangular Wave and a Dc Voltage

the duty cycle is increased. Using the same technique, if less duty cycle is required, then the magnitude of the reference voltage is decreased.

Sig1' is found by passing Sig1 through a **not** gate and Sig2' is found by passing Sig2 through a **not** gate. Q1 is generated by taking **or** of Sig1 and the inverse of Sig2. That

means when both of the signals are zero it will generate zero. Otherwise if either of both of them have value, it will keep generating values. The generation of the switching signal is showed in figure 2.5.

The signal Q2 is generated by passing both of the inverse of Sig1 and Sig2 through an **or** gate. The signal wave-shapes to generate Q2 is shown in figure 2.6.

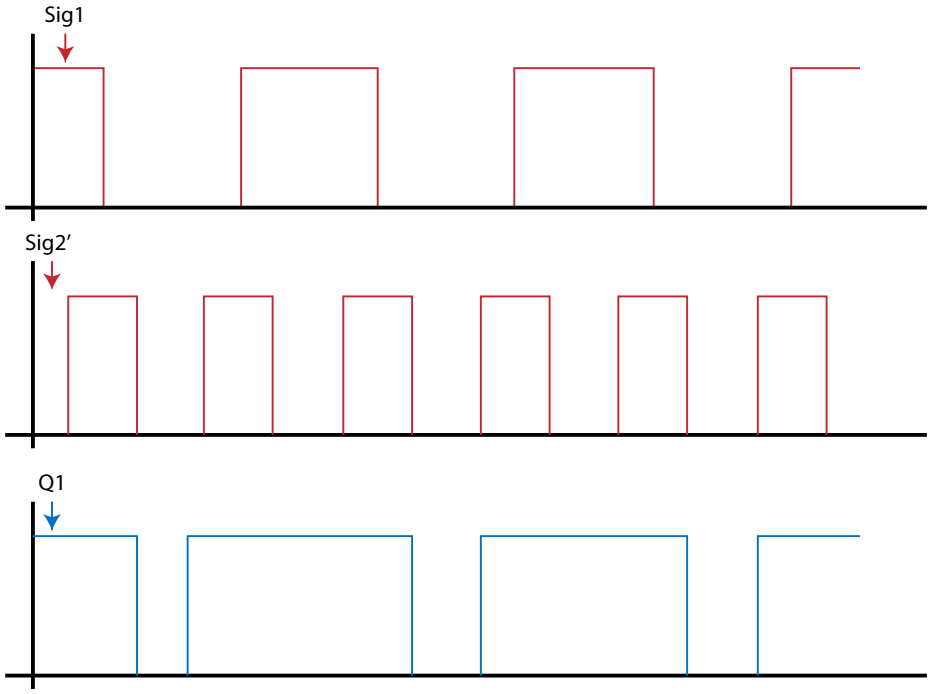

Fig. 2.5. Generation of Q1 from Sig1 and Sig2

2.3 Single Input Dual Output Dc-dc Converter

In [50], a single input dual output converter was presented but it requires control system constituting both duty cycle and frequency. Changing duty cycle is easily possible but changing frequency to control a load could be a complex and cost inducing method. In addition to it, the lower load was loosely connected to the transformer primary winding. So to utilize similar control method for both of the loads, the conventional dc-dc converter to supply two separate loads is explored in this section.

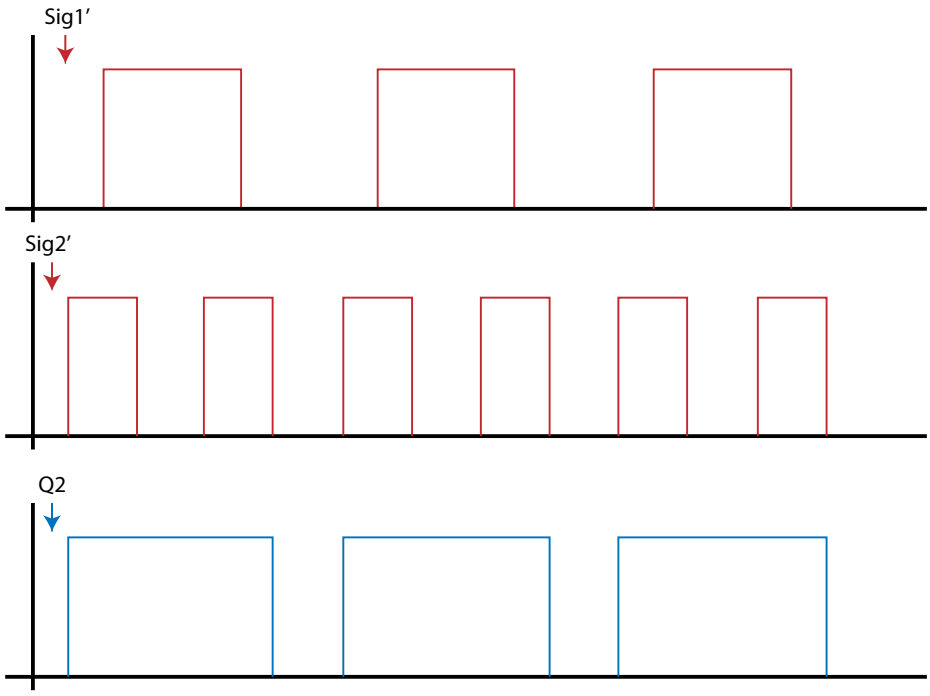

Fig. 2.6. Generation of Q2 from Sig1' and Sig2'

2.3.1 Converter Configuration

To implement using the conventional single input single output circuitry, supplying dual output from a single source requires a parallel connection from the source. This ensures that both of the load can have the whole source voltage in the primary side. The converter is shown in figure 4.1. The input voltage is Vin and there are two loads R1 and R2 connected to it. There are four switches for each of the primary side and hence there are eight switches altogether.

2.3.2 Gating Signal Circuitry

As discussed in the previous section, the switching signals are generated using logic gates. Figure 2.8 shows the logic circuit that generates the gating signals.

Three operational amplifiers generate the required pulses. From these signals through the **not** gates and **or** gates, four gating signals for the eight switches are generated.

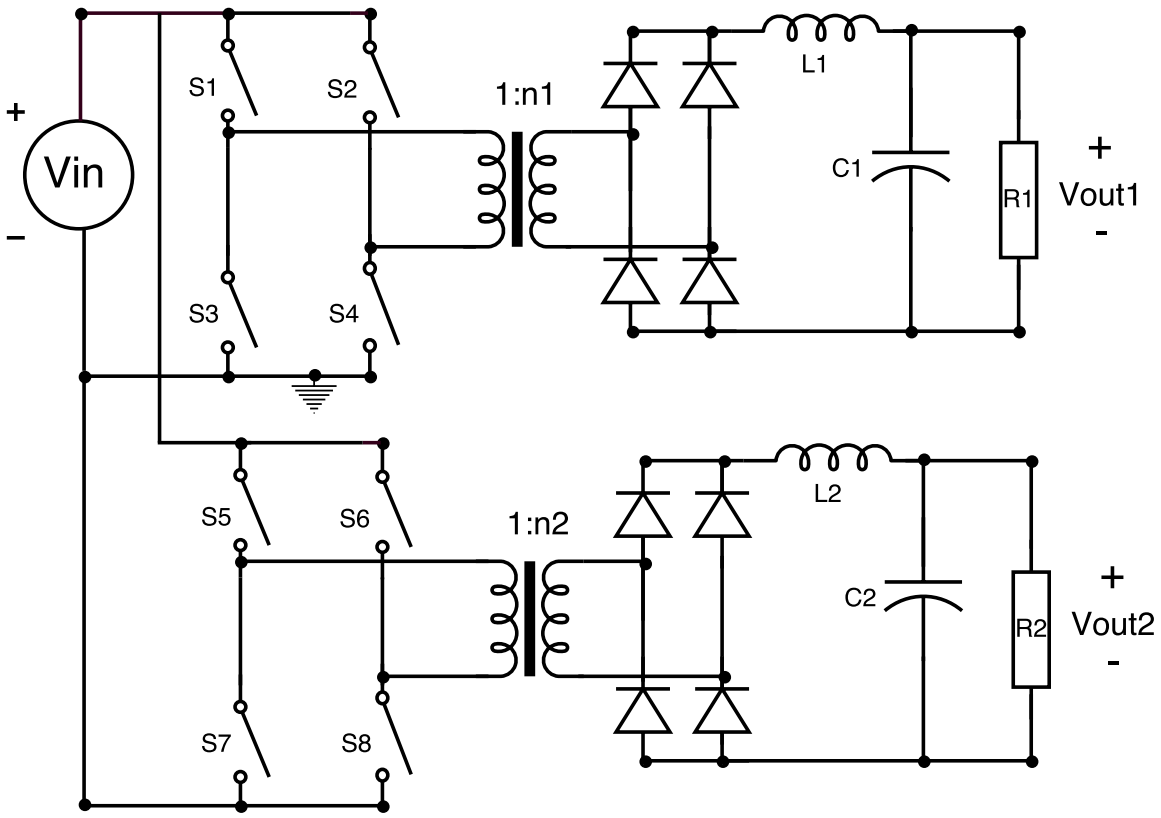

Fig. 2.7. Full-bridge Single Input Dual Output Dc-dc Converter

The signal Sig1 is the switching signal for the switches S1 and S2, Sig2 is for the switches S2 and S3, Sig3 is for the switches S5 and S8 and Sig4 is for the switches S6 and S7 in figure 4.1.

2.3.3 Transfer Function

If the turns ratios of the transformers are n1 and n2 and duty cycles of the signals are D1 and D2 for load1 and load2 respectively, then the transfer functions are:

$$\frac{Vout1}{Vpri1} = n1 * D1 \tag{2.2}$$

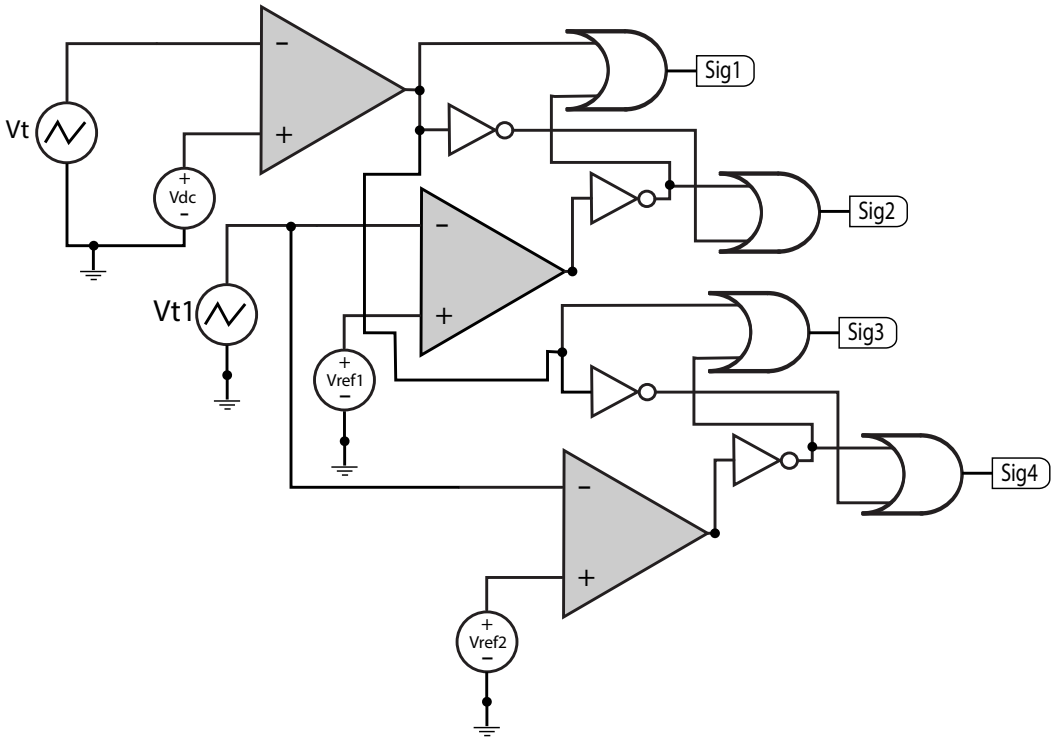

Fig. 2.8. Logic Circuit to Generate Switching Signals

$$\frac{Vout2}{Vpri2} = n2 * D2 \tag{2.3}$$

In these cases, the primary side voltages can reach the value of the input voltage.

2.4 Dc-Ac Converter

For the applications where ac output is required, an inverter portion is integrated at the load side in order to provide alternating current. The typical converter that converts the dc input to a required ac value is shown in figure 2.9.

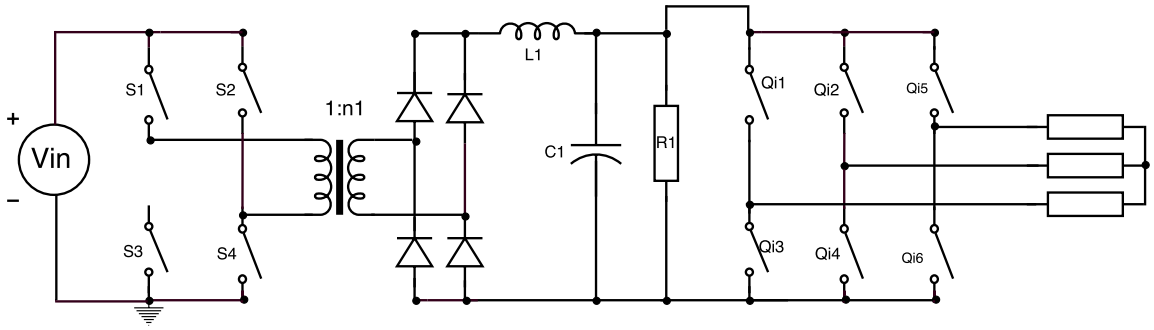

Fig. 2.9. Conventional Single-Input Single-output Inverter

Figure 2.9 presents the converter with only one input and one output. Like the previous section, if the converter is made to supply two separate loads, then the traditional configuration looks like the one in figure 2.10.

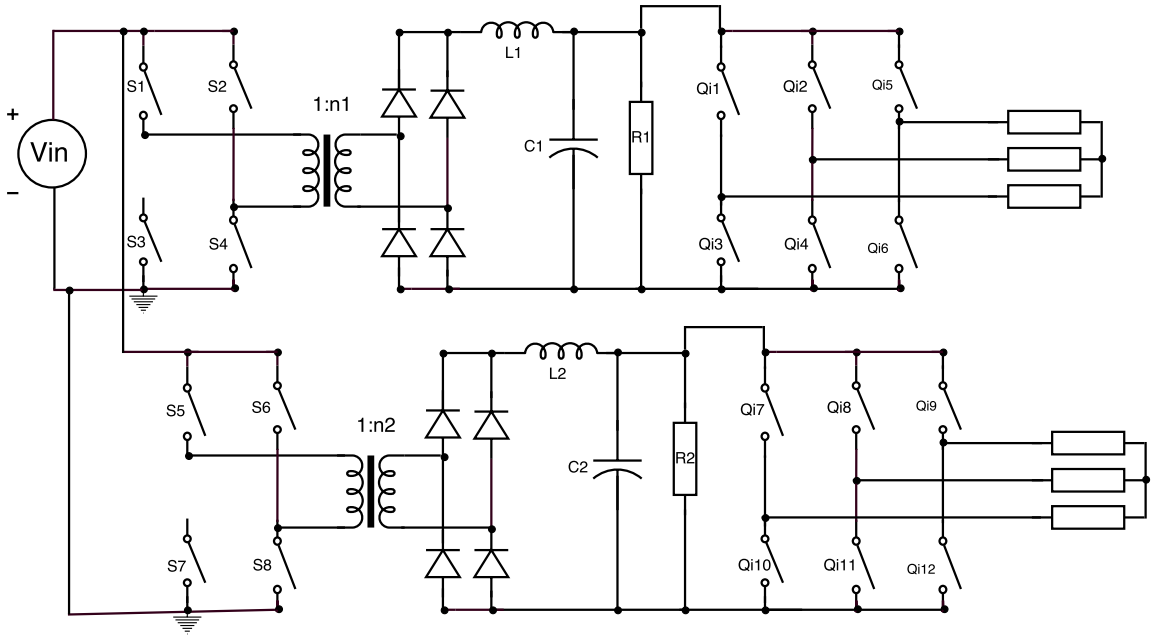

Fig. 2.10. Single-input Dual-output Dc-dc-ac Converter with Eight Switches

The single input converter that supplies two ac loads in figure 2.10 is consists of eight switches in total. For this circuit configuration, the gating signals for the dc-dc converters are similar to the ones generated in an earlier section. The switching signals of the eight switches in the left side of the design are generated using a similar circuit shown in figure 2.8.

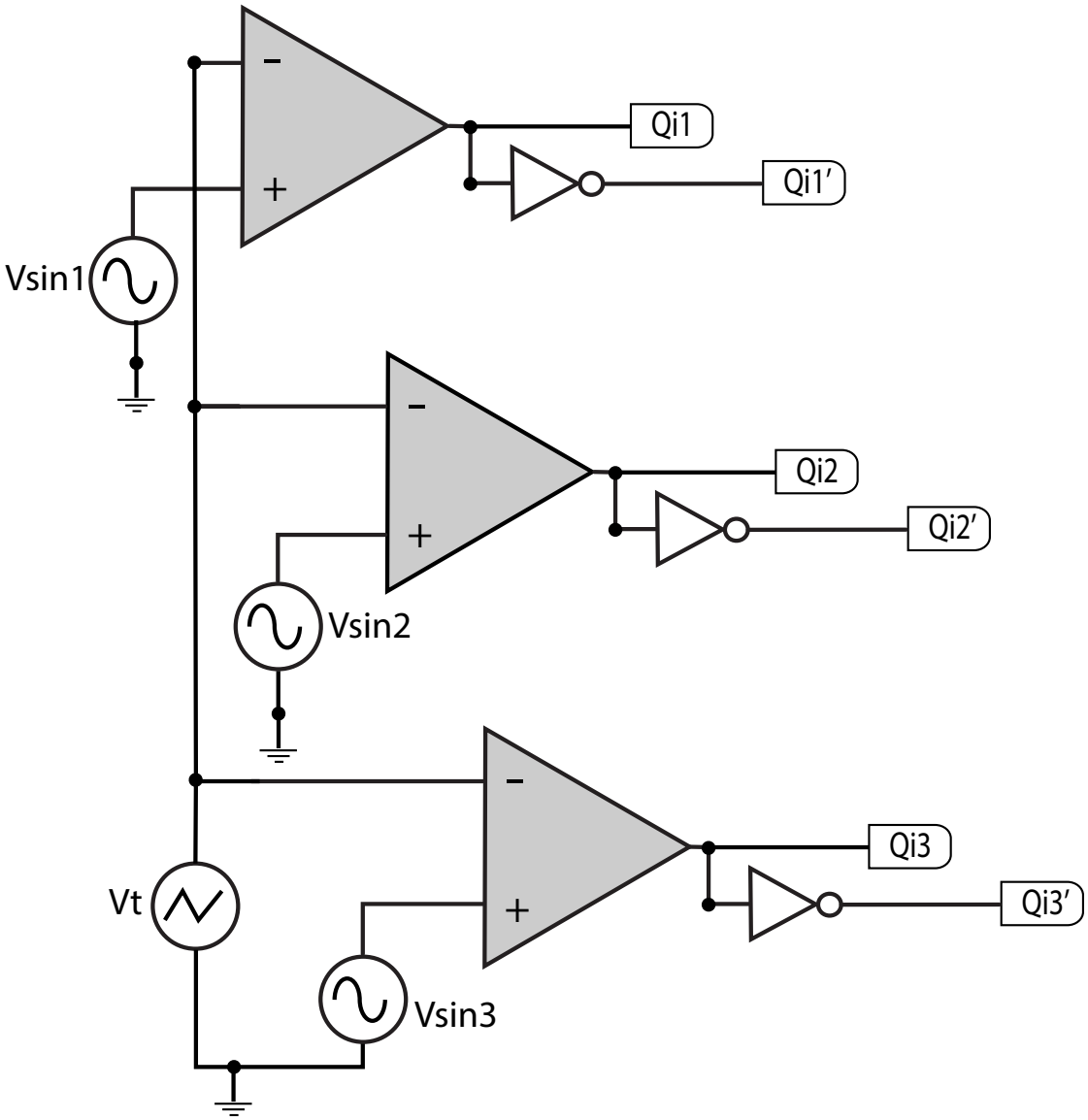

Fig. 2.11. Switching Signal Generation of Dc-ac Converter

For the generation of six set of signals at the dc-ac converter side, the similar gating signal generation circuit for a conventional inverter is used. The circuitry is shown in figure 5.6. These generated signals can be used for both of the loads.

3. PROPOSED DC-DC CONVERTER

3.1 Introduction

The proposed dc-dc converter have reduced number of switches comparing to the conventional single input dual output converter. As discussed in the previous chapter, the conventional single input dual output dc-dc converter requires eight switches in total to operate two loads separately. In the proposed converters several possibilities were explored to reduce the number of switches. Then it was designed with only six switches and a unique switching signal was proposed to reach the optimum number of logic gates to generate the switching signals.

3.2 Motivation

It was explained in [51], using three switches instead of four switches in the dual output buck converter is able to save silicon area with suitable design of power switches. Similarly for a full-bridge dc-dc converter, if a dual output converter can be designed with reduced number of switches, it should be able to reduce cost in implementation of the regulator switches. In [52], three switch dual output buck converter was explored to alleviate space and platform cost in PC platform that hosts various subsystems such as the central processing unit (CPU), memory and I/O control hubs, the memory subsystem, graphics, audio, LAN etc. Because with increased features, the power delivery network is required to be able to supply different voltage levels which increases cost, requires more space and consequently reduces efficiency. For this kind of PC platform, compact and high efficiency power conversion system is needed.

In the field of renewable energy, the power electronic system and hence high efficiency power conversion system is also a necessity. Due to the increased demand of power gener-

ation, the utilization of renewable energy has increased and has become more popular over the traditional fossil resources [53]. The drop in photo-voltaic pricing trend is demonstrated in [54]. Not only the use of renewable energy is cost effective than the diesel fuel, but also it has increased reliability [55]. For dispersed power generation systems, power electronic interfaces are a necessity [56]. Especially for the integration of renewable energy sources to the grid [57]. To increase robustness of these interfaces many configurations have been proposed. To reduce power coupling and improve system stability in distributed generation unit, implementation of virtual impedance is found useful [58].

In microgrid system, cluster of small energy generators such as solar cells, fuel cells, wind turbine along with electrical loads exist within the main grid that includes embedded management and control system which requires power electronic converters [59]. Detailed analysis at power converter level of microgrid structures and control techniques were discussed in [60]. Power electronic interface for distributed energy has the following advantages:

1. By mitigating harmonic elements and maintaining power factor within range, PE interface improves power quality. In addition to it, PE interface ensures uninterrupted power flow which have much faster response time than non-PE based system especially for sensitive loads and induction and synchronous generator systems [61].

2. In radial distribution system, PE system in voltage regulation has the benefit of controlling voltage and reactive power at the generation [62].

3. By employing enhanced phase locked loop [EPLL] as the synchronization method provides more frequency adaptivity with unbalanced or polluted signals that has noise, harmonics etc. and with variable frequency environments [63].

4. Reliability analysis and was conducted in [64] through reliability prediction metrics by evaluating reliability, failure rate, mean time to failure (MTTF), mean time to repair (MTTR) and availability. Then the improvement of reliability of the system was provided by component assessments and fault analysis which is possible in power electronic system.

Power electronic converters are used to convert energy suitable for distribution. In solar PV micro-inverter, the generated input voltage is required to be boosted to a higher voltage level for practical use [65]. Especially in module integrated PV micro-inverters. The feasibility of dispatchable converters was presented in the researches in [66] and [67]. High step-up converters [15] are required for these kind of applications.

For various applications like electric tractor locomotives or elevators, doubly fed machines are required to operate from one input source [27]. Multiple outputs also wide range applications in hybrid electric vehicles [28], LED lighting [29], dc based nano-grids [30], stand-by power supplies etc. [31], [32]. In addition to it, the setup where to loads can be operated from the same source reduce the bulkiness of the conventional converters and provide more compactness, cost effectiveness [33] and have higher efficiency [34]. A single input dual output buck converter is presented and utilization of power switches are shown in [35] and in [36], it was presented for both unidirectional and bidirectional operations.

Isolated converter is preferred over conventional one as it provides full dielectric isolation between input and output. In case of internal failure, the input voltage is prevented to be transmitted to the output. In addition to it, this type of converters protects the person handling it.

3.3 Design Requirements

From the motivation to design a novel isolated dc-dc converter, the converter was designed to meet the following specifications:

1. It has the same transfer function as the conventional one so that the output is similar.
2. The output voltages can be controlled separately with load requirement.
3. Switching and conduction losses are less than the conventional one.

3.4 Converter Design and Layout

To ensure the control of the loads separately, each primary side requires four switches in the conventional one. The upper pairs of switches connects the positive input and the lower pairs ensure the connection to ground.

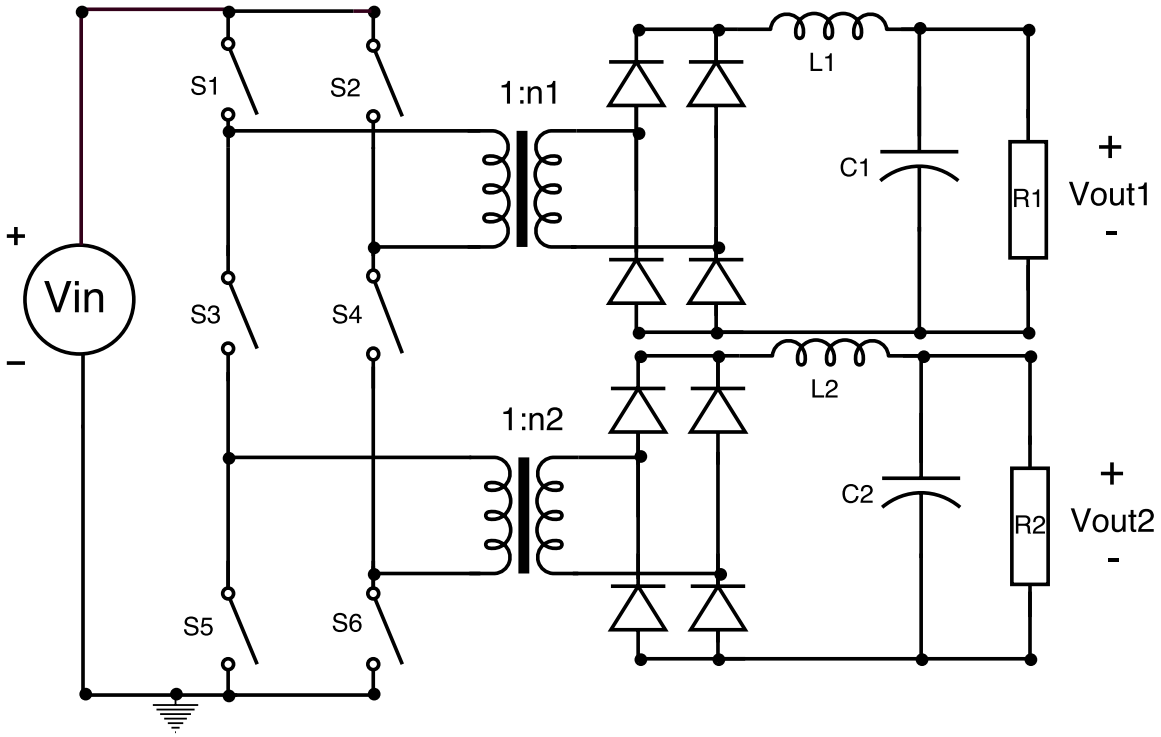

Fig. 3.1. Proposed Single Input Dual Output Dc-dc Converter

The number of switches can be reduced by using only a pair of switch in the middle for both of the loads instead of the lower pair of switches of the upper load and upper pair of switches in the lower load. The layout of the converter is shown in figure 3.1.

3.5 Switching States

The next challenge of the design procedure is finding the correct switching state for the converter to supply regulated voltage. By changing the switching states, the converter can

have serial or parallel connection for both of the loads. For six switches with two states (on and off), the converter can have $2^6 = 64$ states. By changing the states of each switch, the voltage at the primary sides are calculated for all 64 states.

Table 3.1.: All topological states

State	Q1	Q2	Q3	Q4	Q5	Q6	Vpri1	Vpri2
1	0	0	0	0	0	0	0	0
2	0	0	0	0	0	1	0	0
3	0	0	0	0	1	0	0	0
4	0	0	0	0	1	1	0	0
5	0	0	0	1	0	0	0	0
6	0	0	0	1	0	1	0	0
7	0	0	0	1	1	0	0	0
8	0	0	0	1	1	1	0	0
9	0	0	1	0	0	0	0	0
10	0	0	1	0	0	1	0	0
11	0	0	1	0	1	0	0	0
12	0	0	1	0	1	1	0	0
13	0	0	1	1	0	0	0	0
14	0	0	1	1	0	1	0	0
15	0	0	1	1	1	0	0	0
16	0	0	1	1	1	1	0	0
17	0	1	0	0	0	0	0	0
18	0	1	0	0	0	1	0	0
19	0	1	0	0	1	0	0	0
20	0	1	0	0	1	1	0	0
21	0	1	0	1	0	0	0	0
22	0	1	0	1	0	1	0	0

continued on next page

Table 3.1.: *continued*

State	Q1	Q2	Q3	Q4	Q5	Q6	Vpri1	Vpri2
23	0	1	0	1	1	0	0	-Vin
24	0	1	0	1	1	1	0	0
25	0	1	1	0	0	0	0	0
26	0	1	1	0	0	1	0	0
27	0	1	1	0	1	0	-Vin	0
28	0	1	1	0	1	1	-Vin	0
29	0	1	1	1	0	0	0	0
30	0	1	1	1	0	1	0	0
31	0	1	1	1	1	0	-Vin	-Vin
32	0	1	1	1	1	1	-Vin	0
33	1	0	0	0	0	0	0	0
34	1	0	0	0	0	1	0	0
35	1	0	0	0	1	0	0	0
36	1	0	0	0	1	1	0	0
37	1	0	0	1	0	0	0	0
38	1	0	0	1	0	1	Vin	0
39	1	0	0	1	1	0	0	0
40	1	0	0	1	1	1	Vin	0
41	1	0	1	0	0	0	0	0
42	1	0	1	0	0	1	0	Vin
43	1	0	1	0	1	0	0	0
44	1	0	1	0	1	1	0	0
45	1	0	1	1	0	0	0	0
46	1	0	1	1	0	1	Vin	Vin
47	1	0	1	1	1	0	0	0

continued on next page

Table 3.1.: *continued*

State	Q1	Q2	Q3	Q4	Q5	Q6	Vpri1	Vpri2
48	1	0	1	1	1	1	Vin	0
49	1	1	0	0	0	0	0	0
50	1	1	0	0	0	1	0	0
51	1	1	0	0	1	0	0	0
52	1	1	0	0	1	1	0	0
53	1	1	0	1	0	0	0	0
54	1	1	0	1	0	1	0	0
55	1	1	0	1	1	0	0	-Vin
56	1	1	0	1	1	1	0	0
57	1	1	1	0	0	0	0	0
58	1	1	1	0	0	1	0	Vin
59	1	1	1	0	1	0	0	0
60	1	1	1	0	1	1	0	0
61	1	1	1	1	0	0	0	0
62	1	1	1	1	0	1	Vin	0
63	1	1	1	1	1	0	0	0
64	1	1	1	1	1	1	0	0

All 64 topological states and the respective primary side voltages are shown in table 3.1.

3.6 Gating Signals

Careful consideration was made during choosing the desired states among the 64 states. There are several ways to choose the switching signals. All these ways will be discussed in this section.

3.6.1 Serially Connected Loads Operate Together

One configuration of switching signals connect the loads in series. If both loads operate at the same time then the source voltage gets divided among the primary sides voltages. None of the loads can have the primary voltage as Vdc. It is always less than Vdc and very difficult to control.

If both load1 and load2 require reduced voltage, then if the controlling duty cycle for load1 is reduced it provides reduced voltage at Vpri1. But at the same time it will force to increase the voltage at Vpri2 regardless of the decreased duty cycle of load2 controlling signal. Because from Kirchhoff's voltage law, after having a lesser voltage drop at load1, the rest of the voltage from Vdc have to drop at load2 for a balanced connection. The same difficulty will be faced in case of the need of increased voltage. If one or both of the loads have a certain limitation of input voltage, then this operation of uncontrolled load will lead to damage and may bear serious safety issues.

In addition to it, this connection fails to utilize the whole source voltage at primary side. To achieve the required voltage level at secondary sides of the transformers the turns ratios are needed to be much greater than the conventional one due to small primary voltage.

At the initial stage of this converter design, gating signals for this configuration was selected and generated using logic circuitry. Then the output was predicted by drawing equivalent circuits and calculation. The results were verified by simulation. And it possessed high risk and less efficiency for practical use as expected.

3.6.2 Serially Connected Loads Operate Separately

The previous connection had the disadvantage of not getting the whole Vdc at each of the primary sides. One way to avoid the problem can be to choose a gating signal in such a way that the loads do not operate at the same time. In that way one of the loads will have the whole input voltage at the primary side and the other will have zero. For example if the first load has zero voltage at the primary side, the second one will have +Vdc or -Vdc at the primary side and vice versa. For this state the desired states are chosen from table 3.1.

Load-1 with positive primary voltage and load-2 with zero primary voltage can be generated from switching state 38, 40, 48 or 62. Then load-1 with zero primary voltage and load-2 with positive voltage can be generated from the switching state 42 or 58. Load-1 with negative primary voltage and load-2 with zero primary voltage can be generated from switching state 27, 28 or 32. Then load-1 with zero primary voltage and load-2 with negative voltage can be generated from the switching state 23 or 56.

Table 3.2.
States Considered to Generate the Gating Signals

Q1	**Q2**	**Q3**	**Q4**	**Q5**	**Q6**	V_{Pri1}	V_{Pri2}
1	0	0	1	0	1	Vdc	0
0	1	0	1	1	0	0	Vdc
0	1	1	0	1	0	-Vdc	0
1	0	1	0	0	1	0	-Vdc

Several attempts were made with different configurations of the states. The most convenient one to implement is presented in table 3.2. The selected states to generate the gating signals are 38, 23, 27 and 42. From the table, it is observed that switching signal Q1 and Q6 are same and switching signals Q2 and Q5 are same. Also the signals Q3 and Q4 are inverse to each other.

Table 3.3.
Logic Table to Generate the Gating Signals

Q4	**Sig2**	**Q4⊕Sig2=Q2=Q5**	**!Q2=Q1=Q6**	**!Q4=Q3**
1	1	0	1	0
1	0	1	0	0
0	1	1	0	1
0	0	0	1	1

Table 3.3 presents the generation of gating signals using logic gates. Sig2 is a signal similar to Q4 but has double the frequency of Q4. These two signals can be used to generate the signal Q2 through **xor**. The signal Q1 and Q3 can be generated by simply using **not** in the signals Q2 and Q4 respectively. As mentioned before, Q5 is the same signal as Q2 and Q6 is the same signal as Q1.

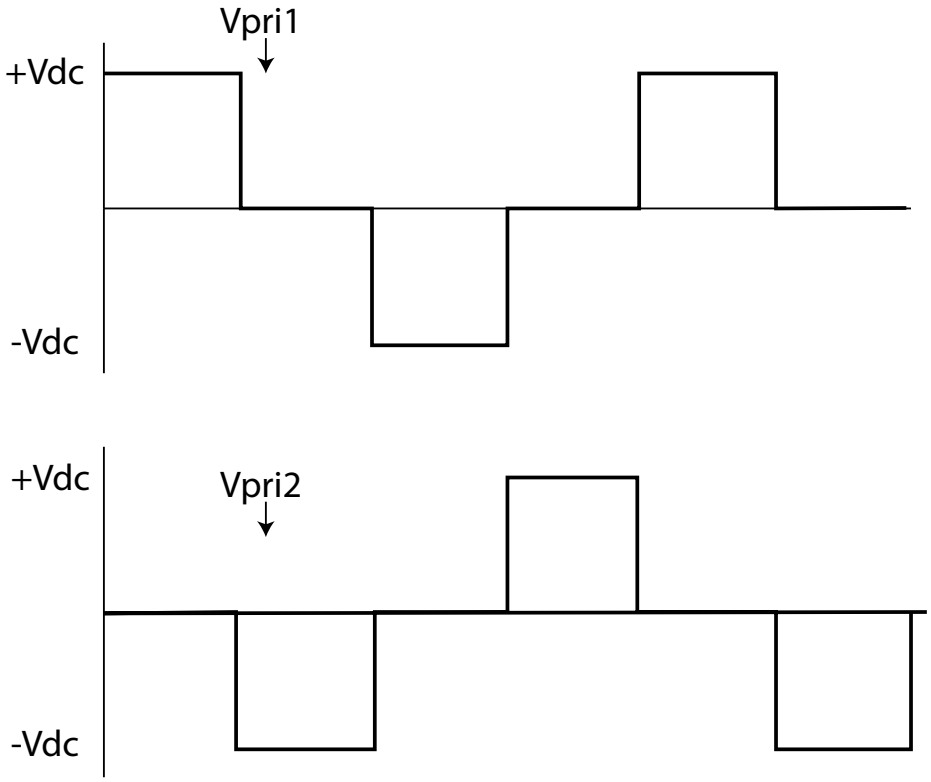

Fig. 3.2. Primary Side Voltages of the Loads for Series Connection

If the signals are implemented, the voltages at primary sides of the loads will be like the one in figure 3.2. In this case, the problem faced about having the source voltage at the primary side in the previous design was eliminated. As the loads do not operate at the same time, the input voltage is present with the whole magnitude in the primary side voltage.

If the generated input voltage is lesser than the required input voltage, then the output voltage at the loads will be less too. In that case, to reach the required voltage level, the duty cycle needs to be boosted. Figure 3.3 shows the primary sides for the loads if the duty

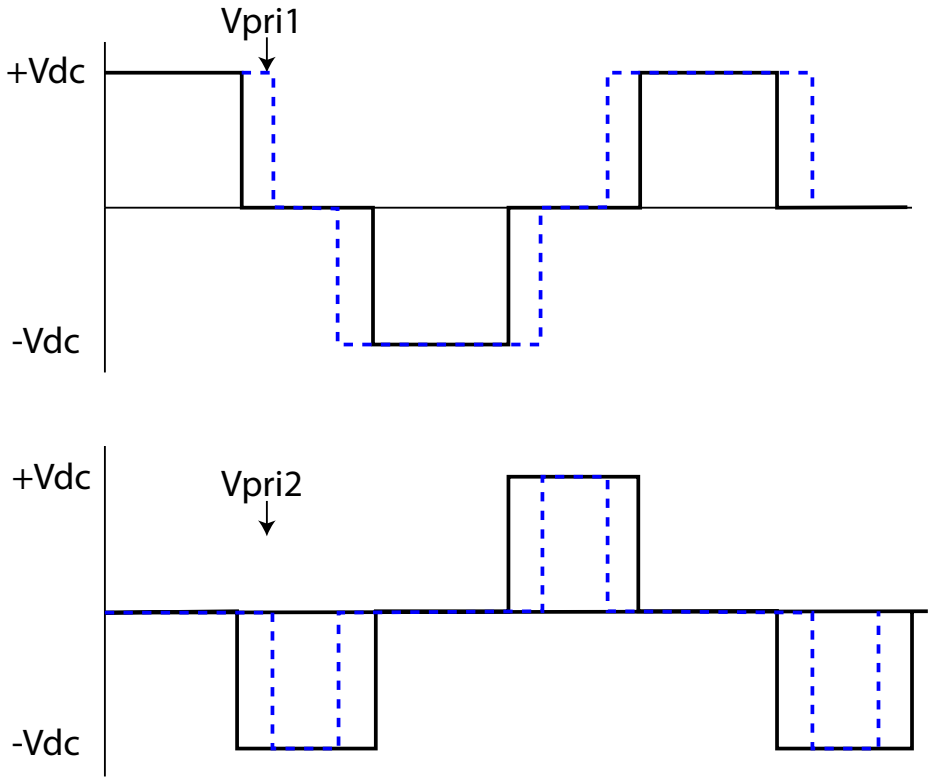

Fig. 3.3. Primary Side Voltages with Increased Duty Cycle for Load-1

cycle for load-1 in increased. From the figure, it is observed that, when the duty cycle for load-1 increases, to ensure the voltage level Vdc at the primary side for the load-1, the duty cycle for load-2 has to be decreased. If the duty cycle for load-1 is same as the before, then for a particular time, both switches that control the loads will be on. Hence the source voltage will get divided among the loads. The problem of not having Vdc as primary side voltage like the previous design will still remain. Also depending on the load condition, the voltage level will fluctuate and hence will be difficult to control. Similarly, if the duty cycle for load-2 in needed to be increased, then duty cycle for load-1 must have to decrease to ensure consistent voltage at primary sides. So this arrangement lead to either compensate one of the loads for the other or have different unwanted and unpredictable voltage levels at the primary sides. It also makes the duty cycles dependent on each other as the load that

is being compensated is forced to a smaller duty cycle to ensure larger duty cycle to the other. Similar situations are applicable when lower voltage is required.

This configuration will work great for the situations where both of the loads are complete opposite in terms of voltage requirements and are somewhat dependent on each other in increasing and decreasing load requirements.

So a decision can be made from this design that although the loads can operate with different duty cycle and hence can generate different levels of output voltage, the problem with independent control of the loads still prevalent during this connection.

3.6.3 Parallel Connection of the Load

From another combination from table 3.1, a parallel connection of the loads can be made. For parallel connection, the positive node of the source voltage is connected to the same upper or lower node of both of the loads. Similarly the ground is connected to the same upper or lower node of both of the loads.

During this configuration, both loads can operate at the same time with separate duty cycles. Figure 3.4 shows the primary side voltages of both of the loads. It can be seen that load-1 has greater duty cycle than load-2 and they are capable of operating independently.

This connection solves the problem of dependency on each load and the loads does not have to compensate for the primary side voltages. Therefore, for this design, this connection was chosen.

3.7 Selection of Gating Signal for the Proposed Converter

As discussed in the previous section, the parallel connection was chosen for this design. The states should be chosen such that the switches operate such that the loads get connected in parallel rather than in serial.

From table 3.1, during state 46 both of the loads have positive source voltage at primary sides and during state 31, they have negative source voltage at the primary side. So, these

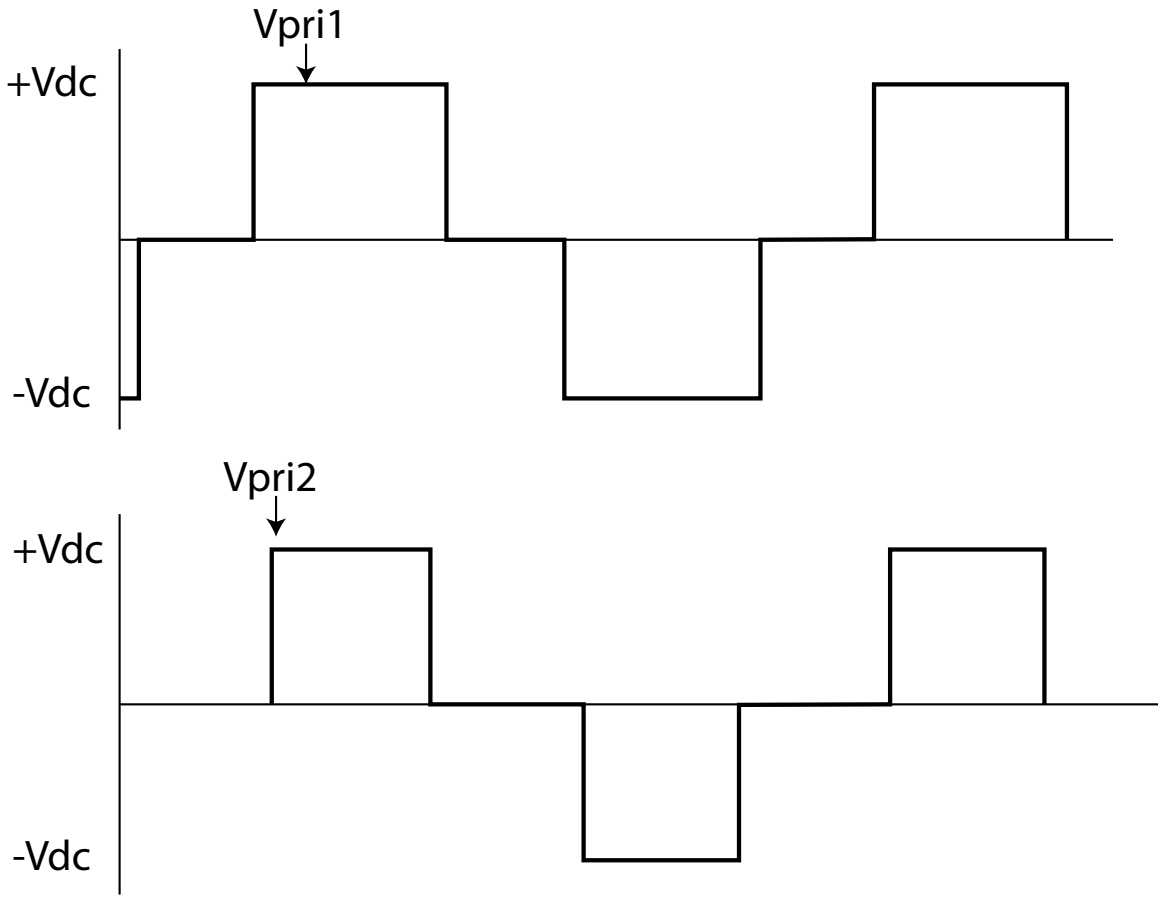

Fig. 3.4. Primary Side Voltages of the Loads for Parallel Connection

two states must be taken into consideration as they definitely ensures parallel connection of the loads.

Table 3.4 shows the desired switching states for generating the gating signals. Other two states, where the loads have zero voltage at primary sides, are chosen such that the logic circuitry to generate the switching signals is convenient. Switching signal Q1 and Q2 are simply the inverse to each other. If signal Q1 can be generated then passing Q1 through a NOT gate will generate the signal Q2.

Two signals Sig1 and Sig2 are utilized to generate the other signals similar to the one in serial connection. Sig1 is generated by comparing a triangular wave with a reference dc

Table 3.4.
Desired Switching States

Q1	**Q2**	**Q3**	**Q4**	**Q5**	**Q6**	**Vpri1**	**Vpri2**
1	0	1	1	0	1	Vdc	Vdc
0	1	0	0	1	0	0	0
0	1	1	1	1	0	-Vdc	-Vdc
1	0	0	0	0	1	0	0

voltage. Sig2 is generated in a similar fashion but from a triangular wave with double the frequency than the one used to generate Sig1.

Table 3.5.
Generation of the Switching Signals for the Switches Q1 and Q2

Sig1	**Sig2'**	**(Sig1$\bigoplus$Sig2')Q1**	**$\overline{\text{Q1}}$=Q2**
1	0	1	0
1	1	0	1
0	0	0	1
0	1	1	0

Sig2' is the inverse of Sig2. Signal Q1 can be generated by passing the signals Sig1 and Sig2' through an XOR gate. Generation of Q1 and Q2 are shown in table 3.5.

Although from table 3.4, it may seem like the signal Q3 is same as Sig2, but this signals contribute to the duty cycle for primary side voltages. So they are needed to be controlled separately.

Table 3.6 shows how the signal Q3 can be generated from Sig2 and Q2. First these signals are passed through an OR gate then an intermediate signal Sig3 is generated. From Sig2 and Sig3, signal Q3 is found.

Table 3.6.
Generation of the Switching Signals for the Switch Q3 (Initial)

Q2	**Sig2**	**(Q2|Sig2)Sig3**	**(Sig2&Sig3)Q3**
0	1	1	1
1	0	1	0
1	1	1	1
0	0	0	0

From the properties of boolean algebra [68] to expand the signals we get,

$$Q2 = \overline{Sig1.\overline{Sig2'} + \overline{Sig1}.Sig2'} \tag{3.1}$$

$$= Sig1.Sig2 + \overline{Sig1}.\overline{Sig2} \tag{3.2}$$

Using the expanded value of the signal Q1 from equation (3.2),

$$Q3 = (Sig2 + Q1).Sig2 \tag{3.3}$$

$$= (Sig2 + Sig1.Sig2 + \overline{Sig1}.\overline{Sig2}).Sig2 \tag{3.4}$$

$$= (Sig2(Sig1 + 1) + \overline{Sig1}.\overline{Sig2}).Sig2 \tag{3.5}$$

$$= (Sig2.1 + \overline{Sig1}.\overline{Sig2}).Sig2 \tag{3.6}$$

$$= (Sig2 + 0).Sig2 \tag{3.7}$$

$$Q3 = Sig2 \tag{3.8}$$

From equation (3.8), it can be seen that the signal Q3 has been reduced to a single term. Apparently it may seem that simply using the generated signal Sig2 as the switching signal at the third switch will provide the desired switching cases. But in this case, to generate the proper primary side voltages, require the switch to turn on and off for specific times depending on both of the loads. The above calculations will work only if the duty cycle for the converters are same. But in most of the practical cases they are not same and it impedes the goal of this configuration. So the signal used to control the duty cycle of the second load, Sig2'2 is used too to generate the signal.

Table 3.7.
Generation of the Switching Signals for the Switch Q3 (Final)

Q2	Sig2'2	(Sig2'2|Q2)Sig3	(Sig2&Sig3)Q3
0	1	1	1
1	0	1	0
1	1	1	1
0	0	0	0

Table 3.7 shows the ways to generate the signal for switch Q3 by using both the controlling signal for load-1 and load-2.

Although signal Q4 looks same as signal Q3 from the table, but as these switches are in the middle, they work for controlling both the upper load and lower load. So their time of operation should be different depending of load-1 and load-2. Also, in this case the signals Sig2 that controls the duty cycle for load-1 and Sig2'2 that controls the duty cycle for load-2 need while generating the switching signal for Q4.

Table 3.8 shows the generation logic for Q4. First an intermediate signal Sig4 is formed from Q2 and Sig2'2. Then from this Sig4 and Q1, another intermediate signal Sig5 is formed using OR gate. Then again from this Sig5 and Sig2, the signal Q4 is generated through an AND gate.

3.8 Switching State Diagrams

Equivalent diagrams for different states are shown in this section to show how the converter operates. The duty cycle is the time the load is on. For convenience let, to have duty cycle D1, load-1 needs to operate for Ton1 time and to have duty cycle D2, load-2 needs to operate for Ton2 time when Ts is the whole period.

State 1 For positive voltage generation at Vpri1, the switches Q1, Q4 and Q6 have to be conducting for Ton1. During this state, switch Q3 conducts for Ton2 time. Only the

Table 3.8.
Generation of the Switching Signals for the Switch Q4

Q2	Sig2'2	(Q2(AND)Sig2'2)Sig4
0	1	0
1	0	0
1	1	1
0	0	0

Q1	(Sig4(OR)Q1)Sig5	(Sig5(AND)Sig2)Q4
1	1	1
0	0	0
0	1	1
1	1	0

switch Q3 during this time ensures connection of load-2. During Ton2, load 2 has positive voltage on the primary and secondary sides.

This situation is shown in figure 3.5. The parallel connection of the loads ensure positive voltage at both of the primary sides. As can be seen from the figure that when both of the loads are operating, switch S1 and S3 are connected to the same node +Vin and the switches S4 and S6 are connected to the same ground node.

State 2 Zero voltage can be generated by following several configurations. For this particular configuration, only switches Q2 and Q5 are conducting. As no path is fulfilled, no current flows and the source get disconnected from the load. Hence it results zero voltage. The equivalent circuit without any path to flow current is shown in figure 3.6.

As the switching signals are generated separately, it needs to be ensured that switches Q3 and Q4 are open for (Ts-Ton1) time, so that they don't create any path for current

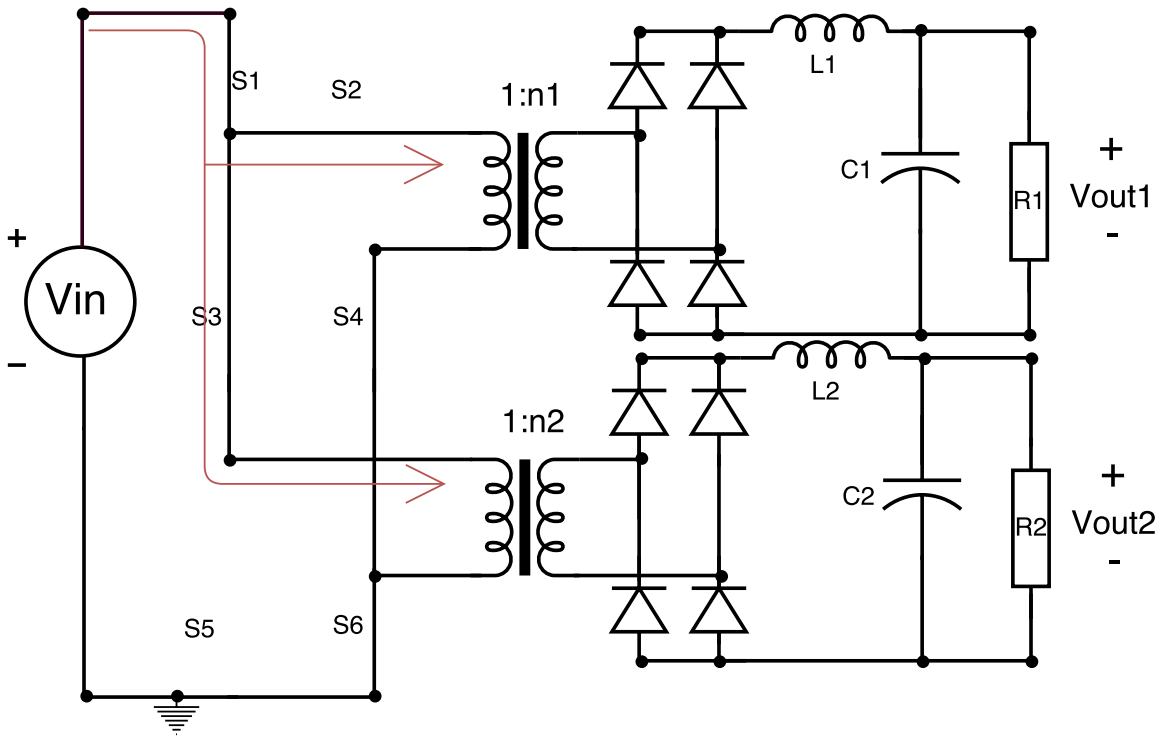

Fig. 3.5. Equivalent Circuit for the First State

flow and result in unwanted voltage at the loads. The switching signals at Q3 and Q4 have to follow Q1 at this stage.

State 3 For negative voltage generation, pulses at switches Q2, Q3 and Q5 controls load1. During this time, pulse for Ton2 time at switch Q4, controls operation of load2.

Figure 3.7 shows the equivalent circuit and the direction of current flow during this state. During this state, the switches S3 and S5 are connected to the ground when operate and switches S2, S4 and S6 are connected to the same node as +Vin when operate. So the voltages at primary sides of the loads are

$$0 - (+Vin) = -Vin$$

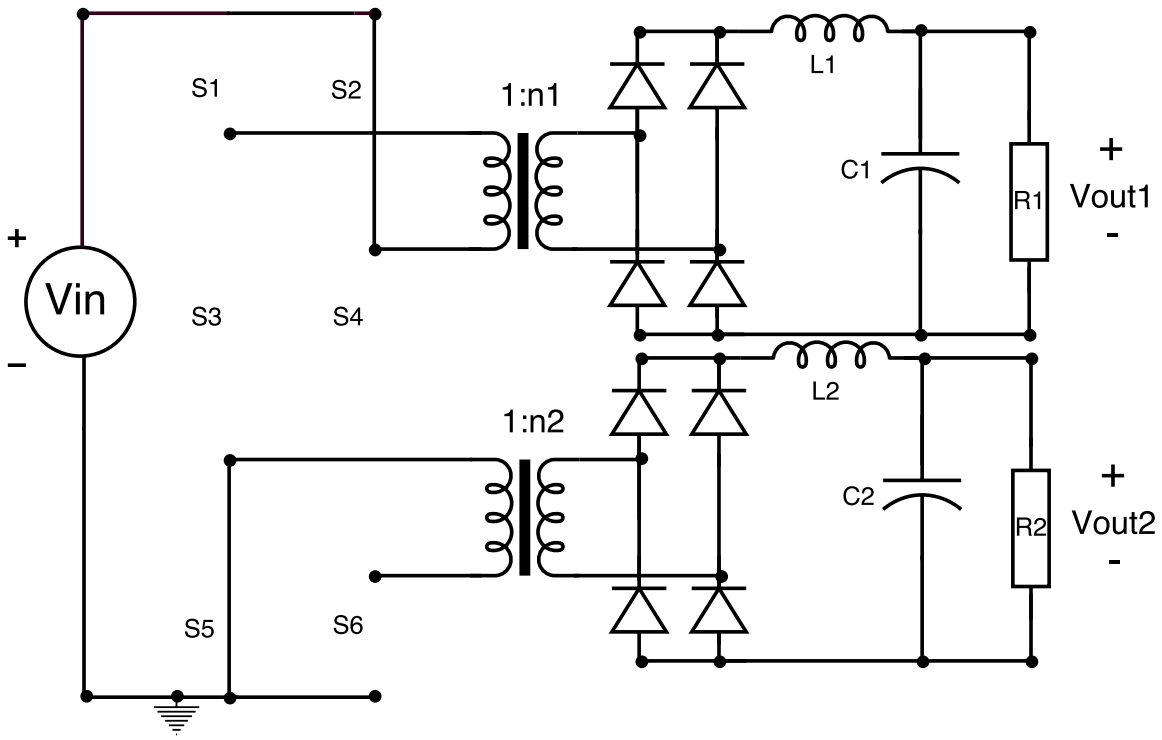

Fig. 3.6. Equivalent Circuit for the Second State

Thus both of loads have negative voltage at primary sides and the operating time of Q4 ensures the duty cycle for load-2.

State 4 This state is similar to state-2. Switches Q1 and Q6 are closed without making any circuit path. All other switches have to stay open for the same amount of time as these switches are operating. They need to follow the signal at Q2 for this stage.

Figure 3.8 shows the equivalent circuit for this state. No path is made for the flow of current.

3.9 Switching Signal Circuitry

While generating switching signals, a triangular wave is compared with the reference voltage. Another triangular wave is required to control the loads which is of twice the

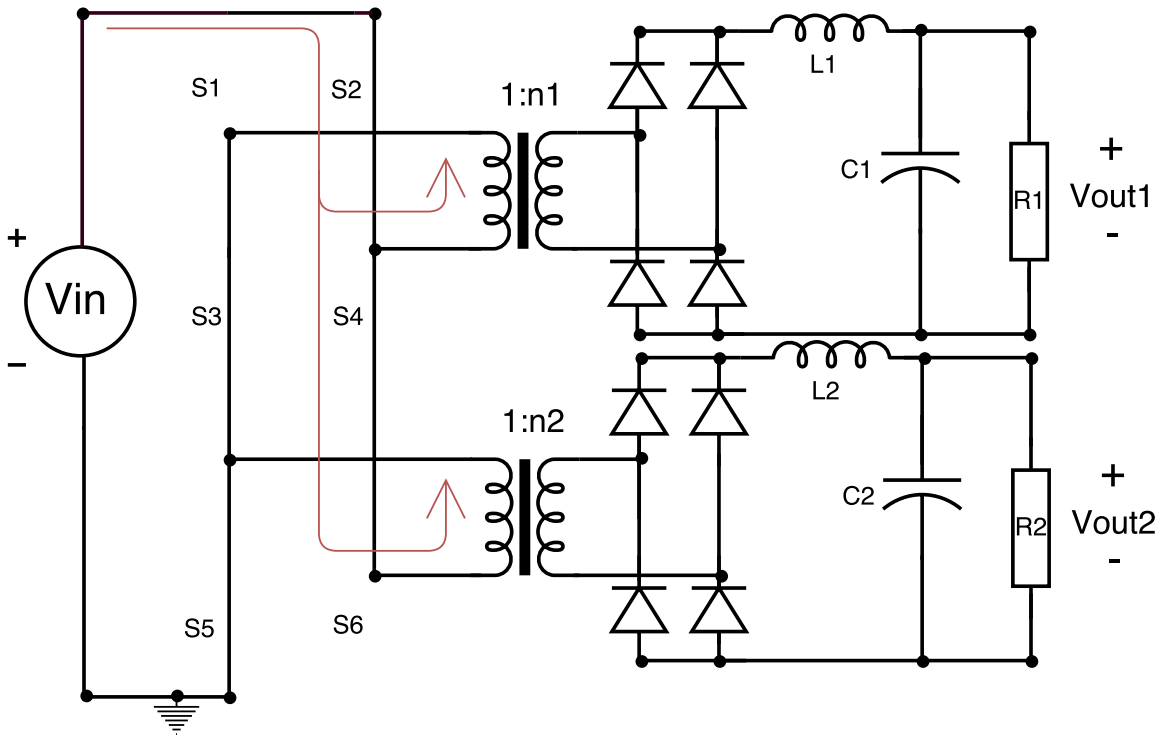

Fig. 3.7. Equivalent Circuit for the Third State

switching frequency. For output1, the duty cycle can vary up to the maximum, which is 1. But output2 can reach the duty cycle equal to D1. The reference voltage can vary according to the output voltage considering the range.

Figure 3.9 shows the all six switching signals of this converter. In this figure Q1 to Q2 are the switching signals for the switches S1 to S6 respectively.

The first switch has the pulse equal to the defined duty cycle for load-1. The signal at the second switch is just inverse to switch-1. In other others, it has a zero value or it is off for the same time as switch-1 is on that is the defined duty cycle for load-1. The signals at the third and fourth switch are a little complicated. The first part of the signal at the third switch operates for the required duty cycle at load-2. It requires keeping the zero value apart from the required operating time. After that instead of repeating the first part again, the signal follows the signal at the second switch for the rest of the time period. The signal

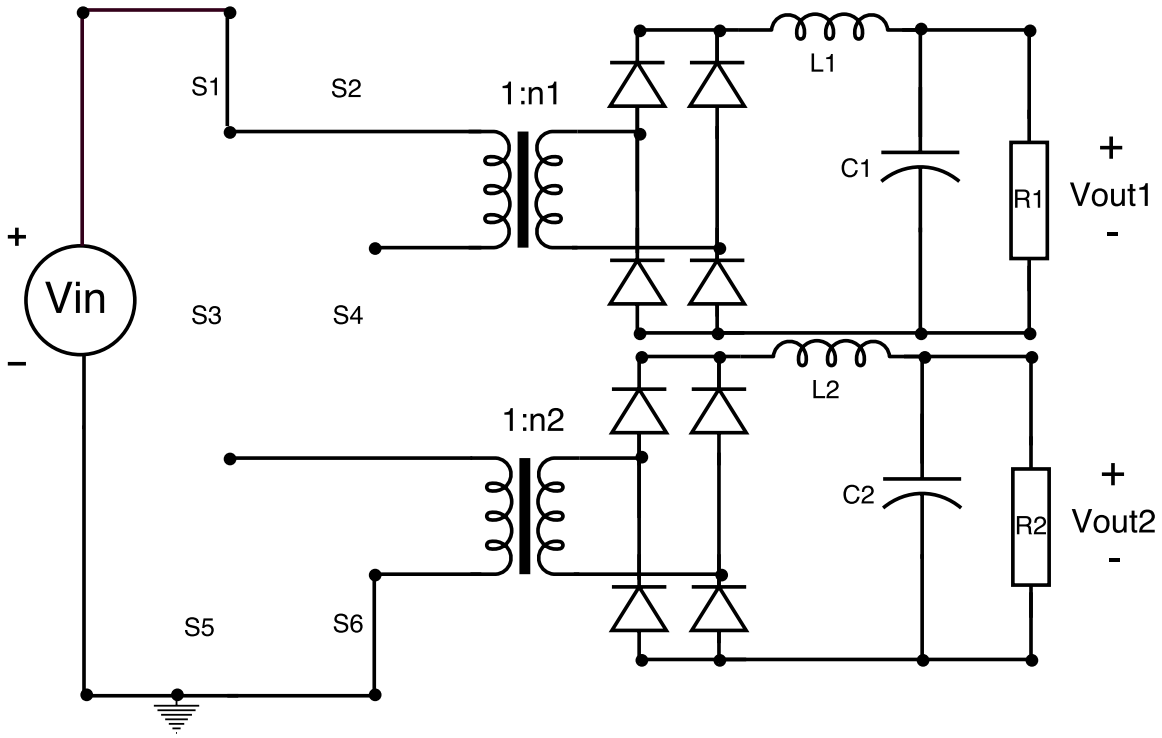

Fig. 3.8. Equivalent Circuit for the Fourth State

at the fourth switch, follows the signal at first switch for the first part. Then it operated for the duty cycle for load-2. The signals at switch-5 is same as the second signal and the signal at switch-6 is same as the first switching signal.

Figure 3.10 shows the gating signal circuitry that generates the switching signals. In the figure, the labels Sig1, Sig2, Sig3 and Sig4 refers to the switching signals at first four switches. As the signals Q5 and Q6 are same as the signals Q2 and Q1 respectively, they were not generated separately using other gating circuits.

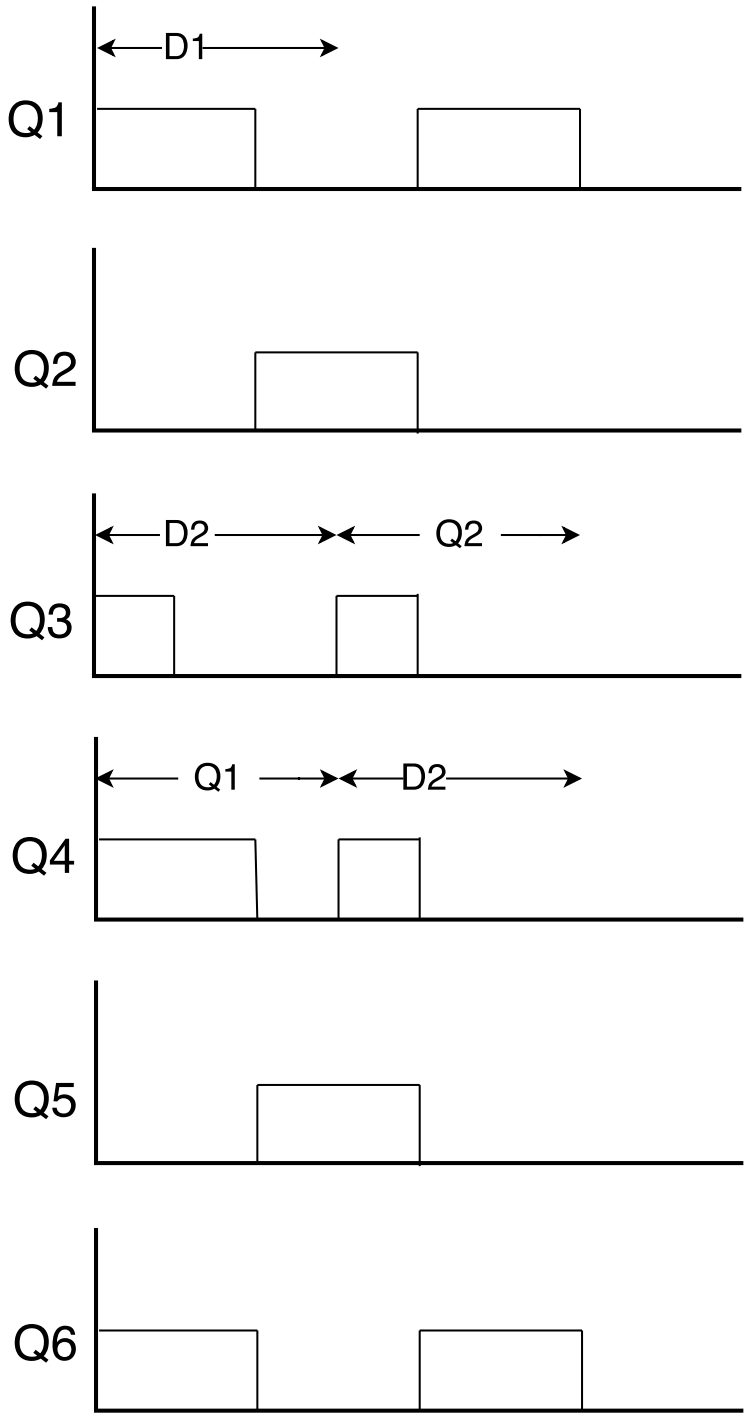

Fig. 3.9. All Six Switching Signals

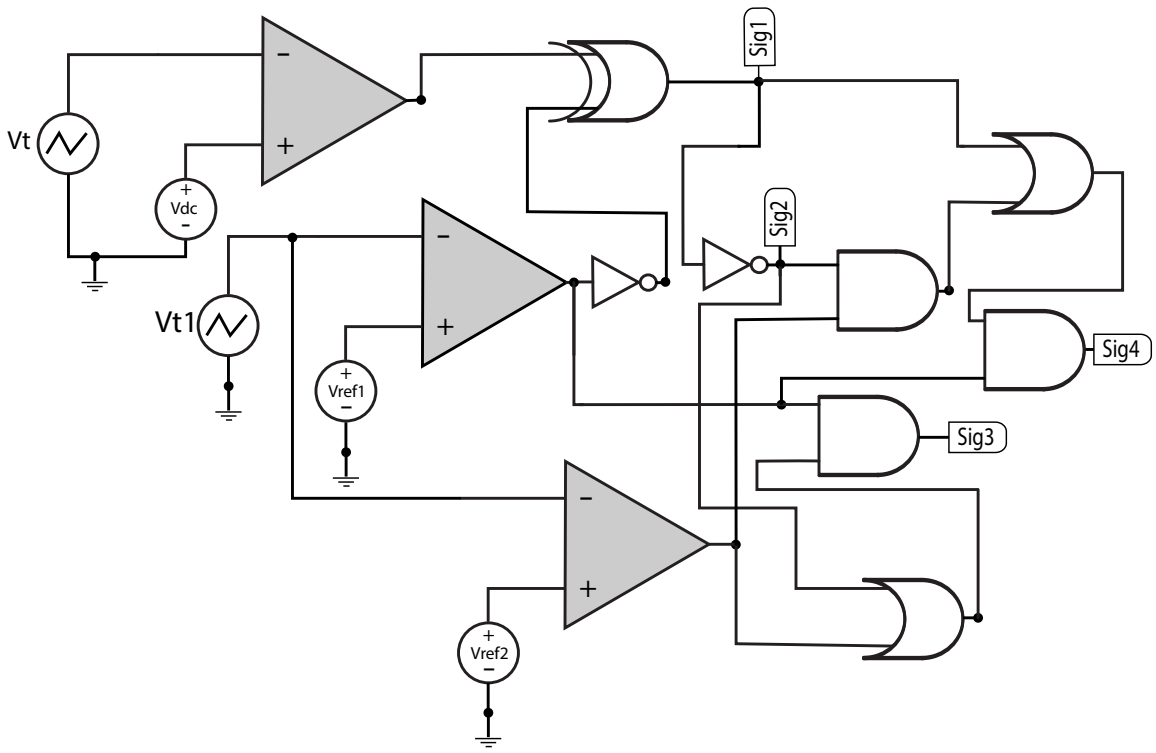

Fig. 3.10. Circuitry to Generate Gating Signals

3.10 Steady State Analysis

If the turns ratios of the high frequency transformers are n1 for output1 and n2 for output2, then as the voltage of the secondary side is turns ratio times the voltage of the primary side,

$$Vsec1 = n1 * Vpri1$$

$$Vsec2 = n2 * Vpri2$$

For state 1, the switches Q1, Q4 and Q6 are closed for the time $Ton1$ which controls output1. The switch Q3 is conducting for $Ton2$ time, that controls output2. Here, $Ton2 \leq Ton1$.

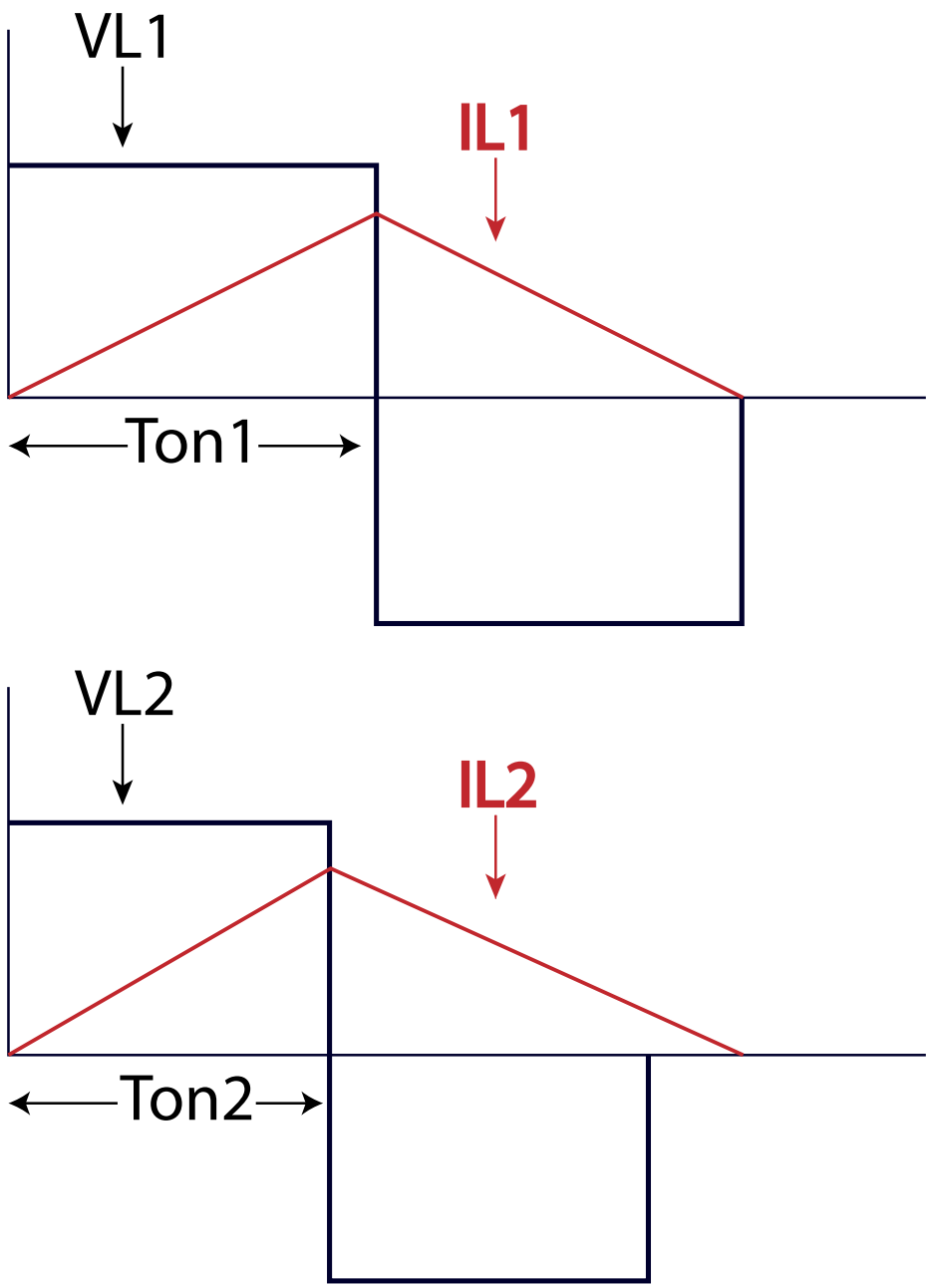

Fig. 3.11. Inductor Voltages and Currents for Output1 and Output2

The inductors have an integral voltage of zero over a period. From figure 3.11.

$$Ton1 * (nVpri1 - Vout1) = (Ts - Ton1) * (-Vout1)$$

$$or, Ton1 * (nVpri1 - Vout1) = (Ts - Ton1) * Vout1$$

$$\frac{Vout1}{Vpri1} = \frac{Ton1}{Ts} * n1$$

Here, $\frac{Ton1}{Ts} = D1$ which is the duty cycle for the switching signal. Also, $|Vpri1| = |Vin|$ The calculation is same for the second load. So, the transfer functions for the loads are:

$$\frac{Vout1}{Vpri1} = n1 * D1 \tag{3.9}$$

$$\frac{Vout2}{Vpri2} = n2 * D2 \tag{3.10}$$

As, $Ton2 \leq Ton1$, $D2 \leq D1$. The second load is controlled independently, but the maximum duty cycle it can have will be equal to the duty cycle of the first load.
It can be seen by comparing equations (3.9) and (3.10) with equations (2.2) and (2.3), the transfer function of the proposed design matches the conventional one.

3.11 Feedback Control System

A control system is an interconnection of components forming a system to provide desired system response. The use of a signal, that is proportional to the error between desired and actual response, to control the process results in a closed loop sequence of operations. This is called a feedback system [69]. Most power electronic system rely on feedback control system. Figure 3.12 shows a basic feedback control system for the converter.

While designing the feedback controller to regulate the output voltage, the following objectives are taken into consideration [70]:

- Zero steady state error
- Fast response to changes in the input voltage and the output load

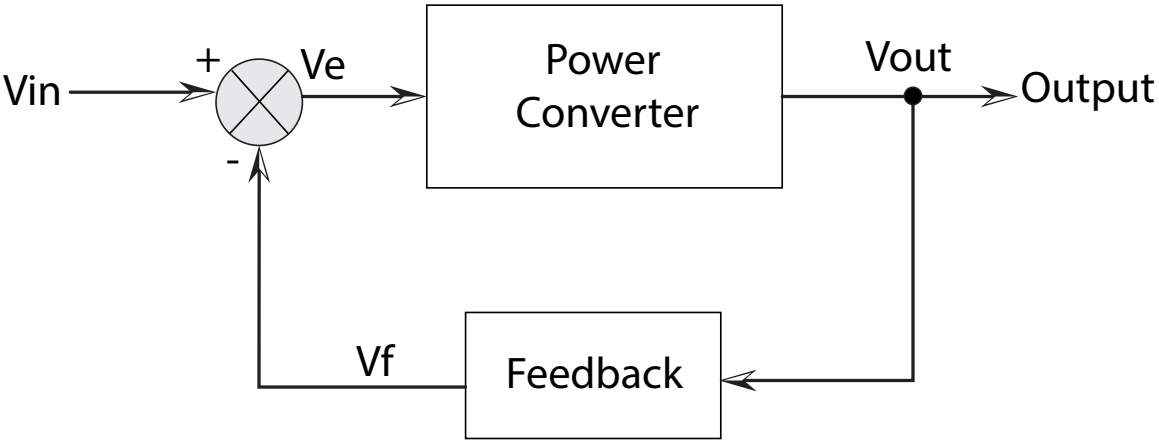

Fig. 3.12. Basic Feedback Control System for the Converter

- Low overshoot
- Low noise susceptibility

The feedback control system [71] in figure 3.13, the output voltage Vout is measured and compared with a reference value Vout*. The difference between these two signals is called the error and it acts on the controller.

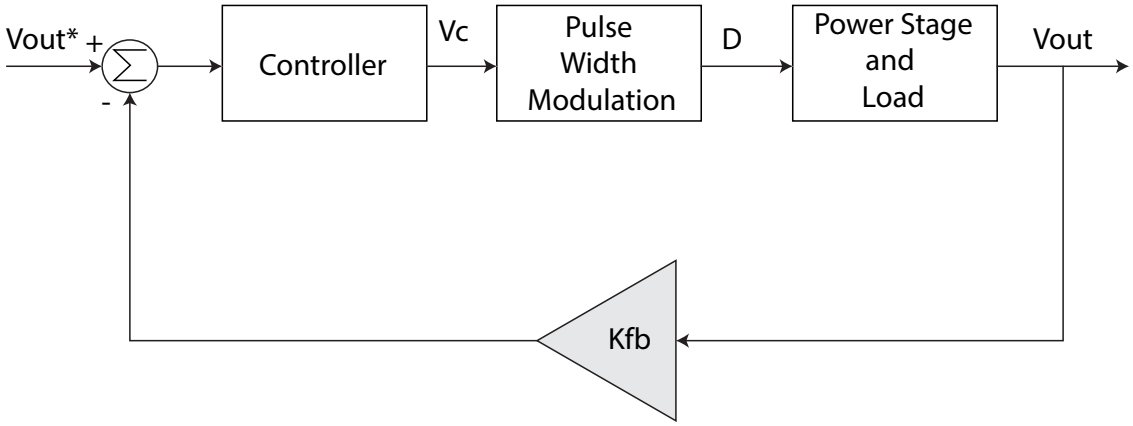

Fig. 3.13. Feedback Control System for the Converter

The voltage produced by the controller is Vc(t). This control voltage is the input to the pulse-width modulator that produces a switching signal. The average value of that signal is d(t). The duty cycle is D. Linearizing around the steady state operating point, small-signal perturbations are assumed. The equations are shown below:

$$\overline{Vout}(t) = Vout + V\tilde{o}ut(t) \tag{3.11}$$

$$d(t) = D + \tilde{d}(t) \tag{3.12}$$

$$Vc(t) = Vc + \tilde{V}c(t) \tag{3.13}$$

The average value of the output voltage including the small-signal perturbation would be like the one in equation (3.11). As mentioned earlier, d(t) is the average value. There is no switching frequency component present in Vc(t).

From figure 3.13, the feedback gain is Kfb. The transfer function of the voltage-sensing networks can be represented by this gain. This gain is usually less than unity.

This feedback control system is integrated with the designed converter to regulate the output voltage within the specified tolerance band in order to ensure uninterrupted power supply for the machines.

4. RESULTS OBTAINED FROM THE PROPOSED DC-DC CONVERTER

4.1 Introduction

Any design that meet the requirements theoretically is needed to be tested to ensure that the design works for real-life situations. The converter designed in the previous chapter was drawn and simulated to guarantee the feasibility of the design.

In this chapter, the results obtained from the simulations are discussed and verified for different conditions. Switching and conduction losses are obtained and calculated for both of the converters. The comparative analyses are also presented in this chapter.

Electronic circuit simulation software package PSIM was used to simulate the designed converter. PSIM has different modules are very useful in power electronic design and can be easily implemented and integrated with other popular platforms, such as TI kits, JMAG, Modelsim, and Simulink [72].

4.2 Circuit Diagrams to Simulate Proposed Dc-dc Converter

While implementing the design initially, the ideal MOSFETs were used in the schematic. From the menu bar in PSIM, ”Elements” was clicked. Then from the drop down menu, Power → Switches → MOSFET was selected to and placed six times in two columns as the switches of the converter. The source in a dc voltage and so Elements → Sources → Voltage → DC was selected as the input dc voltage. The values of the components are given by double clicking of the elements and entering the magnitudes. The other components are selected from the Elements → Power module. From the module, the resistors, capacitors and inductors are placed from ”RLC Branches”. There is a subsection named

”Transformers” in the ”Power” module. The transformers are selected from that subsection. The diodes here are placed from the ”Switches” subsection.

After the placement of the elements in their convenient positions, they are connected through wires. The ground was connected at the bottom of the diagram for proper current flow through the circuit. Connecting the gating signals to the diagrams by wires can make the diagram complicated and cumbersome as it contains different logic gates and there are chances of wrong connections and misplaced nodes. For that reason, the gating signal circuitry was placed separately and the labels were used to provide signal inputs in the switches. The switches cannot be connected to the labels through wires or placing close to it. An additional element is required between the switch and the signal. Elements → Other → Switch Controllers → On-Off Controller was selected and placed between all switches and their corresponding signal labels.

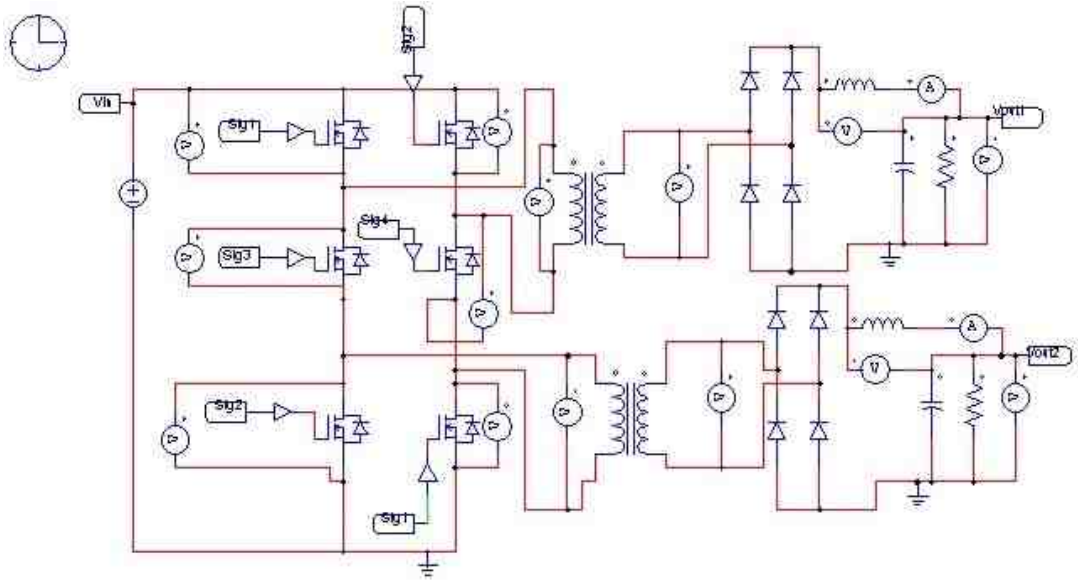

Fig. 4.1. Diagram in PSIM to Simulate the Designed Converter

Figure 4.1 is the diagram drawn on PSIM. For the primary stage of the simulation, ideal MOSFETs were used as switches for simplicity. After successful evaluation of the design, practical switches are employed in stead of the ideal ones.

The MOSFET switches are an active switch with an anti-parallel diode. It is turned on when the gating signal is a logic high and the switch is positively biased (drain-source voltage is positive).Whenever the gating signal is low or the current drops to zero it turns off.

For the gating circuit, the logic gates are selected from Elements → Control → Logic Elements. The Op-Amps are found in the ”Other” subsection of the ”Power” module.

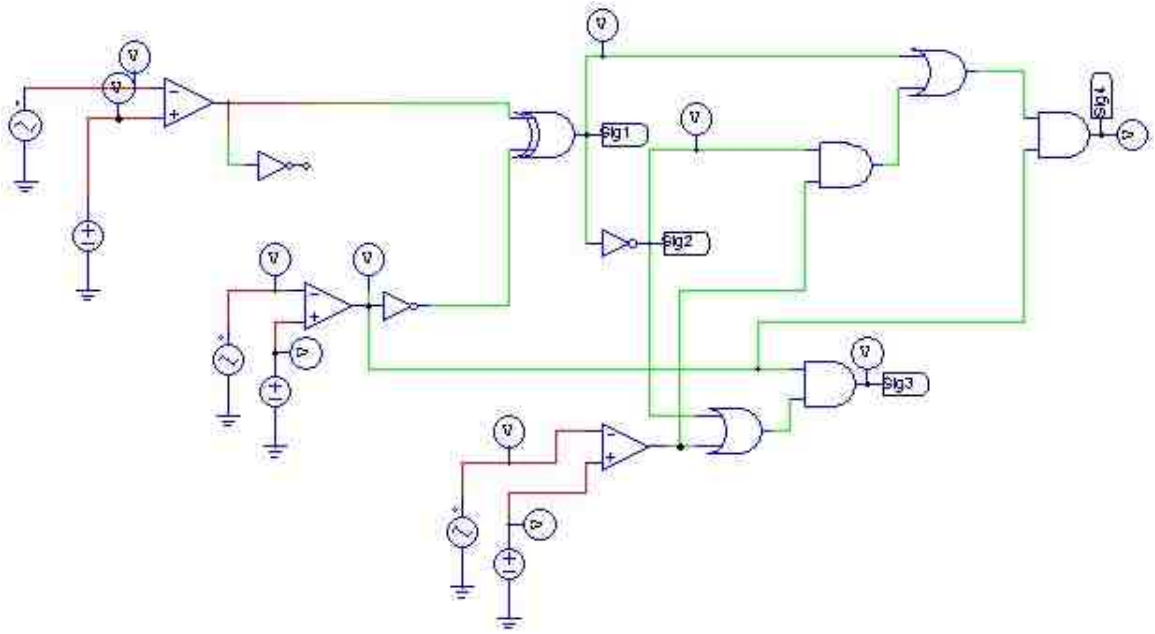

Fig. 4.2. Gating Circuitry to Generate the Switching Signals

Figure 4.2 is the gating circuitry in PSIM that generate the switching signals. Four signals were generated here as signals Sig1 and Sig2 were used as the switching signals for the sixth and fifth switches respectively apart from the first and second switches. The labels are placed in the parts where the desired signals are generated.

As mentioned before, while connecting these labels as the gating signals to the switches, the ”On-Off Controllers” are required. On-off switch controller works as the interface between the control gating signals and the power switches. The switches are controlled by the gating signal which are the input logic signal generated from the control circuit is passed to the power circuit [73]. The ”On-Off Controllers” are placed between the signal labels and the power switches.

4.3 Results From Simulation

After all the circuits are completed, from the menu bar ”Simulation” is clicked and from the drop down menu, ”Simulation Control” is selected. Then the cursor changes into a clock symbol. This clock is placed at a side on the schematic. The properties like time step, total time etc. can be changed by double clicking on the symbol.

Table 4.1.
Parameters of Simulation Control

Parameters	**Value**
Time step	4E-006
Total time	4
Print time	1
Print step	1

The parameters that are included in ”Simulation Control” are shown in table 4.1. Other parameters are left as it was. Then the simulation is run by selecting ”Run Simulation” from ”Simulation” menu. After the simulation is completed, ”Run SIMVIEW” is selected from the same menu to launch the waveform display program. Then by selecting the waveforms of the previously placed probes, the waveforms are displayed.

The required switching signals found from the simulation are shown in figure 4.3. Note that these switching signals are similar to the expected switching signals.

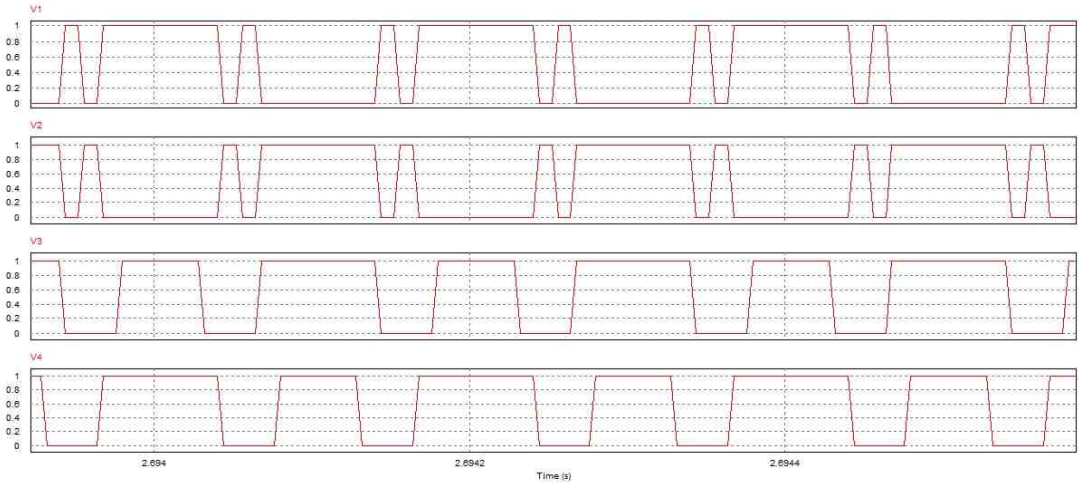

Fig. 4.3. Four Switching Signals Generated to Control the Voltage at Primary Side

Load-1 was given a reference voltage of 0.8 magnitude and Load-2 was given a reference voltage of 0.5 magnitude during this simulation. So the duty cycle for load-1 (the upper load) is 0.8 and the duty cycle for load-2 (the lower load) is 0.5 as the magnitude of the triangular voltage was 1.

Figure 4.4 shows the voltages at primary sides according to the given duty cycles.

For this simulation, the input voltage is set as 40 volts. The turns ratios of the transformers are given as 1:2 for both of the loads. The output voltages of both of the loads found from this simulation are shown in figure 4.5. Apparently, the output voltage of load-1 is higher than the output voltage of load-2.

4.4 Calculations

From the transfer function of the converter, the output voltages can be calculated. Equation (3.9) in chapter 3 of this thesis gives the transfer function of load-1 of the converter and equation (3.10) gives the transfer function of load-1 of the converter.

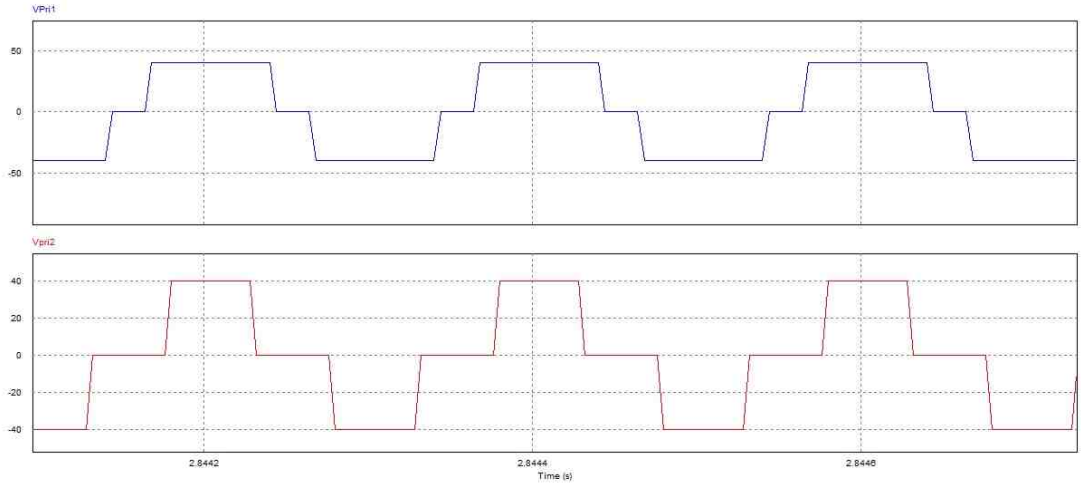

Fig. 4.4. Primary Side Voltages [Upper one with 0.8 duty cycle and lower one with 0.5 duty cycle]

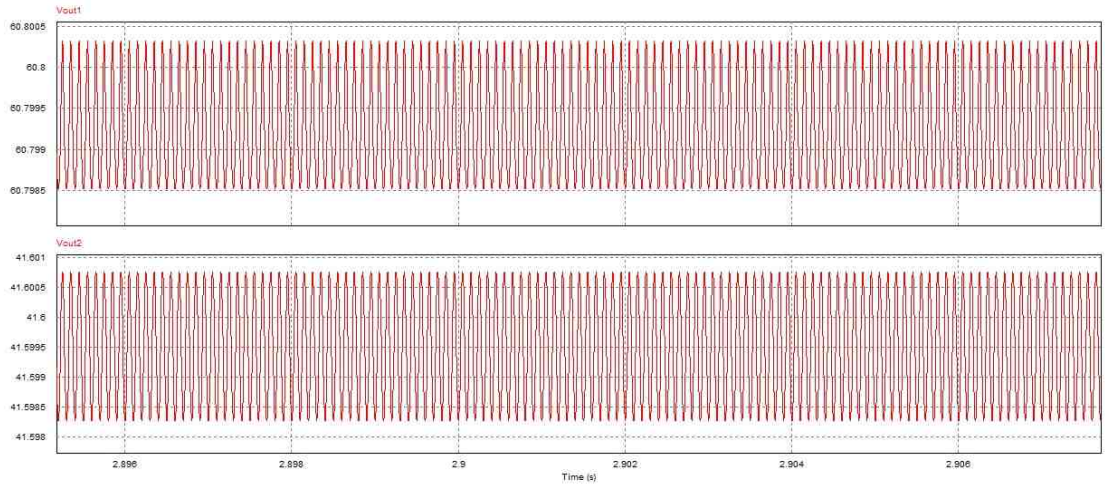

Fig. 4.5. Output Voltages of Load-1 and Load-2

From figure 4.5, the output voltage for load-1 is approximately 61 volts and the output voltage for load-2 is approximately 41.6 volts.

For load-1, the output voltage calculated for this case is,

$$Vout1 = n1 * D1 * Vpri1 \tag{4.1}$$

$$= 2 * 0.8 * 40V \tag{4.2}$$

$$Vout1 = 64 \tag{4.3}$$

For load-2, the output voltage calculated for this case is,

$$Vout2 = n2 * D2 * Vpri2 \tag{4.4}$$

$$= 2 * 0.5 * 40V \tag{4.5}$$

$$Vout2 = 40 \tag{4.6}$$

Both equation (4.3) and (4.6) match the simulated output results in figure 4.5

4.5 Special Condition

The designed converter works for any duty cycle for both of the loads independently but the maximum duty cycle for load-2 is limited to the duty cycle of load-1 at that point. For this case, the duty cycle for load-1 was given as 0.5 and for load-2, it was 0.8. Figure 4.6 shows that although the duty cycle for load-2 should be greater than that of load-1, the active duty cycle for both of the loads are 0.5. It is clearly evident that the duty cycle of load-1 is limiting the duty cycle of load-2.

It is also evident from the output voltages shown in figure 4.7 that the output voltages are same although as per the transfer function equation, the lower load is supposed to generate higher voltage.

This is the drawback of the designed converter that although the loads can be controlled separately, the voltage range of one of the loads is always defined by the other one.

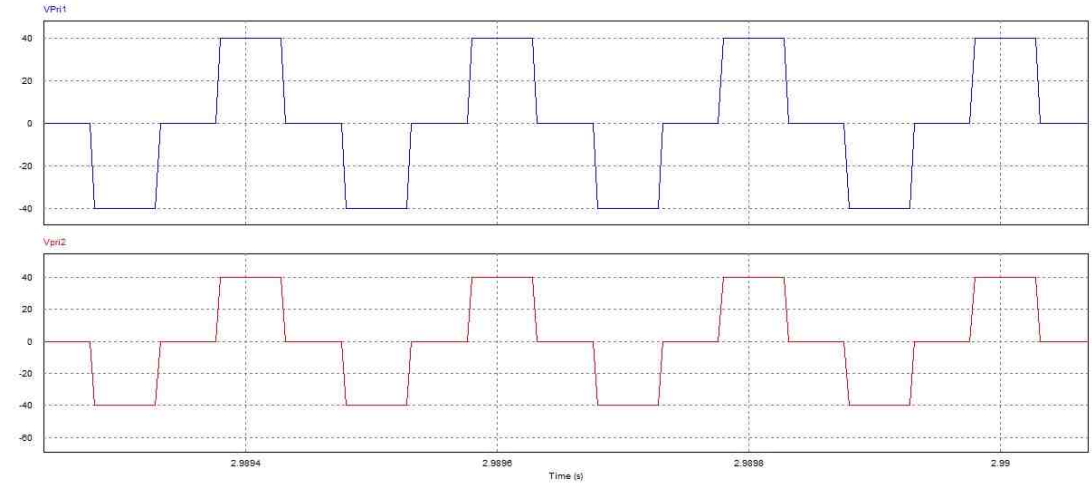

Fig. 4.6. Primary Side Voltages [Upper one with 0.5 duty cycle and lower one with 0.8 duty cycle]

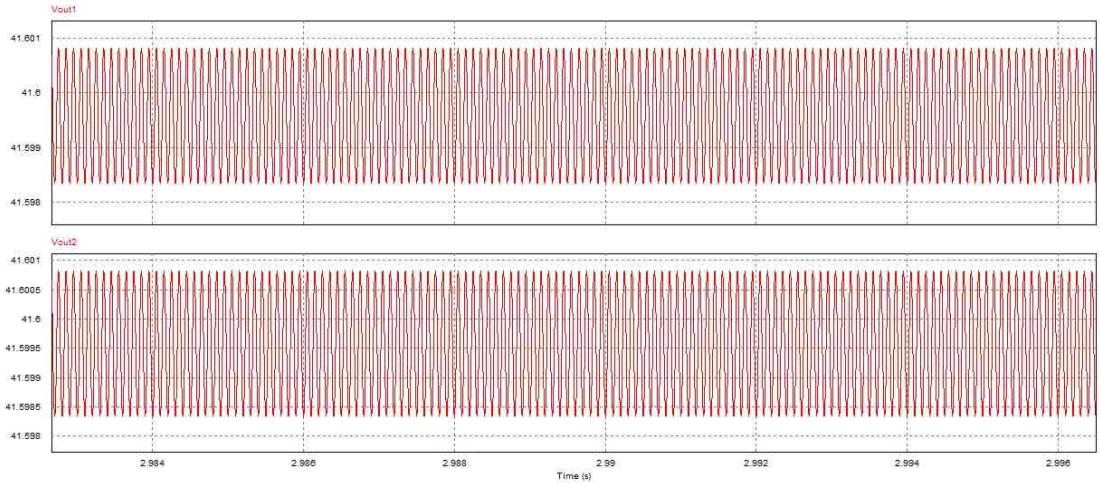

Fig. 4.7. Output Voltages of Load-1 and Load-2 [Upper one with 0.5 duty cycle and lower one with 0.8 duty cycle]

4.6 Comparison with The Conventional Converter

4.6.1 Generation of Output Voltage

In practical use of dc-dc converter, the input voltage can fluctuate. Especially in applications of renewable energy, the dependency on the environment,weather and location is huge and so the generation of power can vary a lot [74]. In that case, the voltage needs to be regulated. For example, if the input voltage reduces, then the generated output voltage will be less to. So the duty cycle needs to be increased to meet the power requirement. With a closed loop feedback control system it can be easily done.

By changing the input voltage, output voltage was generated for similar condition in conventional and the designed converter. The result is presented in table 4.2.

Table 4.2.
Output Voltage of Conventional and Proposed Converter with Changing Input Voltage

Vin	**Vout1,Conv**	**Vout2,Conv**	**Vout1,Proposed**	**Vout2,Proposed**
40V	176.7	124.7	176.7	124.7
35V	154	109	154	109
30V	152	107	151	107
20V	118	83	118	84

It is evident from table 4.2 that the proposed converter generated similar voltages as the conventional one with different input voltages.

So the proposed dc-dc converter is able to meet the requirement just like the conventional one but with increased efficiency to operate with reduced number of switches.

4.6.2 Power Loss

The previous simulations were conducted using ideal power switches. To calculate the switching and conduction loss of practical switches, the conventional and proposed converters were simulated to calculate power loss in both of them.

The switch used for these designs is the MOSFET IRF1010EZ by Infineon technologies. This MOSFET has the following features that makes it suitable for this converter operations [75]:

- Utilizes the advanced process technology
- It can process ultra low on-resistance per silicon area
- Junction operating temperature of 175°C
- Fast switching speed
- Improved repetitive avalanche rating up to the maximum junction temperature
- Lead-free, RoHS Compliant
- Extremely efficient and reliable for use in automotive and other applications

In PSIM, there is a ”Thermal Module” in the ”Power” section of the menu ”Elements”. The losses of the semiconductor devices can be estimated by the thermal module. The device can be chosen from the library or added manually. It was made sure that the properties matches with the ones provided in the data-sheet.

In PSIM menu bar, the ”Utilities” is clicked. Then from the drop down menu ”Device Database Editor” is selected. Then in the ”PcdEditor” window, the MOSFET IR1010EZ is selected to see the device properties. As can be seen in figure 4.8, discrete (n channel) package is selected. The transistor and diode properties are entered according to data-sheet.

Figure 4.9 shows the diode characteristic curve when clicked on the ”Edit” button beside ”Vd vs IF” under the section **Electrical Characteristics-Diode** in the same editor

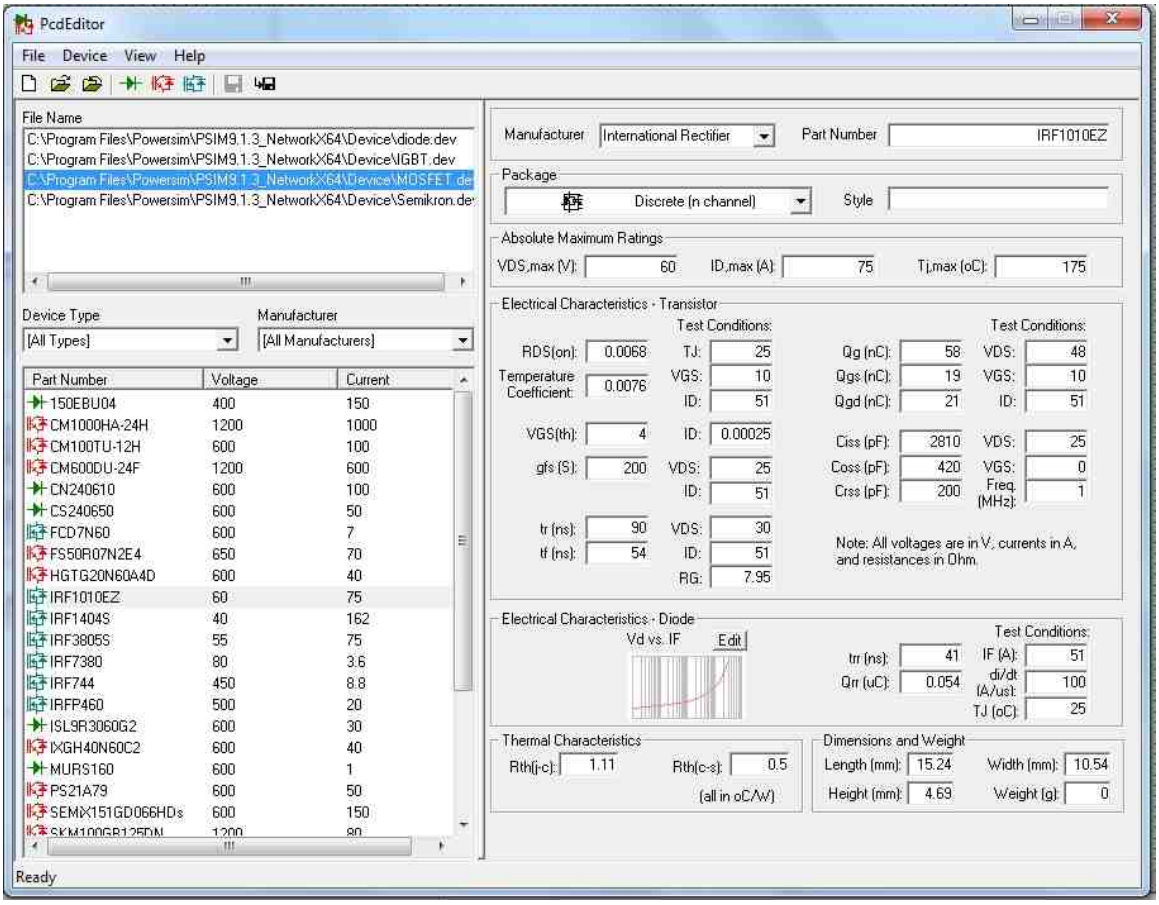

Fig. 4.8. MOSFET Properties in the PcdEditor Window in PSIM

window. The curve can be edited or added by clicking on the ”Add Curve” button. Proper changes can be made by redrawing by selecting points on the curve. After the characteristics of the device is saved, it can be selected from the device browser instead of the ideal MOSFET switch used before.

Then the power losses are calculated. When the same device is placed in the conventional design and simulated, the power loss in the conventional configuration is found. Figure 4.10 shows the circuit diagram to calculate the power losses in the conventional converter. The MOSFETs from the thermal module have four extra nodes besides the usual terminal nodes. The nodes from top to bottom are for transistor conductor losses (the node

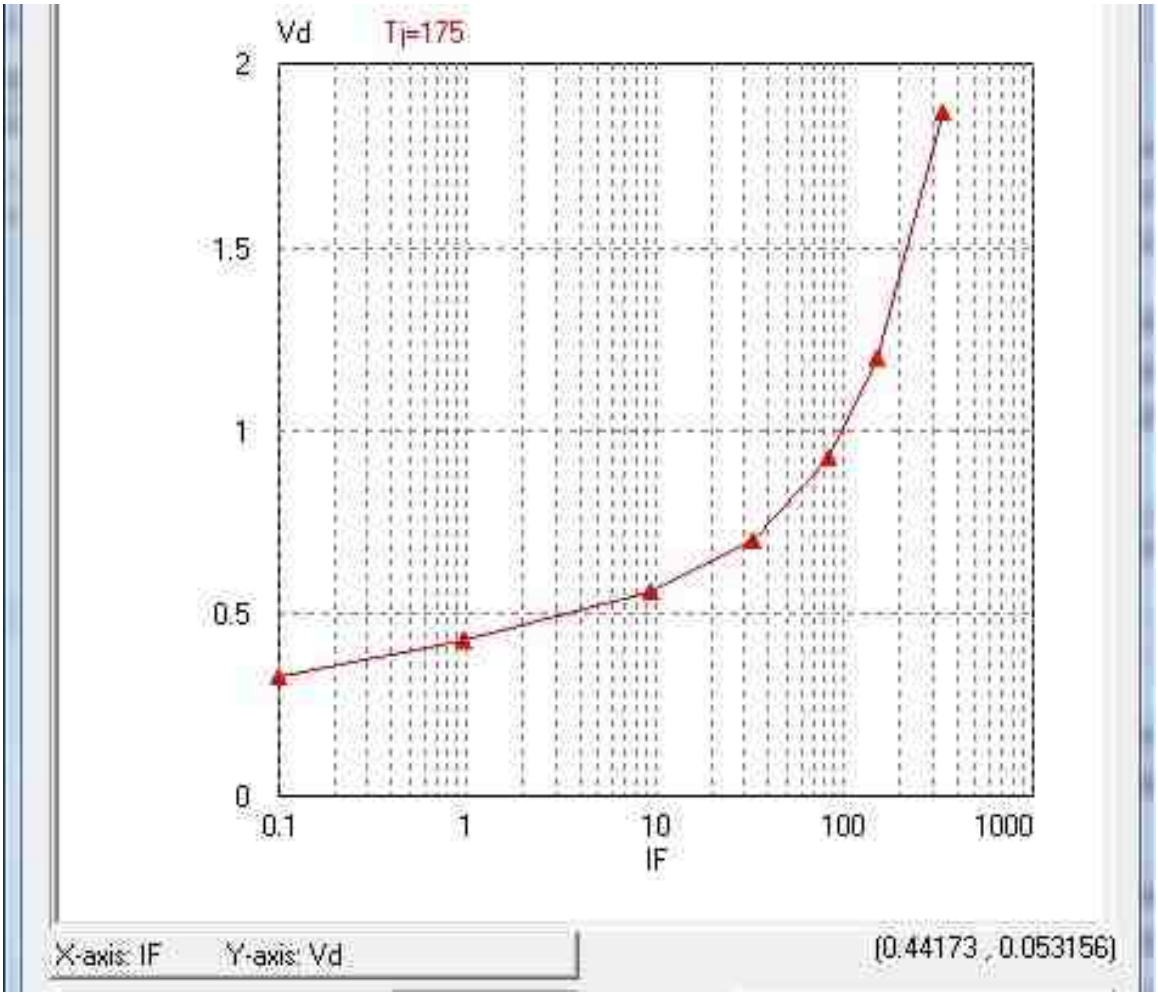

Fig. 4.9. Diode Voltage Drop vs Diode Forward Current of the Switch

with a circle), for transistor switching losses, for diode conductor losses (the node with a square), and for diode switching losses respectively. These MOSFET was used in both of the diagrams in figure 4.10 and figure 4.11. The additional four nodes are connected to the measuring devices to detect the power losses. After placing the MOSFET devices on the schematic, the diagram for the proposed design looks like the one in figure 4.11.

For calculating and comparing the power loss in the switches, the duty cycle in both the conventional and proposed configuration was kept as 0.5 in both of loads.

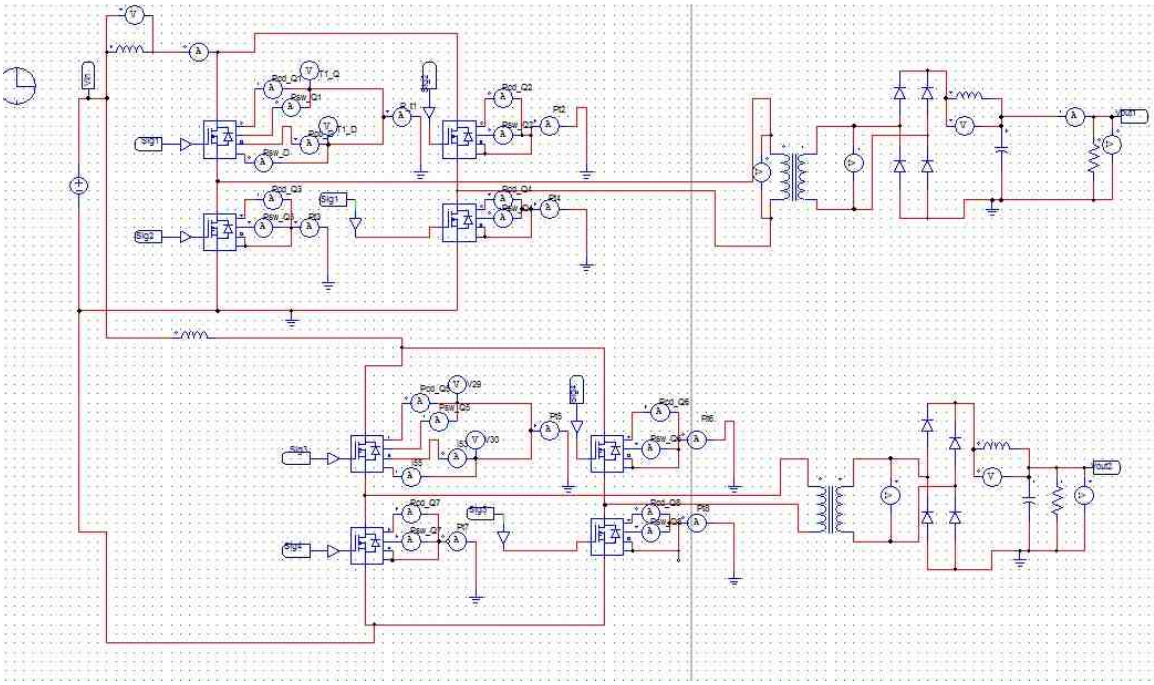

Fig. 4.10. Diagram to Calculate the Losses in Conventional Configuration

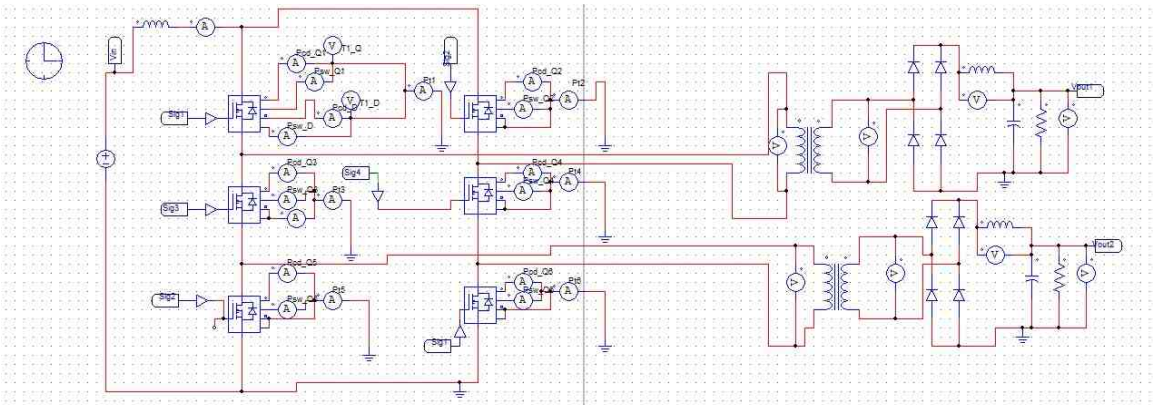

Fig. 4.11. Diagram to Calculate the Losses in Conventional Configuration

The transistor conduction loss is calculated as:

$$TransistorConductionLosses = I_D^2 * R_{DS(on)} \tag{4.7}$$

where I_D is the drain current, and $R_{DS(on)}$ is the static on-resistance.

When the transistor is conducting periodically with an on duty cycle of D, the conduction losses are calculated as:

$$TransistorConductionLosses = I_D^2 * R_{DS(on)} * D \tag{4.8}$$

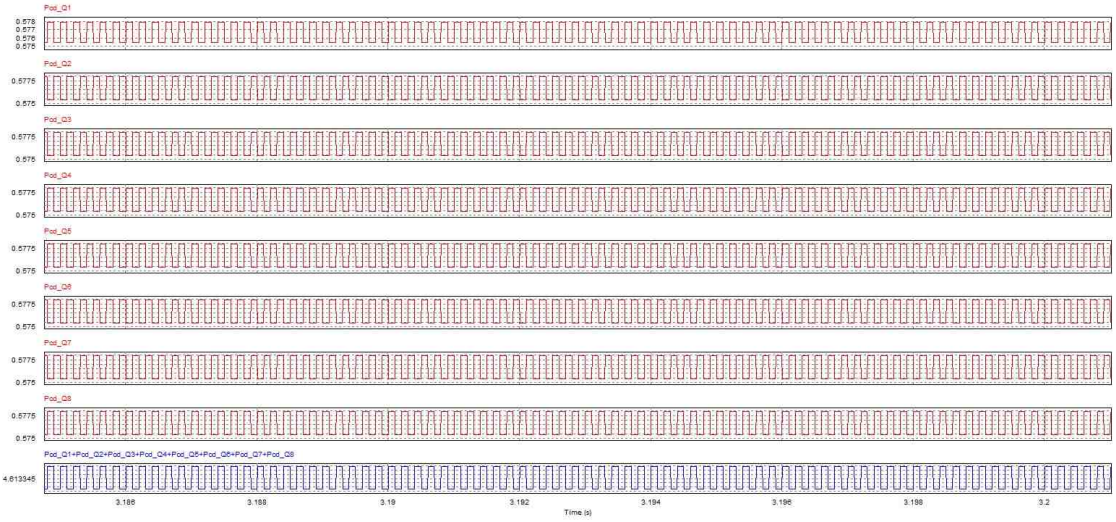

Fig. 4.12. Conduction Losses of the Switches in the Conventional Configuration

Figure 4.12 contains the waveforms in all of the switches in the conventional configuration. The first eight waveforms are the conduction losses for the all eight switches in the configuration. It can be observed that the conduction losses in all eight switches are almost same (approximately 0.58 Watts each). The reason behind this loss is the switches remain on or turn off for almost same amount of time for this configuration. The waveform at the bottom of the figure is the summation of the conduction losses in all eight switches which is the total conduction loss of this configuration.

The conduction losses of the switches in the proposed design is shown in figure 4.13. The first six waveforms are the conduction losses in the six switches. It can be noticed that in this case, the conduction losses of the switches are not same. The losses in the first two and the last two switches are almost similar but the middle two switches are different from

Fig. 4.13. Conduction Losses of the Switches in the Proposed Design

the other four switches. This occurs due to the unequal operational time of the switches in this configuration. Note that even the highest conduction loss among the switches (approximately 0.4 Watts) is less than the lowest conduction loss (approximately 0.575 Watts) of the conventional configuration. In addition to it, the number of switches are less in the proposed configuration than the conventional one. Hence, the total conduction loss is definitely less in the proposed configuration. The waveform at the bottom in figure 4.13 shows the summation of all six switches in the proposed configuration. The total conduction loss is around 1.512 Watts which is much less than the conduction loss in the conventional configuration (approximately 4.613 Watts).

The comparison among the conduction losses are more evident when they are shown as a pie chart. Figure 4.14 contains the pie graph where the blue color shows the amount of total conduction loss in conventional configuration and the total conduction loss in the proposed configuration is shown using orange color. The proposed configuration has three times less conduction loss than the conventional one. This loss is much reduced because of the selection of proper switching signal that has reduced the conduction losses in the middle two switches greatly.

Fig. 4.14. Comparison Between the Conduction Losses of the Conventional and Proposed Configuration

The switching losses of the MOSFETs are the turn on and turn off losses. The transistor turn-on loss is calculated as:

$$TransistorTurn - onLosses = E_{on} * f \tag{4.9}$$

where E_{on} is the transistor turn-on energy losses, and f is the frequency as defined in the input parameter "Frequency". The transistor turn-off loss is calculated as:

$$TransistorTurn - offLosses = E_{off} * f \tag{4.10}$$

where E_{off} is the transistor turn-off energy losses. The energy losses E_{on} and E_{off} are calculated using the rise times and the fall times of the voltage and current waveforms based on the information of the MOSFET gate current, input/output/reverse transfer capacitances and gate charges.

The current rating of the selected MOSFET is sufficient for the current flow in this circuit. Otherwise, if the current rating is too low, it is difficult to calculate rise and fall times. For the conventional configuration, the gate-source voltage level was increased up to 20 Volts (which is kept as 10 Volts for the proposed configuration), so that it does not exceed the maximum allowed current.

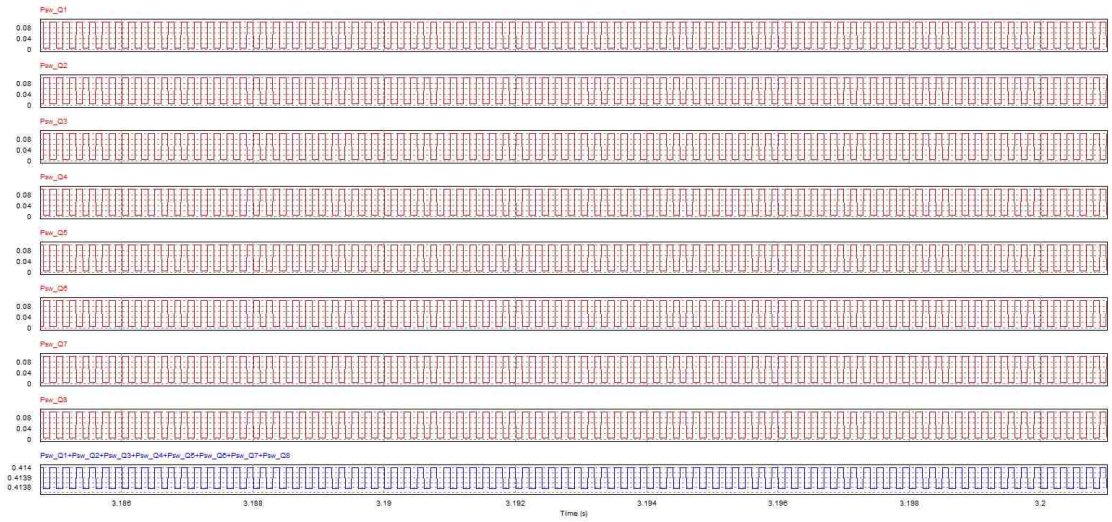

Fig. 4.15. Switching Losses of the Switches in the Conventional Configuration

Figure 4.15 shows the switching losses of all eight switches in the proposed converter. Just like the conduction losses, the switching losses are almost same for all eight switches in this configuration which is approximately 0.08 Watts each. The waveform at the bottom is the total switching loss of all eight switches.

Figure 4.16 contains the waveforms of the switching losses in the proposed design. In this case, the switching losses for the first two and the bottom two switches are almost same (approximately 0.016 Watts each). The middle two switches have a slightly higher switching loss (approximately 0.03 Watts) than the other four switches. Similar to the conduction losses, the higher switching loss in the proposed design is smaller than the lowest conduction loss among the switches. Hence, the total switching loss in the proposed

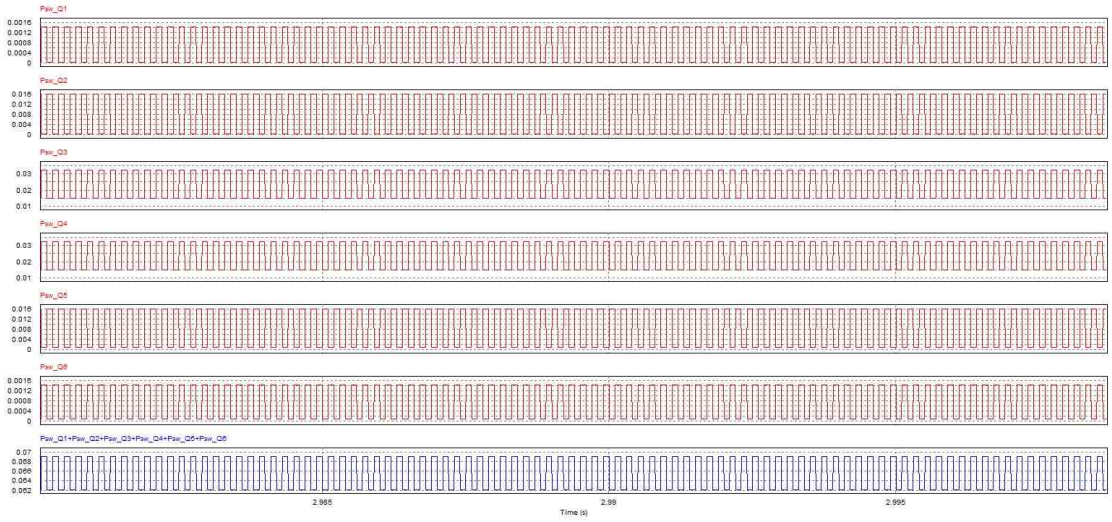

Fig. 4.16. Switching Losses of the Switches in the Proposed Design

converter is much less (approximately 0.07 Watts) which is even less than the switching loss of a single switch in the conventional converter.

The comparison among the total switching losses between the conventional and the proposed converter is shown using a pie chart in figure 4.17. The switching loss in the proposed converter is shown using the color orange and the switching loss in the conventional converter is shown using the color blue. The switching loss is even less compared to the conduction loss. The total switching loss in the proposed converter is about six times less than the total switching loss in the conventional configuration.

The total losses in the switches are calculated by combining all of the losses in the switches. A measuring device (an ammeter in this case) is connected at the node that joins all of the transmission paths from the four nodes that depict the conduction and switching losses of the transistors and diodes. The total loss of the switches conventional configuration are shown in figure 4.18. As the conduction losses and the switching losses were almost same for the switches, the total loss is also similar. The total loss for all of the switches are added and the total loss for the configuration is the bottom waveform. The total loss for the conventional configuration is almost 5.03 Watts.

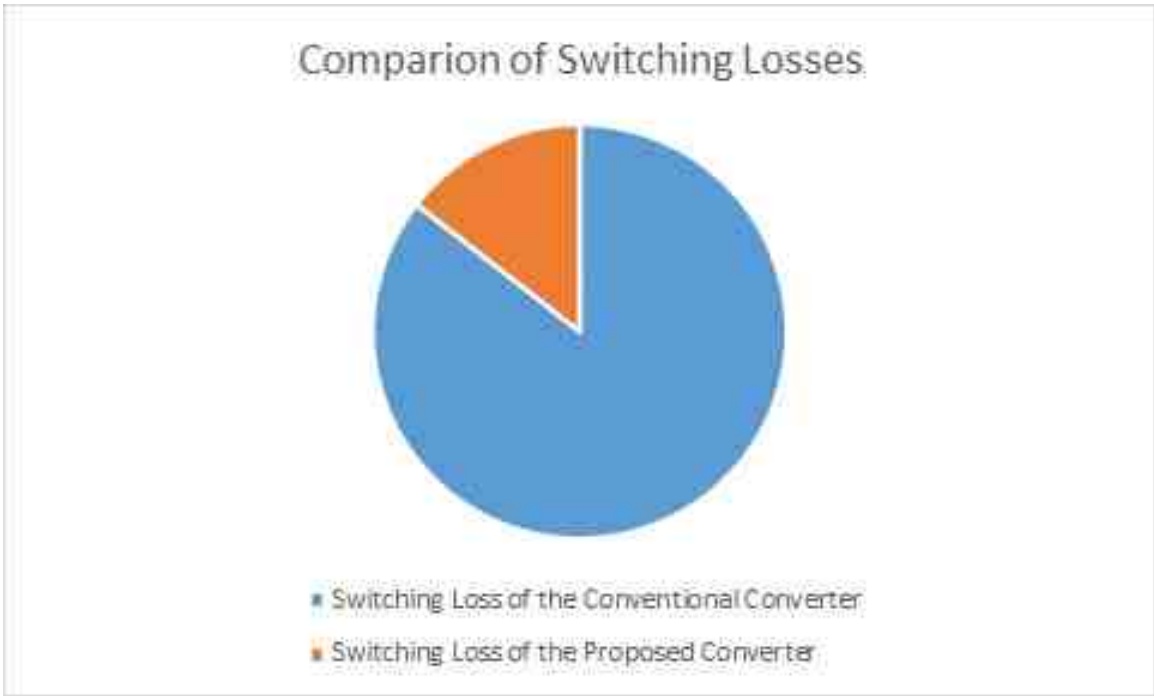

Fig. 4.17. Comparison Between the Switching Losses of the Conventional and Proposed Configuration

Figure 4.19 shows the combination of all kinds of losses for each switch in the proposed converter. The first two and the bottom two switches have similar losses and the middle two switches have similar losses which is different from the other four switches as expected. The last waveform shows the representation of all switches combined. The total loss in the proposed design is only around 1.58 Watts which is less than the conventional configuration.

Total losses in conventional and proposed converter are compared in figure 4.20 by using a pie chart. The total losses of the proposed converter is the orange portion of the graph which is less than a third of the blue portion of the graph representing the total loss in the conventional converter.

For similar loads, transformer ratio, input conditions and duty cycles, the proposed converter has around 68% less switching and conduction loss than the conventional one.

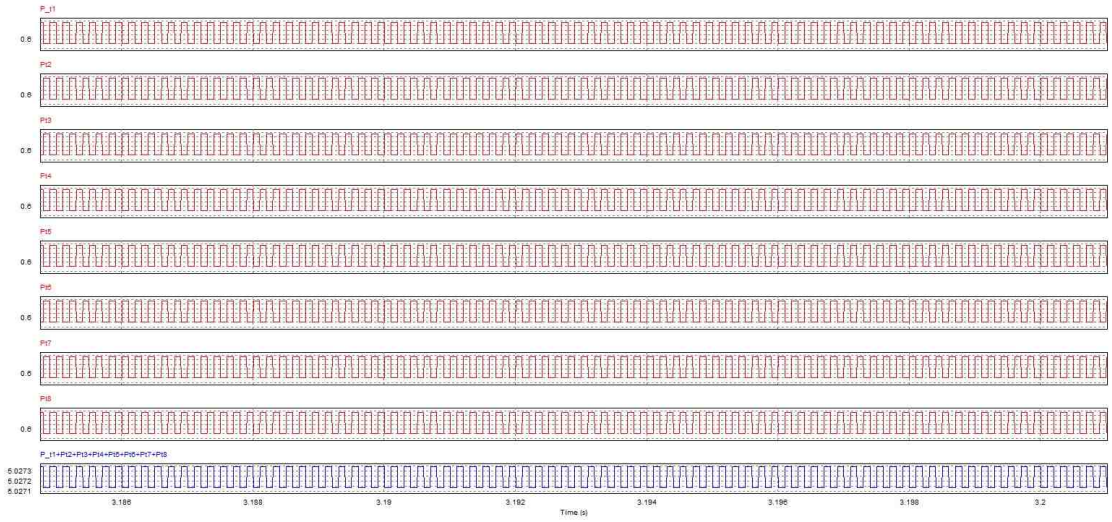

Fig. 4.18. Total Loss in the Conventional Configuration

Fig. 4.19. Total Loss in the Proposed Design

In addition to it, the designed converter has less number of switches than the conventional one. The design is not only cost effective but also much more efficient in reducing losses.

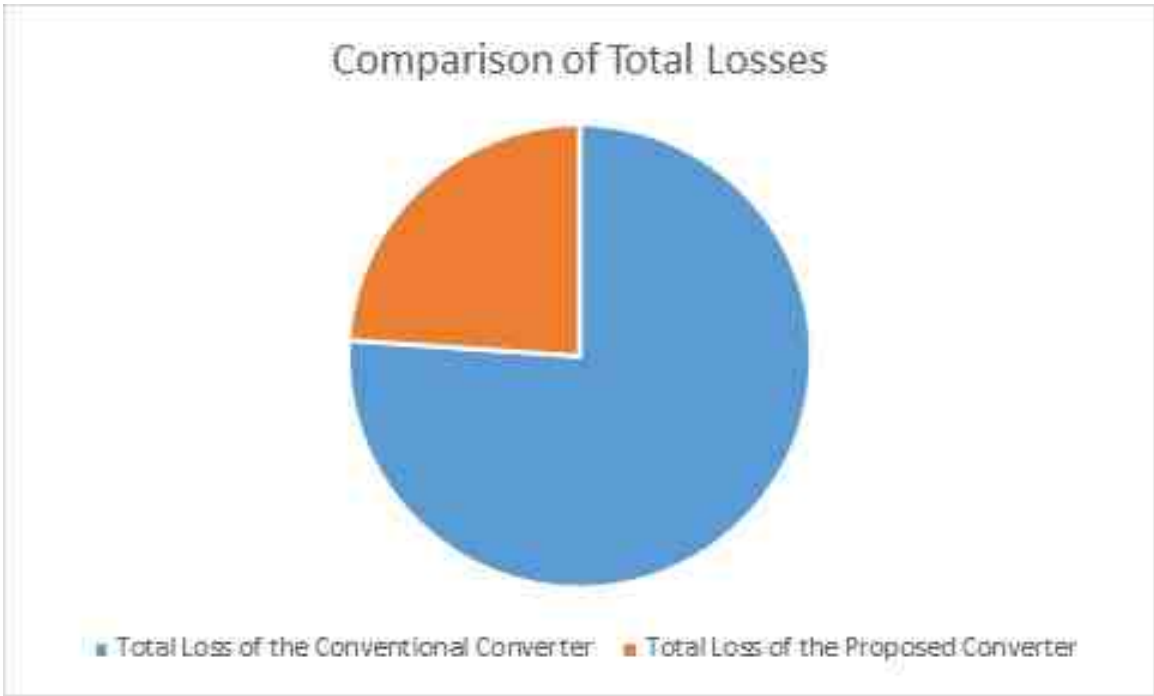

Fig. 4.20. Comparison Between the Total Losses of the Conventional and Proposed Configuration

4.6.3 Number of Components Required

The designed converter has six MOSFETs working as controlling switches at primary side whereas the conventional converter requires eight MOSFETs. The PWM gating circuit for the conventional converter has three op-amps, four OR gates, and four NOT gates. The designed converter needs three op-amps, one XOR gate, three AND gates, one OR gate and two NOT gates. The number of required logic gates required to generate PWM is eight in total for both of the converter.

5. PROPOSED DC-DC-AC CONVERTER

5.1 Introduction

According to [76], the utilization of dc to ac converter includes the following applications:

- Variable voltage/frequency AC supplies in adjustable speed drives (ASDs), such as induction motor drives and synchronous machine drives. In industrial applications adjustable speed drives are widely applied.
- Constant regulated voltage AC power supplies. For example, uninterrupted power supplies (UPSs).
- Static var compensations.
- Active filters.
- Flexible AC transmission systems (FACTSs).
- Voltage compensations.

Power conversion process is often multi-step process that involves more than one type of converter [77]. In this chapter, the converter that converts dc to dc then dc to ac is discussed and designed. Dc to ac converters are designed to provide single phase or three phase output. For larger industrial application three phase is needed. So in this thesis the converter is designed to provide three phase output.

5.2 Motivation

In alternating current electric power generation, transmission and distribution system, three-phase electric power is a common method [78]. Three phase system has advantages over single phase system like:

- Three phase machines enhance power capability for a given machine size.
- Three phase system has greater effectiveness in motors, three phase system ensures the same direction of motor provided maintained connection of phases [79].
- Single phase or two phase inputs can be taken from the three-phase system rather than generated independently. By manipulating supplied three phases, the requirements of more than three phases like in the aluminum industry, where 48 phases are required for melting purposes can be provided [80].
- Instantaneous power of a three phase system is not pulsating [80].
- During transmission, thinner conductor with 25% reduced copper requirement is able to transmit same KVA at same voltage than single phase system. Thus construction and maintenance cost is reduced [81].
- In rotating machinery, three phase keeps the torque on rotor more constant and cause less vibration than single phase due to constant instantaneous power [82].

For these reasons, the machines where alternating current is required, a three phase system seems more feasible. Balanced three-phase system provides very smooth power delivery [83]. So previously boosted dc output voltage was planned to be converted to two three-phase outputs in this design.

5.3 Design Layout

The designed converter discussed in this chapter has two separate stages. The conversion process from dc input to two desired three phase ac output is done during these stages.

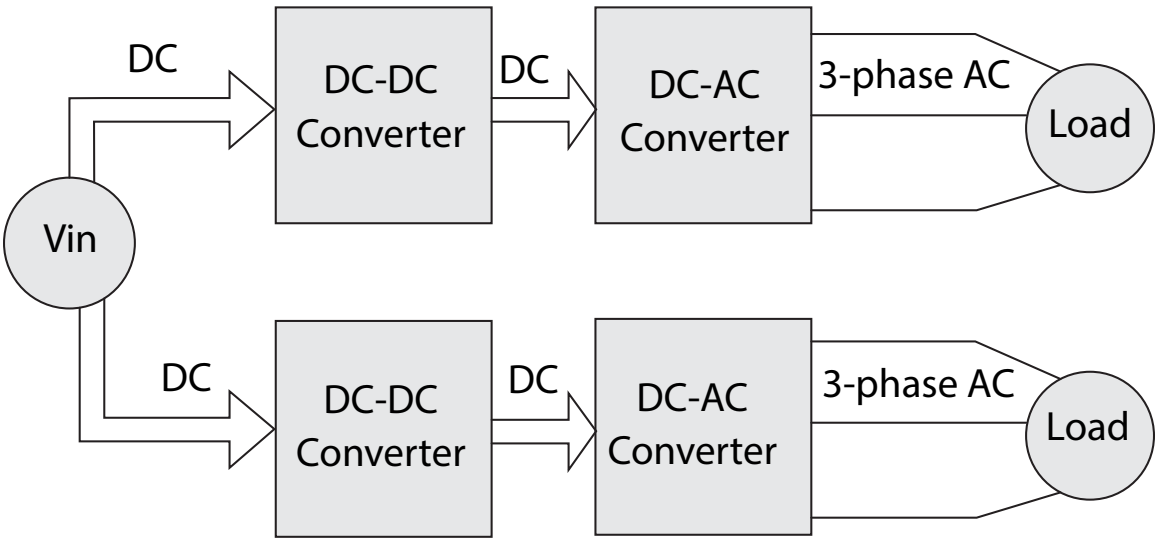

Fig. 5.1. The Planned Layout of the Converter

1. The first stage modifies the input dc voltage to an output dc voltage to meet the requirement of ac output voltage.

2. The second stage converts the dc voltage to the desired three phase ac voltage.

The planned layout is shown in figure 5.1. It can be seen that from this design, two three-phase loads are supplied from a single dc source.

5.3.1 Dc-dc Converter

The transformer turns ratio and duty cycle are given such that it can generate the dc output voltage to provide the desired ac output voltage. Unlike the traditional converter, this converter has only single input and two separate output converters to supply different loads as explained in chapter 3 of this thesis.

Dual dc outputs from this converter work as the input to the dc to ac converter.

5.3.2 Dc-ac Converter

This part of the converter converts the dc voltage to ac output voltage. Dc to ac converter or inverter can be of several types. The main types are [84]:

1. Current Source Converter: This type of converter acts as a constant current source and requires large ac filter for harmonic elimination. Reactive power supply is required for power factor correction. This kind of converter has the capability to limit faulty current.

2. Voltage Source Converter: This type of converter works as a constant voltage source and small ac filter is capable of eliminating higher harmonics. No reactive power supply is necessary for this kind of converter as it can work in any quadrant. As a capacitor is required at the dc side, it has the possibility to discharge into faults.

Evaluating the aspects of the current source and voltage source converts, the voltage source converter seems to be more compatible with the modern machines and other applications. So voltage source converter is considered for this design.

5.4 Three Phase Voltage Source Inverters

According to the circuit arrangement classification, inverter can be voltage source and current source type. A voltage source inverter (VSI or voltage stiff inverter) forms voltage with required magnitude, frequency and phase [85]. Also this inverter has very low internal impedance. For this design, voltage source inverter was chosen. Three phase inverter consists of three half bridges which are mutually phase shifted by 120 degrees to generate three phase voltage waves [86]. Figure 5.2 shows the generation of switching pulses of the inverter from triangular wave and three phase shifted sinusoidal wave.

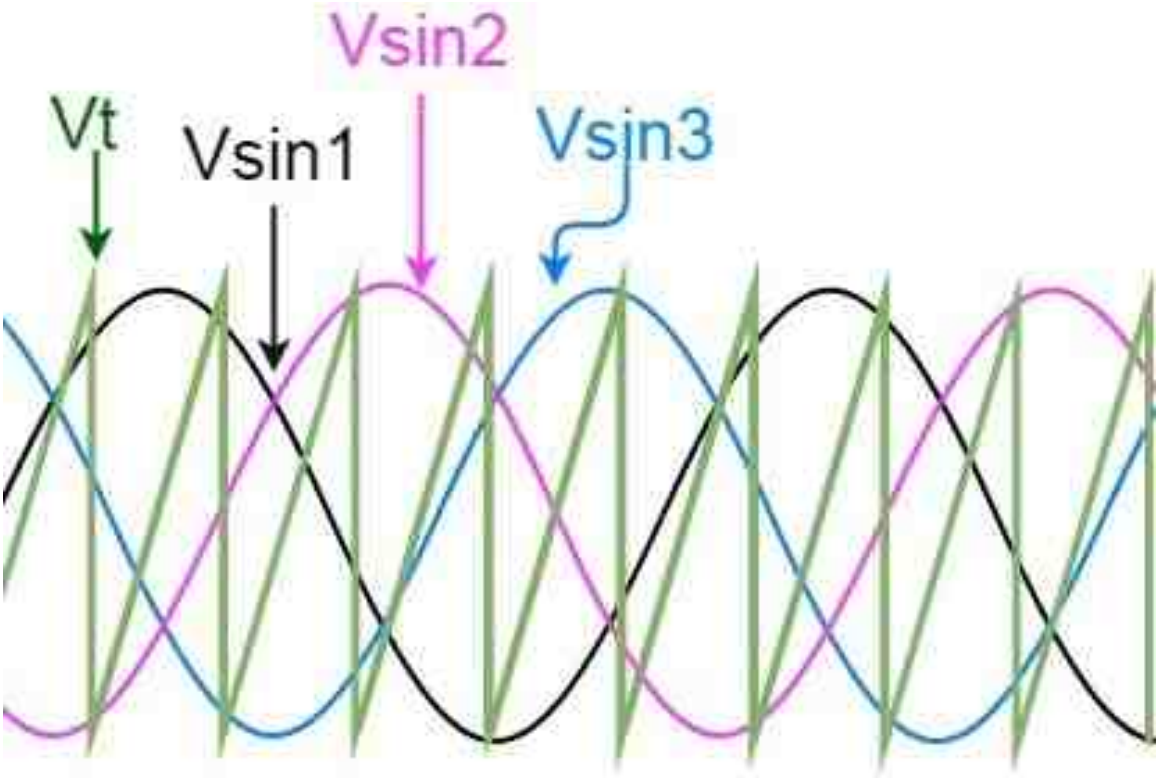

Fig. 5.2. Triangular Wave and Three Sine Waves to Generate Switching Signals

5.5 Converter Layout

5.5.1 Dual Output Converter with Eight Switches

Figure 5.3 shows two inverters connected to the previously discussed converter output. The capacitor keeps a constant voltage at the inverter input. The converter that drives ac devices mostly ranges 1 kW to 500 kW. These are based on gate commutated devices such as the GTO, MOSFET, BJT and IGBT, which can be turned ON and OFF by low power control circuits connected to their control gates [87]. For this design IGBT switches are used.

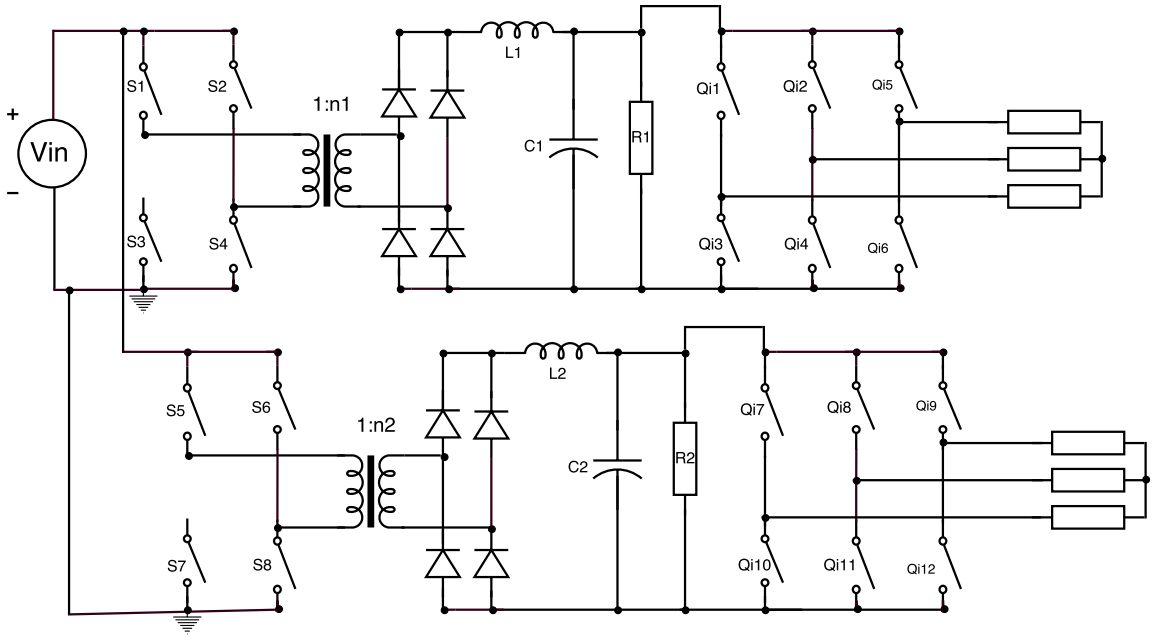

Fig. 5.3. Single-input Dual-output Inverter with Eight Switches

5.5.2 Dual Output Converter with Six Switches

5.5.3 Dual Output Converter with Fault Correction

Fault tolerant drive system is capable of continuing the operation satisfactorily even after a fault. Several topologies were proposed from time to time [88]:

- Switch-redundant topology [89], [90] which incorporates four TRIACs and three fast acting fuses.
- Double switch-redundant topology [91] for four leg inverter with additional fuses and two SCRs per phase leg and capacitors.
- Phase-redundant topology [91], [92], [93] that introduces a spare inverter leg to improve fault tolerance.
- Cascaded inverter [94], [95] topology [88] that allows the full bus voltage to be applied to each of the load phases that increases reliability [96].

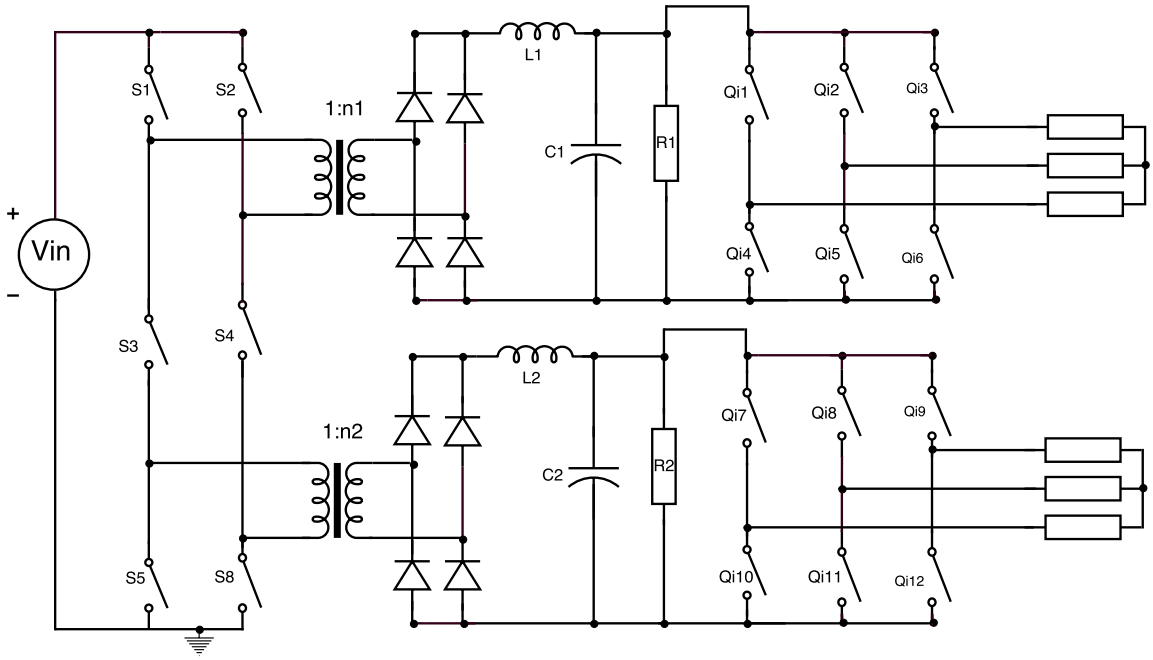

Fig. 5.4. Single-input Dual-output Inverter with Six Switches

- Four-leg inverter topology [97], [98].

The fault tolerance capability can be increased by employing two three leg inverters [99]. Reconfiguration of power converter topology allows compensation in dc link capacitor failure, short circuit failure and open circuit failure of the power switches.

Figure 5.5 shows the pre-fault configuration of open-end winding motor drive system.

5.6 Gating Signal

The gating signal for the dc-dc-ac converter utilizes the gating signal circuitry generated in chapter 3 for the dc to dc conversion part. For the dc to ac conversion part, the IGBT module has the similar gating circuitry of the inverter.

Figure 5.6 shows the gating signal circuitry of the dc to ac conversion part. A triangular wave is compared with three phase shifted sine waves as explained earlier. The waveforms shown in figure 5.2 are the signals Vt, Vsin1, Vsin2 and Vsin3. These waves are compared

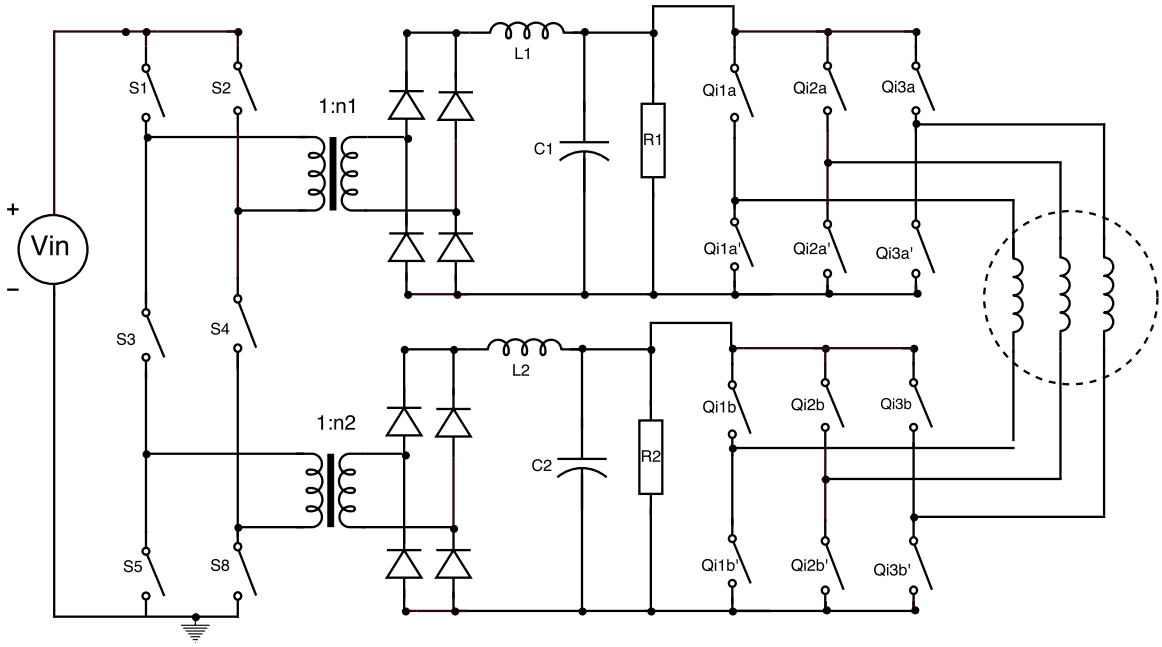

Fig. 5.5. Open-end Winding System

to generate the switching signals Qi1, Qi2 and Qi3 for the switches Qi1, Qi2 and Qi3 respectively in figure 5.4. The inverted signals of these three switching signals are Qi1', Qi2' and Qi3' are the gating signals for the switches Qi4, Qi5 and Qi6 respectively in figure 5.4. The switches for the other load have the similar switching signals. So the generated signals Qi1, Qi2, Qi3, Qi1', Qi2' and Qi3' of figure 5.6 can be used as the gating signals for the switches Qi7, Qi8, Qi9, Qi10, Qi11 and Qi12 respectively in figure 5.4.

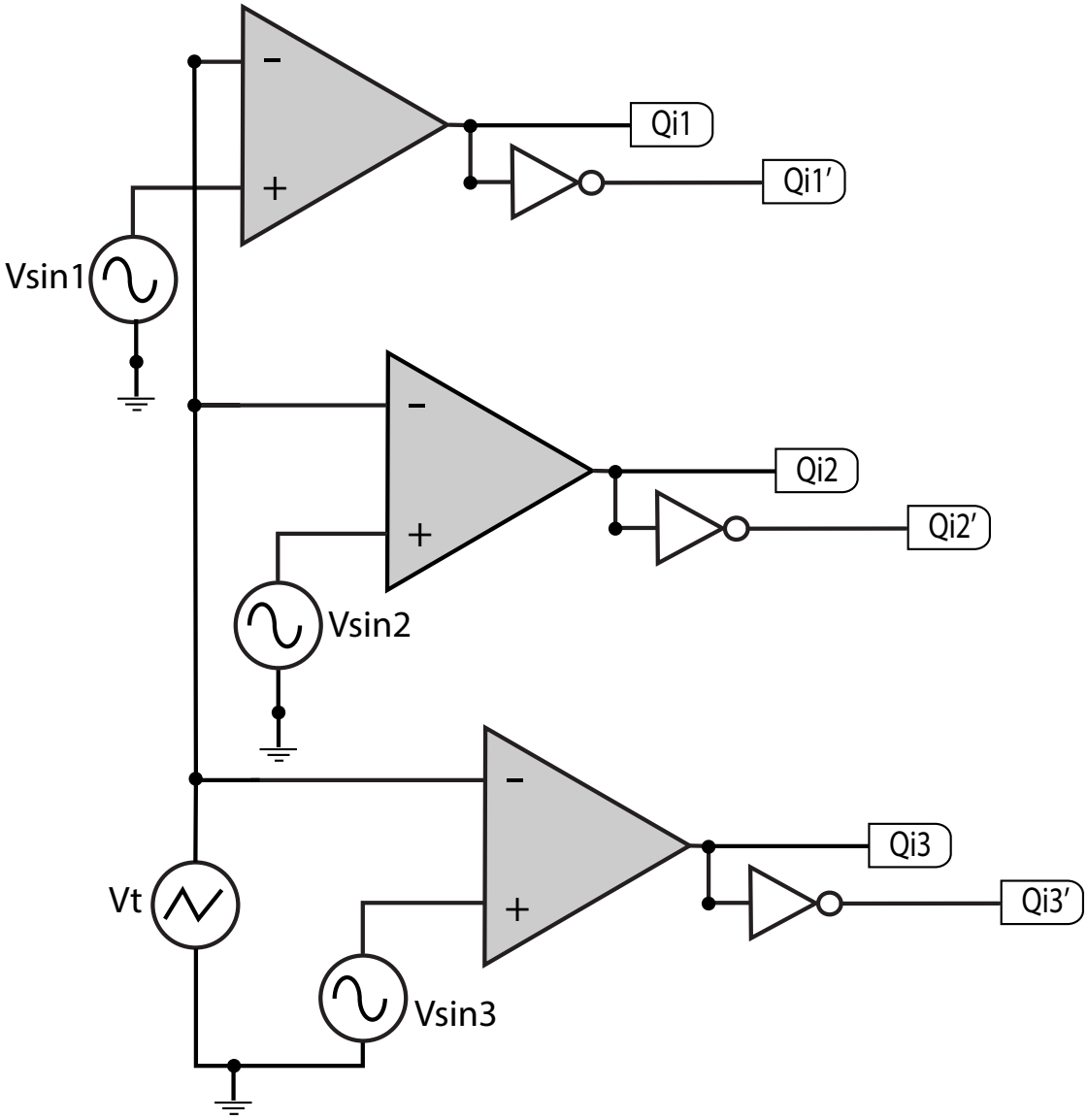

Fig. 5.6. Switching Signal Generation of Dc-ac Converter

6. RESULTS FROM DESIGNED DC-DC-AC CONVERTER

6.1 Introduction

The designed converter in chapter 3 of this thesis was simulated using the simulation software package PSIM. As the PSIM software is very effective in power electronic design and solutions, for the simulation and analysis of the designed converter in chapter 5, the package PSIM was used too.

6.2 Gating Signals

After simulation, the gating signals are found by comparing a triangular wave with three phase shifted sine waves. In this simulation, the parameters were specified to generate the desired wave-shapes.

Table 6.1.
Parameters Included for the Triangular Wave

Parameters	**Value**
V_peak_to_peak	1
Frequency	10k
Duty cycle	0.5
DC Offset	-0.5
Tstart	0
Phase Delay	0

Table 6.1 contains the specified parameters to generate the triangular wave for the switching signals. The triangular signal has a total magnitude of 1 and as the dc offset is set to -0.5, it will be positioned from -0.5 to 0.5 of Y-axis.

Table 6.2.
Parameters Included for the Sine Waves

Parameters	**Value(Sine1)**	**Value(Sine2)**	**Value(Sine3)**
Peak Amplitude	0.5	0.5	0.5
Frequency	500	500	500
Phase Angle	0	120	240
DC Offset	0	0	0
Tstart	0	0	0

Table 6.2 includes the specified parameters for the sine waves. The values of Sine1, Sine2 and Sine3 are the sine waves used for the first, second and third IGBT switches respectively. The sine waves are 120 degrees phase shifted from each other. The frequency for these sine waves are kept less than the triangular wave to generate proper switching signals. Note that, in the case of sine waves, the parameter ”Peak Amplitude” is present instead of peak-to-peak voltage like the triangular wave. As sine wave is generally expanded throughout both positive and negative axis, the peak amplitude takes place in both side of the Y-axis too.

Figure 6.1 shows the drawn circuit diagram in PSIM to generate gating signals. For this circuit, naturally sampled pulse width modulation technique was used [100]. The **not** gates are used for the inversed version of the generated signals. The triangular wave and the three sine waves are shown in figure 6.2. The sine waves and the triangular waves are displayed as specified.

The generated switching signals after comparing the triangular wave and the sine waves are shown in figure 6.3. It shows all six switching signals of the inverter part of the converter. As **not** gates were used for the other three signals than the generated ones, it can

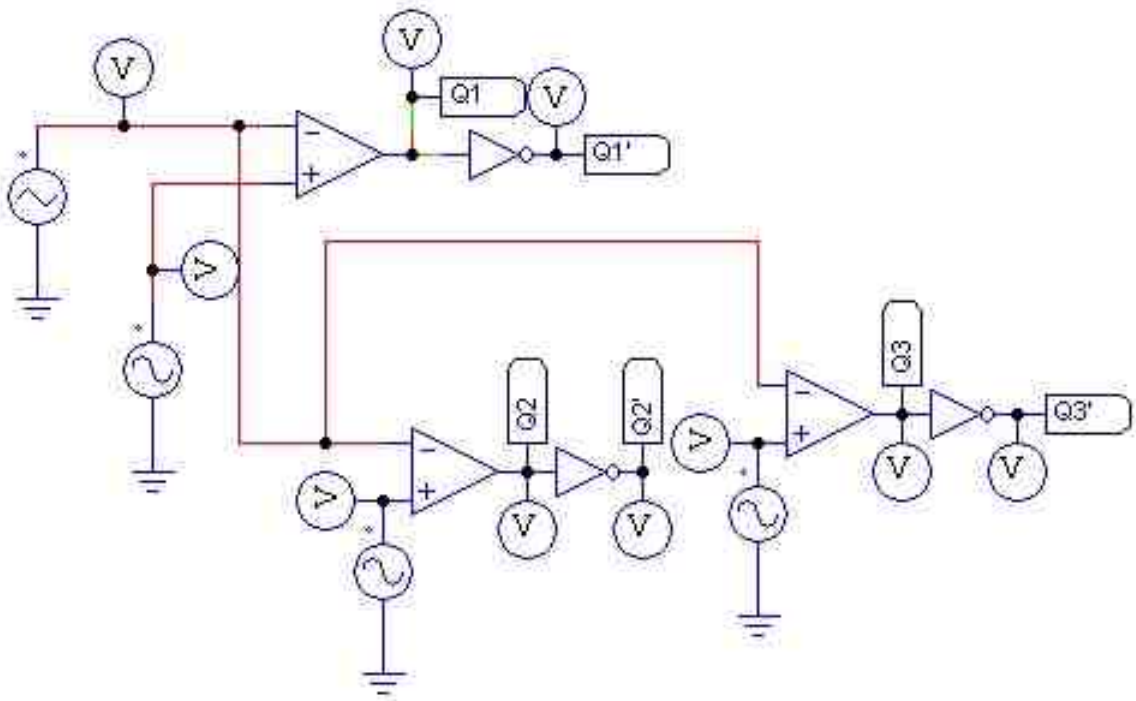

Fig. 6.1. Gating Signal Generation Circuitry

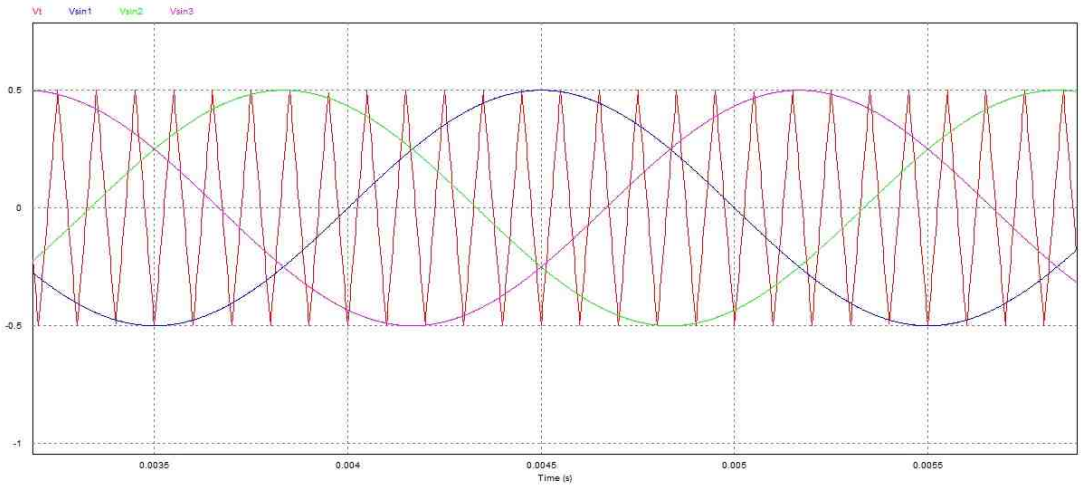

Fig. 6.2. Waves to Generate Switching Signals

Fig. 6.3. Generated Switching Signals for Six Switches

be observed that the last three signals (Q4, Q5 and Q6) are the inversed version of the first three switching signals (Q1, Q2 and Q3) respectively.

6.3 Single Input Dual Output Dc-ac Converter

The proposed circuit diagram on PSIM for simulation is shown in figure 6.4. The schematic diagram of the developed design in chapter 4, is used in the first part (or the left part) of this schematic diagram. The part to convert output dc to three phase ac is connected to the output of the previous design.

For this simulation the upper load was given a duty cycle of 0.8 and the lower had a duty cycle of 0.5.

The ammeters connected to the loads display the current signals. From figure 6.5, it can be observed that the inverter has generated phase shifted output current waves. In addition to it, the current waves in the upper load have larger magnitude than the lower one. The effect of duty cycle explains this result.

Figure 6.6 shows the line to line voltages of the load. The red waves are line voltages (Vab, Vbc and Vca) for load-1 and the blue ones display line voltages (Vab2, Vbc2 and

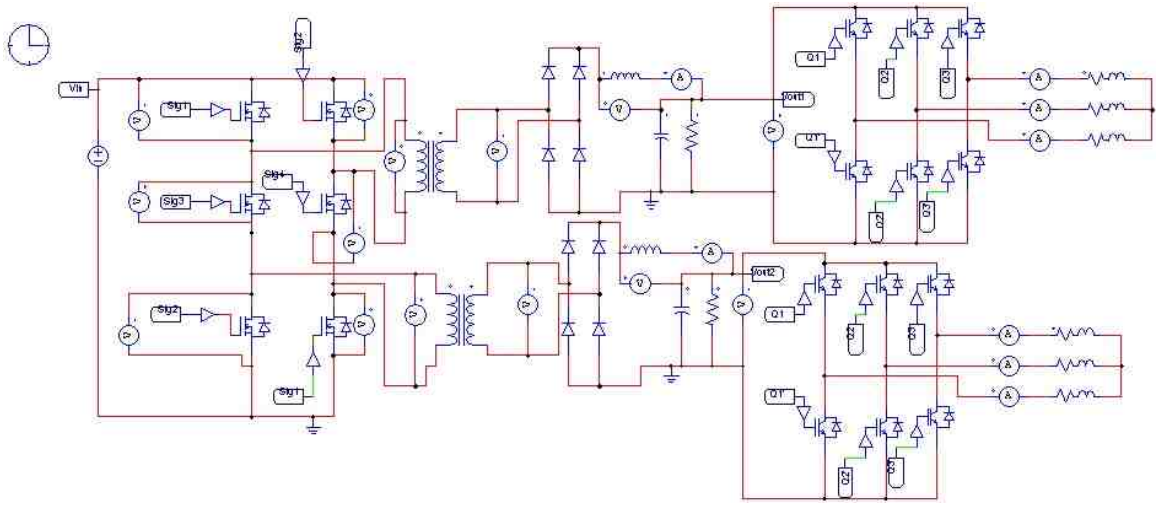

Fig. 6.4. Circuit Diagram for the Proposed Design

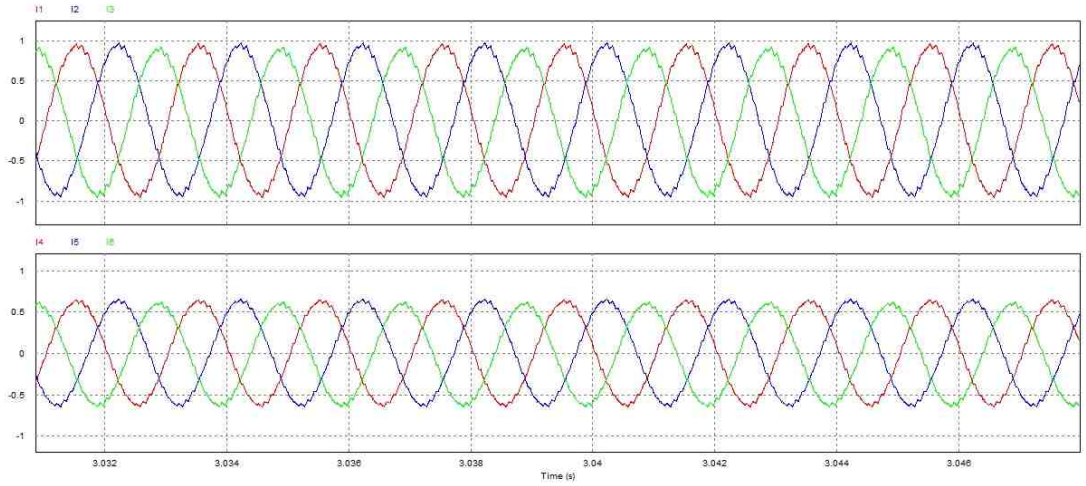

Fig. 6.5. Output Currents

Vca2) of load-2. Just like the output current waves, the magnitude of line voltages of load-2 is less than the ones of load-1 as expected due to the duty cycle.

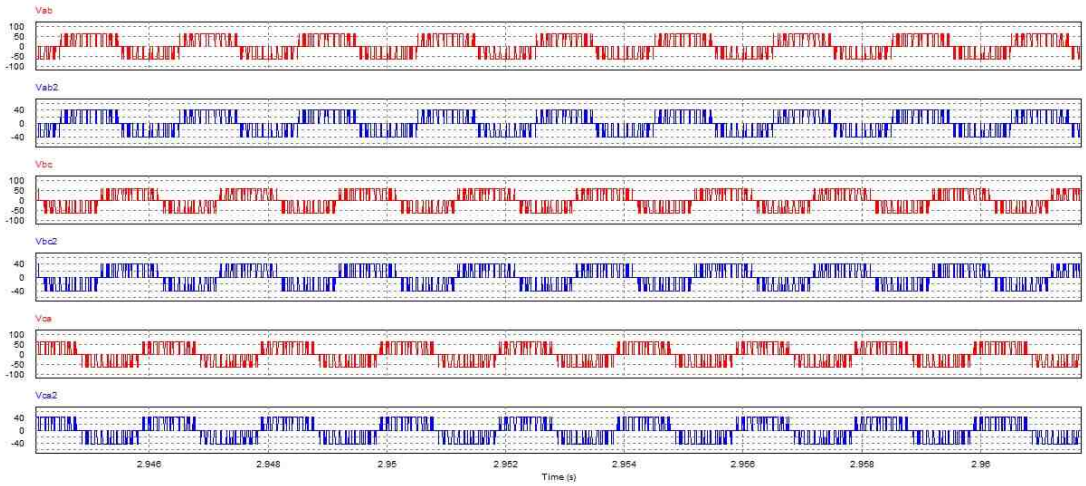

Fig. 6.6. Line to Line Voltages

7. CONCLUSION

7.1 Discussions on the Designed Converters

7.1.1 Single Input Dual Output Dc to Dc Converter

The designed dc to dc converter is capable of transforming the input voltage to any voltage level. According to the requirement, the desired voltage can be achieved by setting a step-up or step-down transformer turns ratio. The converter is capable of conducting the operation similar to the conventional. The results have shown that the designed converter with only six switches generate the same output as the one with eight switches. Moreover, the switching losses are much less than the conventional one. Also the PWM circuitry has almost same number of logic gates as the conventional one. So the designed converter has better efficiency from several points.

7.1.2 Single Input Dual Output Dc to Ac Converter

This converter has two stages. In the first stage it converts dc input voltage to two dc voltage levels. Then the output dc is converted to suitable three phase ac suitable for the loads.

A cascaded fault tolerant system was implemented with the configuration too.

7.2 Suggested Improvements

The designed dc-dc-ac converter is possible to make more efficient by reducing switching more on the secondary ac side. If the conversion to the desired ac signal can be done using shared circuitry like the designed dc to dc converter then the converter should be more improved, cost effective and easier to implement.

Another suggestion on the whole system could be implementation of a wirelesss control system. If a wireless feedback system can be developed that is capable of sending the pulse-width modulated signal to the converter with desired duty cycle, then the converter can be controlled from a remote position according to user requirements. Real-time regulation can be possible by implementing feedback system along with this proposed strategy.

REFERENCES

REFERENCES

[1] M. H. Rashid, *Power electronics handbook: devices, circuits and applications*. Academic press, 2010.

[2] P. C. Hewitt, "Vapor electric apparatus." April 11, 1911, US Patent 989,259.

[3] P. C. Hewitt, "Vapor electric apparatus." September 12, 1916, US Patent 1,198,381.

[4] P. Krein, "Elements of power electronics. Oxford University Press," 1998.

[5] C. C. Herskind and W. McMurray, "History of the static power converter committee," *IEEE Transactions on Industry Applications*, no. 4, pp. 1069–1072, 1984.

[6] E. L. Owen, "History [origin of the inverter]," *IEEE Industry Applications Magazine*, vol. 2, no. 1, pp. 64–66, 1996.

[7] T. M. Jahns and E. L. Owen, "Ac adjustable-speed drives at the millennium: How did we get here?" *IEEE Transactions on Power Electronics*, vol. 16, no. 1, pp. 17–25, 2001.

[8] T. L. Skvarenina, *The power electronics handbook*. CRC press, 2001.

[9] B. K. Bose, "Neural network applications in power electronics and motor drivesan introduction and perspective," *IEEE Transactions on Industrial Electronics*, vol. 54, no. 1, pp. 14–33, 2007.

[10] D. C. Hopkins, S. Mathuna, A. N. Alderman, and J. Flannery, "A framework for developing power electronics packaging," in *Applied Power Electronics Conference and Exposition, 1998. APEC'98. Conference Proceedings 1998., Thirteenth Annual*, vol. 1. IEEE, 1998, pp. 9–15.

[11] R. W. Erickson and D. Maksimovic, *Fundamentals of power electronics*. Springer Science & Business Media, 2007.

[12] F. L. Luo and H. Ye, *Advanced dc/dc converters*. CRC Press, 2016.

[13] M. K. Kazimierczuk, *Pulse-width modulated DC-DC power converters*. John Wiley & Sons, 2015.

[14] A. Chub, D. Vinnikov, F. Blaabjerg, and F. Z. Peng, "A review of galvanically isolated impedance-source dc–dc converters," *IEEE Transactions on Power Electronics*, vol. 31, no. 4, pp. 2808–2828, 2016.

[15] W.-F. Lai, S.-M. Chen, T.-J. Liang, K.-W. Lee, and A. Ioinovici, "Design and implementation of grid connection photovoltaic micro inverter," in *Energy Conversion Congress and Exposition (ECCE), 2012 IEEE*. IEEE, 2012, pp. 2426–2432.

[16] R. E. Torres-Olguin, M. Molinas, and T. Undeland, "Offshore wind farm grid integration by vsc technology with lcc-based hvdc transmission," *IEEE Transactions on Sustainable Energy*, vol. 3, no. 4, pp. 899–907, 2012.

[17] Y. Hu, R. Zeng, W. Cao, J. Zhang, and S. J. Finney, "Design of a modular, high step-up ratio dc–dc converter for hvdc applications integrating offshore wind power," *IEEE Transactions on Industrial Electronics*, vol. 63, no. 4, pp. 2190–2202, 2016.

[18] H. I. Sari, "Dc/dc converters for multi-terminal hvdc systems-based on modular multilevel converter," Master's thesis, Norwegian University of Science and Technology, 2016.

[19] S. Oucheriah and L. Guo, "Pwm-based adaptive sliding-mode control for boost dc–dc converters," *IEEE Transactions on Industrial Electronics*, vol. 60, no. 8, pp. 3291–3294, 2013.

[20] K.-C. Tseng, C.-T. Chen, C.-A. Cheng *et al.*, "A high-efficiency high step-up interleaved converter with a voltage multiplier for electric vehicle power management applications," *source: Journal of Power Electronics*, vol. 16, no. 2, pp. 414–424, 2016.

[21] T.-J. Liang, Y.-T. Huang, J.-H. Lee, and L. P.-Y. Ting, "Study and implementation of a high step-up voltage dc-dc converter using coupled-inductor and cascode techniques," in *Applied Power Electronics Conference and Exposition (APEC), 2016 IEEE*. IEEE, 2016, pp. 1900–1906.

[22] H. Bai and C. Mi, "Eliminate reactive power and increase system efficiency of isolated bidirectional dual-active-bridge dc–dc converters using novel dual-phase-shift control," *IEEE Transactions on Power Electronics*, vol. 23, no. 6, pp. 2905–2914, 2008.

[23] M. Narimani and G. Moschopoulos, "An investigation on the novel use of high-power three-level converter topologies to improve light-load efficiency in low power dc/dc full-bridge converters," *IEEE Transactions on Industrial Electronics*, vol. 61, no. 10, pp. 5690–5692, 2014.

[24] G. Maitre, "Dc-ac converter," July 3, 1973, US Patent 3,743,918.

[25] W. D. Bernardus, "Dc-ac converter," May 9, 1972, US Patent 3,662,249.

[26] M. Luursema, H. Palmers, and D. Wijsboom, "Dc-ac converter," June 18, 1974, US Patent 3,818,312.

[27] E. Reyes, R. Pena, R. Cardenas, J. Clare, and P. Wheeler, "A control scheme for two doubly fed induction machines fed by indirect matrix converter," in *Industrial Technology (ICIT), 2010 IEEE International Conference*. IEEE, 2010, pp. 631–636.

[28] A. Emadi, Y. J. Lee, and K. Rajashekara, "Power electronics and motor drives in electric, hybrid electric, and plug-in hybrid electric vehicles," *IEEE Transactions on industrial electronics*, vol. 55, no. 6, pp. 2237–2245, 2008.

[29] X. Qu, S.-C. Wong, and K. T. Chi, "Noncascading structure for electronic ballast design for multiple led lamps with independent brightness control," *IEEE transactions on Power Electronics*, vol. 25, no. 2, pp. 331–340, 2010.

[30] R. Adda, O. Ray, S. K. Mishra, and A. Joshi, "Synchronous-reference-frame-based control of switched boost inverter for standalone dc nanogrid applications," *IEEE Transactions on Power Electronics*, vol. 28, no. 3, pp. 1219–1233, 2013.

[31] X. Liu, J. Xu, Z. Chen, and N. Wang, "Single-inductor dual-output buck–boost power factor correction converter," *IEEE Transactions on Industrial Electronics*, vol. 62, no. 2, pp. 943–952, 2015.

[32] O. Ray, A. P. Josyula, S. Mishra, and A. Joshi, "Integrated dual-output converter," *IEEE Transactions on Industrial Electronics*, vol. 62, no. 1, pp. 371–382, 2015.

[33] X. Liu, P. Wang, P. C. Loh, and F. Blaabjerg, "A compact three-phase single-input/dual-output matrix converter," *IEEE Transactions on Industrial Electronics*, vol. 59, no. 1, pp. 6–16, 2012.

[34] J.-K. Kim, H.-S. Park, and G.-W. Moon, "A new standby structure using multi-output full-bridge converter integrating flyback converter," in *Power Electronics and ECCE Asia (ICPE & ECCE), 2011 IEEE 8th International Conference*. IEEE, 2011, pp. 615–619.

[35] V. Mayega, J. Chen, J. L. Krug, and D. W. Evans, "Single inductor dual output buck converter with frequency and time varying offset control," June 13, 2006, US Patent 7,061,214.

[36] E. C. dos Santos, "Dual-output dc-dc buck converters with bidirectional and unidirectional characteristics," *IET Power Electronics*, vol. 6, no. 5, pp. 999–1009, 2013.

[37] J. M. Burdio, F. Monterde, J. R. Garcia, L. A. Barragan, and A. Martinez, "A two-output series-resonant inverter for induction-heating cooking appliances," *IEEE Transactions on Power Electronics*, vol. 20, no. 4, pp. 815–822, 2005.

[38] N. Pogaku, M. Prodanovic, and T. C. Green, "Modeling, analysis and testing of autonomous operation of an inverter-based microgrid," *IEEE Transactions on power electronics*, vol. 22, no. 2, pp. 613–625, 2007.

[39] M. D. Manjrekar and T. A. Lipo, "A hybrid multilevel inverter topology for drive applications," in *Applied Power Electronics Conference and Exposition, 1998. APEC'98. Conference Proceedings 1998., Thirteenth Annual*, vol. 2. IEEE, 1998, pp. 523–529.

[40] J. Abraham and D. Neela, "Modeling and performance analysis of hybrid inverter hvac system using colored hybrid petri nets," *Global Journal of Pure and Applied Mathematics*, vol. 12, no. 3, pp. 2355–2366, 2016.

[41] S. Inoue and H. Akagi, "A bidirectional isolated dc–dc converter as a core circuit of the next-generation medium-voltage power conversion system," *IEEE Transactions on Power Electronics*, vol. 22, no. 2, pp. 535–542, 2007.

[42] S. Inoue and H. Akagi, "A bidirectional dc–dc converter for an energy storage system with galvanic isolation," *IEEE Transactions on Power Electronics*, vol. 22, no. 6, pp. 2299–2306, 2007.

[43] T. Nishiyama and K. Ueki, "Isolated dc-dc converter," October 26, 2010, US Patent 7,821,797.

[44] D. Vinnikov and I. Roasto, "Quasi-z-source-based isolated dc/dc converters for distributed power generation," *IEEE Transactions on Industrial Electronics*, vol. 58, no. 1, pp. 192–201, 2011.

[45] F. Standard, "1037c. telecommunications: Glossary of telecommunication terms," *Institute for Telecommunications Sciences*, vol. 7, 1996.

[46] J. F. Cox, *Fundamentals of linear electronics: integrated and discrete*. Cengage Learning, 2002.

[47] S. F. Barrett and D. J. Pack, "Microcontrollers fundamentals for engineers and scientists," *Synthesis Lectures on Digital Circuits and Systems*, vol. 1, no. 1, pp. 1–124, 2005.

[48] T.-Y. Yang, "PWM controller having off-time modulation for power converter," April 8, 2003, US Patent 6,545,882.

[49] S. Buso and P. Mattavelli, "Digital control in power electronics," *Lectures on power electronics*, vol. 1, no. 1, pp. 1–158, 2006.

[50] R. L. Steigerwald, "Dual output dc-dc converter with independently controllable output voltages," December 9, 1986, US Patent 4,628,426.

[51] M. A. Rojas-González, J. Torres, P. Kumar, and E. Sánchez-Sinencio, "Design of an integrated single-input dual-output 3-switch buck converter based on sliding mode control," *Analog Integrated Circuits and Signal Processing*, vol. 76, no. 3, pp. 307–319, 2013.

[52] P. Kumar and M. Rojas-Gonzalez, "Novel 3-switch dual output buck voltage regulator," in *Applied Power Electronics Conference and Exposition, 2006. APEC'06. Twenty-First Annual IEEE*. IEEE, 2006, pp. 7–pp.

[53] A. Tomaszuk and A. Krupa, "High efficiency high step-up dc/dc converters-a review," *Bulletin of the Polish Academy of Sciences: Technical Sciences*, vol. 59, no. 4, pp. 475–483, 2011.

[54] D. Feldman, *Photovoltaic (PV) pricing trends: historical, recent, and near-term projections*. Lawrence Berkeley National Laboratory: Lawrence Berkeley National Laboratory., 2014, LBNL Paper LBNL-6019E.

[55] R. Karki and R. Billinton, "Reliability/cost implications of pv and wind energy utilization in small isolated power systems," *IEEE Transactions on Energy Conversion*, vol. 16, no. 4, pp. 368–373, 2001.

[56] F. Blaabjerg, Z. Chen, and S. B. Kjaer, "Power electronics as efficient interface in dispersed power generation systems," *IEEE transactions on power electronics*, vol. 19, no. 5, pp. 1184–1194, 2004.

[57] J. M. Carrasco, L. G. Franquelo, J. T. Bialasiewicz, E. Galván, R. C. PortilloGuisado, M. M. Prats, J. I. León, and N. Moreno-Alfonso, "Power-electronic systems for the grid integration of renewable energy sources: A survey," *IEEE Transactions on industrial electronics*, vol. 53, no. 4, pp. 1002–1016, 2006.

[58] J. He and Y. W. Li, "Analysis, design, and implementation of virtual impedance for power electronics interfaced distributed generation," *IEEE Transactions on industry Applications*, vol. 47, no. 6, pp. 2525–2538, 2011.

[59] S. M. Sharkh, M. A. Abu-Sara, G. I. Orfanoudakis, and B. Hussain, *Power electronic converters for microgrids*. John Wiley & Sons, 2014.

[60] J. Rocabert, A. Luna, F. Blaabjerg, and P. Rodriguez, "Control of power converters in ac microgrids," *IEEE transactions on power electronics*, vol. 27, no. 11, pp. 4734–4749, 2012.

[61] B. Kroposki, C. Pink, R. DeBlasio, H. Thomas, M. Simoes, and P. K. Sen, "Benefits of power electronic interfaces for distributed energy systems," *IEEE Transactions on Energy Conversion*, vol. 25, no. 3, pp. 901–908, 2010.

[62] P. P. Barker and R. W. De Mello, "Determining the impact of distributed generation on power systems. i. radial distribution systems," in *Power Engineering Society Summer Meeting, 2000. IEEE*, vol. 3. IEEE, 2000, pp. 1645–1656.

[63] M. Karimi-Ghartemani and M. R. Iravani, "A method for synchronization of power electronic converters in polluted and variable-frequency environments," *IEEE Transactions on Power Systems*, vol. 19, no. 3, pp. 1263–1270, 2004.

[64] Y. Song and B. Wang, "Survey on reliability of power electronic systems," *IEEE Transactions on Power Electronics*, vol. 28, no. 1, pp. 591–604, 2013.

[65] M. Joshi, E. Shoubaki, R. Amarin, B. Modick, and J. Enslin, "A high-efficiency resonant solar micro-inverter," in *Power Electronics and Applications (EPE 2011), Proceedings of the 2011-14th European Conference*. IEEE, 2011, pp. 1–10.

[66] M. Emmanuel and R. Rayudu, "Evolution of dispatchable photovoltaic system integration with the electric power network for smart grid applications: A review," *Renewable and Sustainable Energy Reviews*, vol. 67, pp. 207–224, 2017.

[67] H.-J. Chiu, Y.-K. Lo, C.-C. Chuang, C.-Y. Yang, S.-J. Cheng, M.-C. Kuo, Y.-M. Huang, Y.-B. Jean, and Y.-C. Huang, "A module-integrated isolated solar microinverter without electrolytic capacitors," *International Journal of Circuit Theory and Applications*, vol. 42, no. 6, pp. 572–583, 2014.

[68] L. L. Kinney and C. H. Roth, *Fundamentals of Logic Design*. Cengage Learning, 2014.

[69] R. C. Dorf and R. H. Bishop, *Modern control systems*. Pearson, 2011.

[70] N. Mohan, T. M. Undeland, and W. P. Robbins, "Power electronics," *Wiley*, 1988.

[71] N. Mohan, *First Course on Power Electronics and Drives*. Minnesota Power Electronics Research & Education, 2003.

[72] "Psim modules," https://powersimtech.com/products/psim/, Last Date Accessed: 2017-07-09.

[73] "Psim users guide," 2016, Powersim Inc.,Version 5.

[74] M. Kaltschmitt, W. Streicher, and A. Wiese, *Renewable energy: technology, economics and environment*. Springer Science & Business Media, 2007.

[75] *Automotive Grade*, Infineon Technologies AG, 9 2015, rev. 1.

[76] F. L. Luo, H. Ye, and M. H. Rashid, *Digital power electronics and applications*. Academic press, 2010.

[77] D. W. Hart, *Power electronics*. Tata McGraw-Hill Education, 2011.

[78] W. D. Stevenson, *Elements of power system analysis*. McGraw-Hill, 1975.

[79] B. M. Weedy, B. J. Cory, N. Jenkins, J. B. Ekanayake, and G. Strbac, *Electric power systems*. John Wiley & Sons, 2012.

[80] C. K. Alexander and M. no Sadiku, "Electric circuits," *Transformation*, vol. 135, pp. 4–5, 2000.

[81] R. L. Boylestad, *Introductory Circuit Analysis*. Prentice Hall PTR, 2002.

[82] W. Hayt, J. Kemmerly, and S. Durbin, *Engineering Circuit Analysis*. McGraw-Hill, Inc., 2007.

[83] J. D. Irwin and R. M. Nelms, *Basic engineering circuit analysis*. John Wiley & Sons, 2010, vol. 900.

[84] V. K. Sood, *HVDC and FACTS controllers: applications of static converters in power systems*. Springer Science & Business Media, 2006.

[85] V. Vodovozov, *Introduction to Power electronics*. Bookboon, 2010.

[86] B. K. Bose, *Power electronics and AC drive*. Prentice Hall, Inc., Old Tappan, NJ, 1986.

[87] M. Barnes, *Practical variable speed drives and power electronics*. Newnes, 2003.

[88] B. A. Welchko, T. A. Lipo, T. M. Jahns, and S. E. Schulz, "Fault tolerant three-phase ac motor drive topologies: a comparison of features, cost, and limitations," *IEEE Transactions on power electronics*, vol. 19, no. 4, pp. 1108–1116, 2004.

[89] T.-H. Liu, J.-R. Fu, and T. A. Lipo, "A strategy for improving reliability of field-oriented controlled induction motor drives," *IEEE transactions on industry applications*, vol. 29, no. 5, pp. 910–918, 1993.

[90] J.-R. Fu and T. A. Lipo, "A strategy to isolate the switching device fault of a current regulated motor drive," in *Industry Applications Society Annual Meeting, 1993., Conference Record of the 1993 IEEE*. IEEE, 1993, pp. 1015–1020.

[91] S. Bolognani, M. Zordan, and M. Zigliotto, "Experimental fault-tolerant control of a pmsm drive," *IEEE Transactions on Industrial Electronics*, vol. 47, no. 5, pp. 1134–1141, 2000.

[92] R. Ribeiro, C. Jacobina, E. Da Silva, and A. Lima, "A fault tolerant induction motor drive system by using a compensation strategy on the pwm-vsi topology," in *Power Electronics Specialists Conference, 2001. PESC. 2001 IEEE 32nd Annual*, vol. 2. IEEE, 2001, pp. 1191–1196.

[93] R. L. de Araujo Ribeiro, C. B. Jacobina, E. R. C. Da Silva, and A. N. Lima, "Fault-tolerant voltage-fed pwm inverter ac motor drive systems," *IEEE Transactions on Industrial Electronics*, vol. 51, no. 2, pp. 439–446, 2004.

[94] H. Stemmler and P. Guggenbach, "Configurations of high-power voltage source inverter drives," in *Power Electronics and Applications, 1993., Fifth European Conference*. IET, 1993, pp. 7–14.

[95] K. Corzine, S. Sudhoff, and C. Whitcomb, "Performance characteristics of a cascaded two-level converter," *IEEE Transactions on Energy Conversion*, vol. 14, no. 3, pp. 433–439, 1999.

[96] W. Song and A. Q. Huang, "Fault-tolerant design and control strategy for cascaded h-bridge multilevel converter-based statcom," *IEEE Transactions on Industrial Electronics*, vol. 57, no. 8, pp. 2700–2708, 2010.

[97] M. B. de Rossiter Correa, C. B. Jacobina, E. C. Da Silva, and A. N. Lima, "An induction motor drive system with improved fault tolerance," *IEEE Transactions on Industry Applications*, vol. 37, no. 3, pp. 873–879, 2001.

[98] R. Ribeiro, C. Jacobina, A. Lima, and E. Da Silva, "A strategy for improving reliability of motor drive systems using a four-leg three-phase converter," in *Applied Power Electronics Conference and Exposition, 2001. APEC 2001. Sixteenth Annual IEEE*, vol. 1. IEEE, 2001, pp. 385–391.

[99] E. Dos Santos and E. R. da Silva, *Advanced Power Electronics Converters: PWM Converters Processing AC Voltages*. John Wiley & Sons, 2014, vol. 46.

[100] B. W. Williams, *Power electronics: Devices, drivers, and applications*. John Wiley and Sons Inc., New York, NY, 1987.